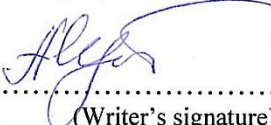




University of
Stavanger

Faculty of Science and Technology

MASTER'S THESIS

Study program/ Specialization: Offshore Technology Marine and Subsea Technology	Spring semester, 2015 Open
Writer: Arkhat E. Sultabayev	 (Writer's signature)
Faculty supervisor: Professor Ove Tobias Gudmestad External supervisor(s): Associate Professor Aleksey V. Dengaev (Gubkin University)	
Thesis title: Development Concepts for the Northern Caspian Sea	
Credits (ECTS): 30	
Key words: Offshore, the Northern Caspian Sea, Ice loads, Ice mechanics, Ice rubble, FEM, Development concepts, Kashagan, ANSYS	Pages:131..... + enclosure:16... Stavanger, 14.06.2015 Date/year

ABSTRACT

Today the Northern Caspian Sea is considered to be a very perspective region for oil and gas growth. However, the challenges encountered in the Northern Caspian Sea are not usually met in such combination in another regions, so this imposes special requirements for the further development of hydrocarbon fields in this region.

This thesis is focused on the field development in the Kazakh sector of the Northern Caspian Sea and it is addressed to a discussion of development concepts that might be applied for these conditions. Possible options for production drilling, production of hydrocarbons, oil and gas transportation and processing are discussed on basis of the analysis of existing solutions for similar conditions. Attention is also given to ice load mitigation measures and other aspects that should be taken into consideration during the development of fields in the Northern Caspian Sea.

In the second part the issue of the ice-structure interaction is described with respect to the shallowness of the Northern Caspian Sea. After gaining understanding of the physical processes related to the ice action on vertical and sloping structures, numerical modelling is performed in ANSYS 15.0 Workbench. The numerical set-up of the model is described in accordance with the theoretical background of the finite element method. The results obtained from the modelling of the ice action on vertical and sloping structures are discussed and compared with actual theoretical models for the ice loads calculation. It was proven that there is some discrepancy between the numerical and theoretical solutions when grounded ice rubble adjacent to the structure partially dissipates the ice loads into the seabed.

Finally, conclusions and suggestion for further research wrap up the thesis in order to summarize the acquired findings.

Acknowledgments

Studying for a Master Degree at Gubkin University and University of Stavanger has been an exciting period of my life. There are many persons who supported me throughout the last two years and who made this thesis possible.

First of all I would like to sincerely appreciate my supervisor Professor Ove Tobias Gudmestad for his support and for his supervision during this spring. His comments and advises during my study in Norway made my own knowledge stronger and deeper.

I also wish to give my thanks to Professor Anatolyi Borisovich Zolotukhin for sharing his outstanding knowledge and experience in oil industry. I would like to thank him for the opportunity to study in Norway and to get an international experience. I believe that Mr.Gudmestad and Mr.Zolotukhin are key persons that heartily supported me during the study and from whom I have learned a lot.

Special tanks also to Rauan Zamangarin for guiding advices that were helpful during the finite element analysis carried out in this thesis.

I would take this opportunity to thank my group mates for a great support thorough my study in Moscow and Stavanger. I will definitely never regret the time spent together in preparing for exams. I also want to thank my friends who help me in all endeavours.

Last but not least, I would like to give thanks to my family who has never stopped believing in me and supporting me.

TABLE OF CONTENTS

Abstract.....	i
Acknowledgments	ii
List of figures.....	vii
List of tables	xiii
List of symbols and abbreviations	xiv
Chapter 1. Introduction	1
1.1 Problem Description.....	4
1.2 Purpose and Scope	4
1.3 Thesis organization.....	5
Chapter 2. Aspects of Sea Ice	7
2.1 Physical properties.....	8
2.1.1 The structure of ice	8
2.1.2 Density.....	10
2.2 Mechanical properties	10
2.2.1 Compressive strength	10
2.2.2 Tensile strength.....	12
2.2.3 Flexural strength.....	13
2.2.4 Shear strength.....	13
2.2.5 Young’s modulus and Poisson’s ratio.....	13
2.2.6 Friction coefficient between ice and different materials.....	14
2.3 Ice features.....	15
2.4 Summary.....	15
Chapter 3. Environmental Conditions of the Northern Caspian Sea	16
3.1 Bathymetry	17
3.2 Air Temperature and Wind	17
3.3 Water Temperature	19
3.4 Water Salinity	20
3.5 Currents	21

3.6 Waves.....	22
3.7 Sea Level	23
3.7.1 Long-term sea level changes.....	24
3.7.2 Short-term sea level changes.....	25
3.8 Ice Conditions.....	26
3.8.1 Landfast ice.....	27
3.8.2 Drift Ice.....	30
3.8.3 Shear Zone	30
3.8.4 Ridges and Stamuchas	30
3.9 Summary.....	31
Chapter 4. Challenges in the Northern Caspian Sea.....	32
Chapter 5. Development Concepts for the Northern Caspian Sea.....	41
5.1 Production drilling systems	42
5.1.1 Ice islands.....	42
5.1.2 Drilling barge.....	44
5.1.3 Jack-up protected by ice protection barriers.....	46
5.1.4 Platform drilling rigs.....	47
5.2 Production system.....	48
5.2.1 Technical solutions	48
5.2.2 Concept of a Semi ice tolerant platform.....	53
5.2.2 Concept of a Stand-alone platform.....	55
5.2.3 Wellhead platforms.....	56
5.3 Ice barriers.....	57
5.3.1 Breakwaters.....	58
5.3.3 Grounded satellite barges	60
5.3.4 Rubble generators	61
5.3.2 Ice Protection Piles.....	63
5.3.5 Grounded ice as an ice barrier	64
5.3.6 Ice barriers arrangement	65
5.4 Processing system	69
5.5 Transportation system	71
5.6 Summary.....	72

Chapter 6. Ice action in shallow water.....	74
6.1 Design scenarios.....	75
6.2 Interaction geometry.....	76
6.3 The effect of Ice Rubbles in shallow waters	77
6.4 Ice loads on vertical structures.....	79
6.4.1 Simple equation of the global ice action	81
6.4.2 Korzhavin’s approach	82
6.4.3 Michel and Thussaint approach.....	83
6.4.4 Empirical correlation based on field measurements	84
6.5 Ice action on sloping structures.....	84
6.5.1 Croasdale’s approach	86
6.5.2 ISO approach.....	88
6.6 Summary.....	90
 Chapter 7. The FEM Theory.....	 91
7.1 State-of-the-Art: Computational Methods for the ice-structure interaction modelling.....	 92
7.2 The conventional FEM combined with element erosion scheme	94
7.2.1 Analysis system	95
7.2.2 The constitutive model.....	97
7.2.3 The damage initiation criterion and the damage evolution law	100
7.2.4 Meshing.....	101
7.2.5 Erosion	102
7.2.6 Boundary, initial and loading conditions	103
7.3 Summary.....	103
 Chapter 8. The Finite Element Analysis of ice-structure interaction in shallow waters of the North Caspian Sea.....	 105
8.1 Interaction scenarios realized in the finite element analysis.....	106
8.2 Finite element analysis of ice loads on vertical structures.....	106
8.3.1 Geometry	106
8.3.2 The simulation results.....	108
8.3.3 Comparison of numerical results and analytical solution.....	109
8.4 Finite element analysis of ice loads on sloping structures	111

8.4.1 Geometry	112
8.4.2 The simulation results	114
8.4.3 Comparison of numerical results and analytical solution.....	114
8.5 Discussion of the results	116
8.6. Summary.....	117
Chapter 9. Conclusions and Suggestion for further work.....	118
9.1 Conclusions.....	118
9.2 Further work.....	120
References.....	121
Appendix A. Summary of the materials properties	131
Appendix B. A concrete armor block with improved interlocking ability	134
Appendix C. Simulation results	140
Appendix D. Dimensions of the SIB and ice rubble	146

List of figures

Figure 1.1: Potential of the Caspian Sea (Zolotykhin, 2014a) 1

Figure 1.2: Perspective fields within the Kazakh sector of the North Caspian Sea. 2

Figure 2.1: Idealized arrangement of atoms in Ih ice wherein oxygen atoms are presented in white circles and view of crystal lattice looking a) along the c-axis and b) along basal-plane layers (after Palmer and Croasdale, 2012)..... 8

Figure 2.2: a) Typical morphology of a sheet ice layer; b) typical temperature profiles during freezing and melting, where T_{freeze} is the freezing temperature of the ice and T_i is the designates the ice temperature; and c) typical salinity profile (Gürtner, 2009). 9

Figure 2.3: Schematic sketch showing the effect of strain rate on the compressive stress-strain behaviour of ice (Sand, 2008). 11

Figure 2.4: Development of the wing crack mechanism: a) Zero load. No cracks. b) Cracks nucleate at a critical compressive stress. Normal stress acts to close cracks and shear stress acts to cause sliding. T denotes tensile zone. c) Wings of length L nucleate in tensile zone at higher stress (after Sand, 2008). 11

Figure 2.5: Flexural strength in the Northern Caspian Sea based on 112 measurements (after Terziev et al., 1992)..... 12

Figure 3.1: Bathymetry chart of the Northern Caspian Sea 17
 (Based on Verlaan and Croasdale, 2011). 17

Figure 3.2: Monthly extreme and average daily air temperatures in Kulaly. The data derives from the period 1977-1985..... 18

Figure 3.3: Frequency of the wind speed for the period 1888-2006. 19

Figure 3.4: Monthly extreme minimum/maximal and average water temperatures at the Kulaly station. The data derives from the period 1977-1991. 19

Figure 3.5: Salinity distribution (ppm) in April for the period 1940-1963 (Terziev et al., 1992)..... 20

Figure 3.6: Monthly extreme minimum/maximal and average water salinity at Kulaly. The data derives from the period 1977-1991. 21

Figure 3.7: Main currents of the Caspian Sea (European Environment Agency, 2005).....	22
Figure 3.8: Distribution of the significant wave height in the Northern Caspian derived from salinity altimetry (October 1992- December 2005). According to Lebedev et al. (2006).	22
Figure 3.9: Significant and maximal wave heights for different return periods (Terziev et al., 1992):	23
Figure 3.10: The Caspian Sea level variability over 1880-2005 and forecast up to 2035 (Karulin et al., 2002). Note that all values of the sea level are given in the Baltic System (BS).	24
Figure 3.11: Monthly extreme minimum/maximal and average sea level at Kulaly. The data derives from the period 1977-1991.....	26
Figure 3.12: Satellite image of the North Caspian Sea taken by NASA’s Terra satellite, February, 2013 (MODIS, 2013).....	26
Figure 3.13: Landfast ice zone (Terziev et al., 1992)	27
Figure 3.14: Ice condition of the Northern Caspian Sea: average duration of ice season, maximal ice thickness and boundaries of drifting ice in mild winter (1), in moderate winter (2) and severe winter (3). According to Kouraev et al. (2004).....	28
Figure 3.15: Chart-map of the Northern Caspian ice conditions based on the satellite images as for March 2015 (based on Planeta, 2015).....	29
Figure 3.16: Rose plot of ice drift. Note that the directions are expressed “from”(Verlaan and Croasdale, 2011).....	30
Figure 3.17: Location of ridges (a) and stomuchas (b) in moderate winters (Terziev et al., 1992).....	31
Figure 4.1: Ice ride-up on low freeboard structure (after Palmer and Croasdale, 2012).....	35
Figure 4.2: Ice encroachment in the Caspian Sea (McKenna et al., 2011).	35
Figure 4.3: a) The Arcktos special amphibious vehicles (Juurmaa and Wilkman, 2002) and b) Ice breaker emergency evacuation vessels (Remontowa Company, 2006).	37
Figure 4.4: The Picture of D Island (Kashagan) wherein an ice wake can be observed behind the structure (Topaz Energy and Marine, 2015)	38
Figure 4.5: the Volga Don Canal and Baltic Sea-Volga waterways (NCOC, 2011).	39

Figure 5.1: Island costs vs. water depth in the Beaufort Sea (Løset, 2014).....	43
Figure 5.2: Gravity berm for the Sunkar barge (Granneman et al., 2001).....	45
Figure 5.3: a) Steel berm foundation that can be used as a barge foundation (based on picture from Granneman et al., 2001) and b) existed example of the steel berm for the SDC drilling platform (Rigzone, 2015).	45
Figure 5.4: Concept of a jack-up with ice protection system (Dudik E., 2009).....	47
Figure 5.5: Sheet pile island built at the Kashagan field (Nymo, 2010).....	49
Figure 5.6: Special shape of a sheet piled island to avoid ice over-ride (not to scale, according to Palmer and Caroasdale, 2012).....	50
Figure 5.7: Tarsiut Island during construction (after Britner-Shen Consulting Engineers Inc.)	51
Figure 5.8: Fill requirement for sacrificial, beach and caisson-retained islands (Comyn, 1984).	52
Figure 5.9: Ice resistant platform at the Pirazlomnaya field (Noyonews.net, 2013).	53
Figure 5.10: Semi-ice tolerant platform built in the Kashagan field (after Atyrau-city.kz, 2011).....	54
Figure 5.11: A stand-alone platform (CRI) for the Kalamkas field development (NCOC, 2013).....	55
Figure 5.12: Wellhead platform with increased ice generating capability (based on the SIB concept).	57
Figure 5.13: Grounded barge in the North Caspian Sea (Bastian et al., 2004).....	60
Figure 5.14: a) a Shoulder Ice Barrier (not to scale) and b) a curve surface barrier proposed by Li et al., 2006.....	62
Figure 5.15: 2D plots of ice rubble profiles at the centre of the SIB (Gürtner, 2009).	63
Figure 5.16: a) The Sunkar Barge is on the location (IMPaC, 2011) and b) Model-scale testing of piles with different spacings (Weihrauch and Gürtner, 2006).	64
Figure 5.17: a) Stomukha resisting moving ice in the Caspian Sea (Lengeek et al., 2003) and b) Spray ice protection barrier around CIDS during its deployment at Antares in the US Beaufort (Matskevitch, 2007).	65

Figure 5.18: Top view of a sheet pile island protected by rock mound ice barriers at Kashagan (SpatialEnergy.com, 2010).	66
Figure 5.19: The Sunkar drilling barge protected by submerged barges. After a) McKenna, 2012, and b) CDE, 2015.....	67
Figure 5.20: Different scenarios of ice action on the central structure as the Sunkar Barge (Jochmann et al., 2003)	68
Figure 5.21: Ice loads on the barge with and without external ice protection (Jochmann et al., 2003).....	68
Figure 5.22: Maximum ice load on a central platform varying with separation of barriers from the platform (Palmer and Croasdale, 2012).	69
Figure 5.23: Processing facility block diagram (Gudmestad et al., 2010).....	70
Figure 6.1: Illustration of factors influencing ice actions (Løset et al., 2006).....	74
Figure 6.2: Design scenarios (Palmer and Croasdale, 2012).	76
Figure 6.3: a) Effective diameter of a multiple legs structure and b) Model-scale testing of piles with different spacing (Løset, 2014c).....	77
Figure 6.4 :Ice rubble built up in front of a wide structure in the Caspian Sea (Loiset et al., 2006 with reference to Evers and Kühnlein, 2001).....	78
Figure 6.5: Air temperature at which it would be possible for rubble of porosity γ to completely consolidate. Note that the initial temperature distribution in the ice sheet is assumed as linear and equal to the air temperature on the top surface (Kry, 1977).....	78
Figure 6.6: Schematic showing localization of action in compressive ice-structure interaction.	80
Figure 6.7: Ice loads during different stages of ice interaction with a vertical structure (a) and a sloping structure (b) in shallow water (Palmer and Croasdale, 2012)	81
Figure 6.8: Phases of ice interaction with a sloping structure in shallow water (Palmer and Croasdale, 2012).....	85
Figure 6.9: Ice rubble in front of a barrier in the North Caspian Sea (Croasdale et al., 2011).85	
Figure 7.1 Representation of a) Tresca's and von Mises yield criteria and b) Mohr- Coulomb and Drucker-Prager yield criteria. (Sand, 2008)	97
Figure 7.2: The hyperbolic Drucker-Prager plasticity model (Lu et al., 2012).....	98

Figure 7.3: Bending failure tests with different layers of continuum element (Lu et al., 2012).	101
Figure 7.4: Representation of the erosion technique (based on ANSYS Inc., 2009b).....	103
Figure 8.1: Mesh for the ice-structure simulation model.	107
Figure 8.2: Simulated horizontal ice forces exerted onto the barge.....	109
Figure 8.3: Interaction of the ice sheet with the barge. Note that the red dots correspond to the free mass points as established in Chapter 7.2.5.	109
Figure 8.4: Comparison of the FEA and the semi empirical solutions described in section 6.4.	110
Figure 8.5: a) The initial stage of the interaction and b) the final stage when the ice rubble is grounded (not to scale).	111
Figure 8.6: Mesh for the ice-structure simulation model when the ice rubble is grounded...	113
Figure 8.7: Interaction of the 0.15-m ice sheet with the sloping face of the SIB.....	114
Figure 8.8: Comparison of ice loads on the SIB (the initial stage) obtained with the finite element simulations and the semi empirical solutions.	115
Figure 8.9: Comparison of ice loads on the SIB (when the ice rubble is grounded in front of the SIB) obtained with the finite element simulations and the semi empirical solutions.	116
Figure C.1: Simulated horizontal component of ice forces exerted onto the SIB (the 0.15-m ice sheet acting on the 45-degree slope).....	141
Figure C.2: Simulated vertical component of ice forces exerted onto the SIB (the 0.15-m ice sheet acting on the 45-degree slope).	141
Figure C.3: Simulated horizontal component of ice forces exerted onto the SIB (the 0.96-m ice sheet acting on the grounded ice rubble in front of the SIB).....	142
Figure C.4: Simulated vertical component of ice forces exerted onto the SIB (the 0.96-m ice sheet acting on the grounded ice rubble in front of the SIB).	142
Figure C.5: Snapshot of ice interaction on the barge revealing the ice failing in crushing. Note that red dots are free mass points (see Chapter 7.2.5).....	143
Figure C.6: Snapshot of the 0.15-m ice sheet acting on the SIB revealing the ice plasticity before the ice failing in bending and before initiation of circumferential cracks.	143

Figure C.7: Snapshot of the 0.96-m ice sheet acting on the grounded ice rubble in front of the SIB revealing the ice failing in rubbing.	144
Figure C.8: Snapshot of the 0.96-m ice sheet acting on the grounded ice rubble in front of the SIB revealing the ice failing in rubbing.(back view).	144
Figure C.9: Snapshot of the 0.96-m ice sheet acting on the grounded ice rubble in front of the SIB revealing the ice failing in rubbing (general view).	145
Figure D.1: The dimensions of the SIB and grounded ice rubble implemented into the simulations. Note that all dimensions are in mm and in degrees.	147

List of tables

Table 1.1. Fields located in the Kazakh sector of the Northern Caspian Sea (According to KazMunayGas, 2013)..... 3

Table 3.1. Ice periods for different types of winters (Terziev et al., 1992). 27

Table 3.2. The 100-return period ice thickness (Gürtner, 2005)..... 29

Table 6.1: Comparison of Korzhavin’s formula with Michel and Thussaint approach..... 83

Table 7.1. Parameter differences between associated and non-associated flow (after Weizhi, 2014)..... 99

Table A.1. Summary of ice properties used for the FEA. 132

Table A.2. Summary of ice rubble properties (Duplenskiy, 2012) 133

Table A.3. Soil properties implemented into the model (Sediments layer of silty sand and soft clay)..... 133

List of symbols and abbreviations

Latin characters

A	nominal contact area
b	body force
b_i	components of the body acceleration
c	cohesion of Mohr-Coulomb material
$C_{1,2}$	slope angle coefficients
D	width of the structure at water level
d	cohesion of Drucker-Prager material
E	Young's modulus
e	porosity of ice rubbles,
F_B	breaking force component
F_H	horizontal force acting on a sloping structure
F_i	forces acting on the node
F_V	vertical force acting on a sloping structure
g	standard acceleration.
h_i	ice thickness
h_r	rubble height
I	indentation factor
h_s	average maximum sail height of the ice rubble
K_1	contact factor
K_2	shape factor
L_c	characteristic length of an ice beam on an elastic foundation
m_i	mass of the node and

w^{int}	internal rate of energy per unit volume
p	average effective pressure
t	time
v	rate of indentation

Greek characters

α	slope of structure face from horizontal
β	friction angle in Drucker-Prager material
$\dot{\varepsilon}_{D/B}$	peak stress
θ	angle of the rubbles inclination to the horizontal
ε	strain
$\dot{\varepsilon}$	strain rate
$\dot{\varepsilon}_0$	reference strain rate
$\varepsilon_{ij}^{\text{cracking}}$	cracking (tertiary) strain
$\varepsilon_{ij}^{\text{delayed}}$	delayed elastic strain
$\varepsilon_{ij}^{\text{elastic}}$	instantaneous elastic strain tensor
$\varepsilon_{ij}^{\text{total}}$	total strain
$\varepsilon_{ij}^{\text{viscous}}$	viscous or permanent strain
μ	friction coefficient
μ_i	ice-ice friction coefficient
ρ	any density
ρ_w and ρ_i	sea water and ice density, respectively
σ_c	unconfined compressive strength of the ice
σ_f	ice flexural strength,
σ_{ij}	stress tensor
σ^T	transposed stress tensor σ

τ	shear stress of the material
φ	angle of internal friction in Mohr-Coulomb material

Abbreviations

BS	Baltic System
CEM	Cohesive Element Method
CRI	Caisson Retained Island
DEM	Discrete Element Method
DP	Drucker-Prager model
FEA	Finite Element Analysis
FEM	Finite Element Method
GBS	Gravity Based Structure
IBEEV	Icebreaker Emergency Evacuation Vessel
MC	Mohr-Coulomb plasticity model
NCOC	North Caspian Operating Company
NE	North-East
NW	North-West
SE	South-East
SW	South-West
W	West
XFEM	Extended finite element method

Chapter 1. Introduction

Although the Caspian Sea, which is shared by Azerbaijan, Iran, Kazakhstan, Russia and Turkmenistan, is one of the oldest oil production regions in the world, its northern part, has been developing over only last two decades. Today the Northern Caspian Sea is considered to be a very perspective region for oil and gas growth.

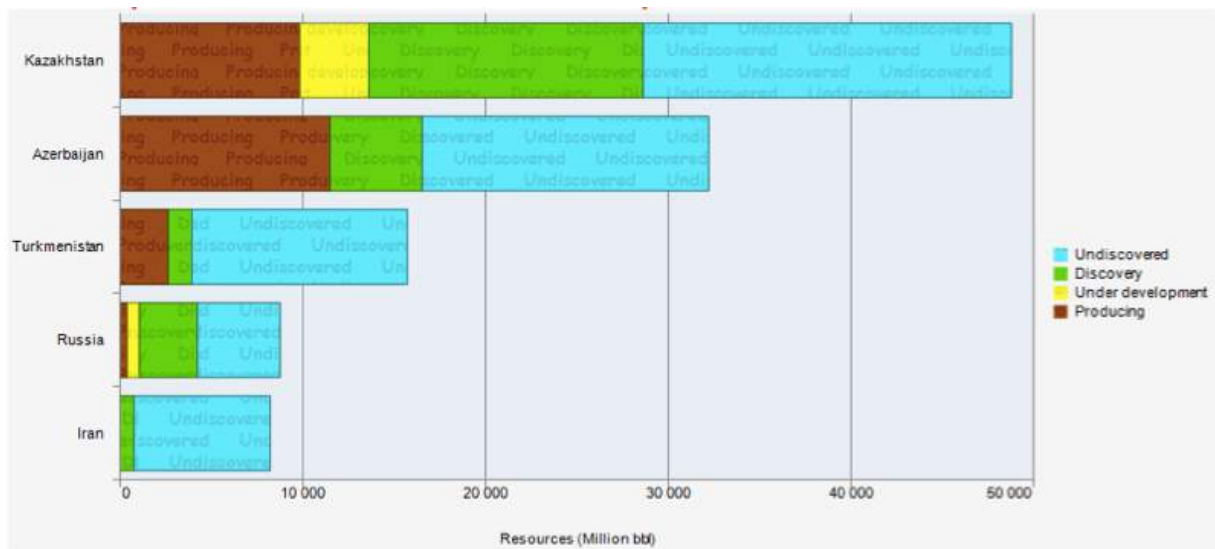


Figure 1.1: Potential of the Caspian Sea (Zolotykhin, 2014a)

The resource potential of the Kazakh sector, which is mainly represented by the Northern Caspian Sea, amounts to ca. 50 billion barrels of oil equivalent, see fig. 1.1. Note that the greatest potential of the Kazakh sector of the Northern Caspian comes from the Kashagan field that is considered as the world’s largest oil discovery in the last 35 years (Henni, 2014).

It is a giant oil field located 80 km southeast of Atyrau. The Kashagan reservoir extends over an area of 75 km by 45 km and holds up to 38 billion of oil-in-place where about 10-13 billion bbl of these reserves is recoverable. As expected the peak production will reach 1.5 million of barrels of oil per day, which will be ca. 5% of global demand by 2022 (Zolotukhin, 2014). North Caspian Operating Company (NCOOC) consisting of Eni, ExxonMobil, Total, Shell, KazMunaiGas, CNPC and INPEX is responsible for the field development.

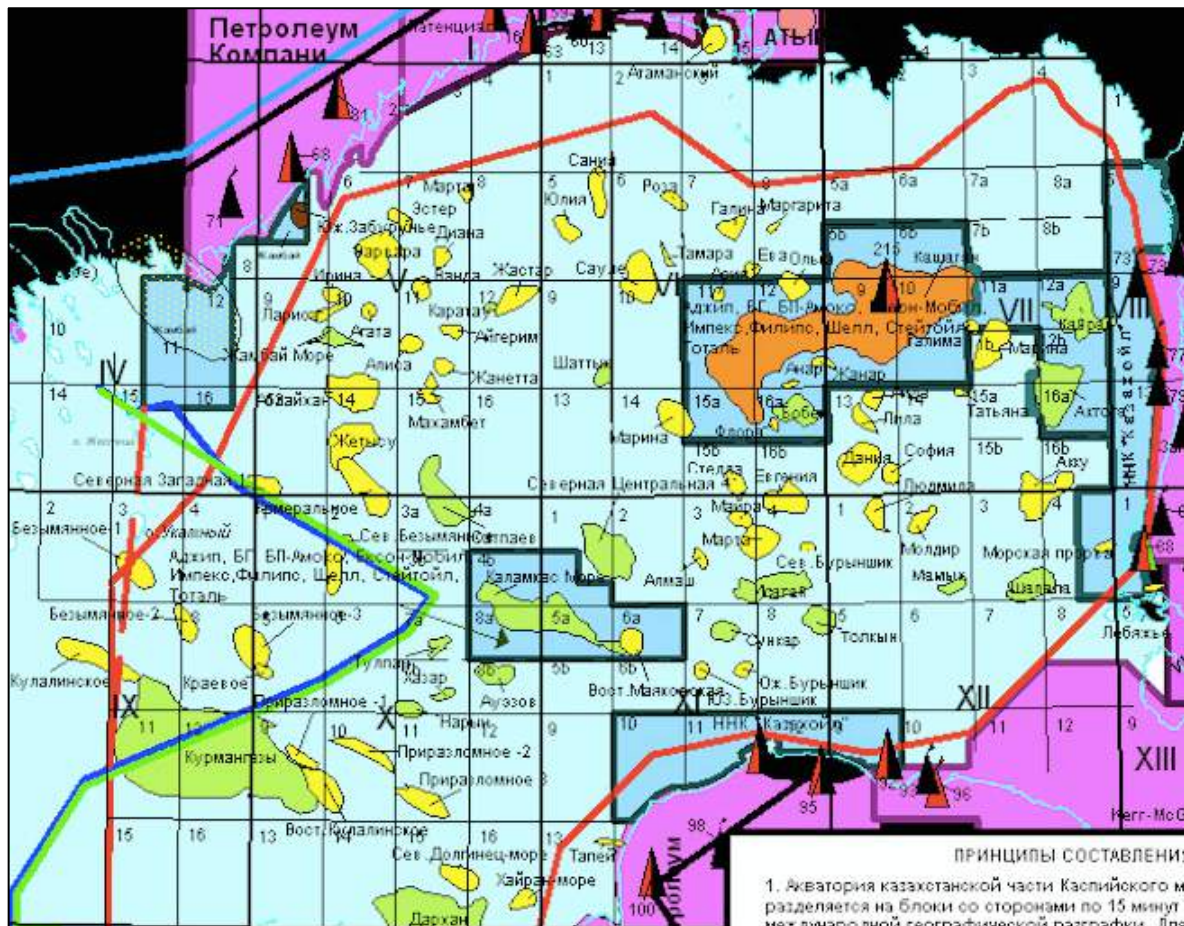


Figure 1.2: Perspective hydrocarbon fields within the Kazakh sector of the North Caspian Sea.

Note that: explored structures are shown in yellow, fields that are ready for the further development are shown in green, fields that have been developed are in brown (based on picture from Wikipedia, 2011).

However, the Kashagan development faced with significant delays and tremendous cost overruns. The production started on 11 September 2013 had to be stopped after two weeks due to leakages of the offshore pipeline running from one of the artificial islands to the onshore processing facility. New date of production beginning is 2016. Currently \$50 billion

has been invested only in the first phase (Helman, 2014) while the final capital expenditures are anticipated to be \$136 billion (Eldesov, 2013).

In addition to Kashagan, about 120 oil fields and perspective structures (table 1.1 & fig. 1.2) have been discovered within the Kazakh sector (Espergen, 2006). However, it worth mentioning that there are still significant uncertainties associated with evaluation of the hydrocarbon amount. Namely, there are such fields as Aktoty, Abai, Kairan, etc, while the reserves of such prospect structures as Makhambet, Zhambyl, Satpayev, Zhenis, Abay, Bobek, Isatay, Darkhan, Shagala are still needed to be estimated.

Table 1.1. Fields located in the Kazakh sector of the Northern Caspian Sea (According to KazMunayGas, 2013)

Field	Year of discovery	Geological Resources	Recoverable Reserves
Aktoty	2003	-	condensate – 77 MM tones <i>gas</i> – 169.5 <i>bcm</i>
Kairan	2003	-	oil - 35.8 MM tones <i>gas</i> -33.5 <i>bcm</i>
Southwest Kashagan	2003	-	oil - 6 MM tones <i>gas</i> - 15.2 <i>bcm</i>
Auezov	2008	oil - 60-70 MM tones	-
Rakushechnoe	2010	oil – 290 MM tones <i>gas</i> - 80 <i>bcm</i>	-
Khazar	2013	oil – 75.3 MM tones	oil – 30.6 MM tones
Kalamkas-offshore	2013	oil – 284.5MM tones	oil - 67.5 MM tones

Even though only limited experience in this region has been gained, this does not prevent many companies including major ones from realizing their own E&P programmes. The North Caspian Sea could become an important centre of oil and gas production in the near future with own exploration and production market, infrastructure, etc.

1.1 Problem Description

However, in order to achieve safe and cost-effective development of the fields introduced above it is of importance to identify and to select an appropriate development concept that is suitable in extreme shallow water coupled with moderate ice conditions. Otherwise great troubles and risks associated with environmental, financial, social challenges should be anticipated.

The term ‘development concept’ refers to systems for production drilling, production, processing and hydrocarbon transportation. The selection of the most optimal option is determined by working conditions (including water depth, soil characteristics, geographic, meteocean conditions, etc.) and expected loads (local and global loads by ice, wave, currents, etc.) that an offshore structure should withstand. One can notice that not every drilling system or type of a production structure can be applied for the Northern Caspian Sea.

Furthermore, it worth mentioning that the development of hydrocarbons in the Northern Caspian Sea imposes special restrictions due to the conditions similar to the Arctic (Løset, 2014a).

1.2 Purpose and Scope

The thesis focuses on the development of fields located in the Kazakh sector of the Northern Caspian Sea and it is addressed to discussion of development concepts that might be applied for these conditions. Moreover, the current research involves the combination of tasks associated with ice mechanics, petroleum engineering, civil engineering, geotechnics, etc.

It is purposed to discuss appropriate options for production drilling, production, transportation and processing of hydrocarbons. In addition, it is anticipated to study the ice-structure interaction mechanism in shallow water of the North Caspian Sea, since empirical models could be not fully correct due to grounded ice rubble in the vicinity of structures. Further aspects, which will be discussed in this thesis with respect to the Canadian/Russian Arctic experience, are:

- Study physical and mechanical properties of sea ice in the Northern Caspian Sea;
- Analyse the Northern Caspian environmental conditions;
- Discuss challenges and risks associated with development activities;
- Discuss of systems that might be applied for production drilling, examine different scenarios of production, processing systems, transportation options;

- Study ice loads mitigation measures and external ice protection systems;
- Study the ice-structure interaction mechanism in shallow water conditions, study the main empirical approaches (including ISO 19906, 2010) for ice loads calculations with respect to this issue;
- Study numerical methods used to simulate the ice-structure interaction process influenced by grounded ice rubble, select the most optimal one and perform finite element analysis;
- Analyse the ice-structure interaction process in shallow waters by introducing an appropriate finite element model;
- Discuss the results, summarize what was done and provide reasonable recommendations regarding to the selection of the development concepts for the Northern Caspian fields (Kazakh sector).

1.3 Thesis organization

Chapter 2 (Aspects of sea ice) describes the basics of ice mechanics required for the further study. The structure and the morphology of sea ice are presented in a concise and easy to understand manner. The main aspects related to the ice molecular structure, its physical and mechanical properties of sea ice and ice features are revealed. Values for each characteristic parameter obtained from field investigations are presented.

Chapter 3 (Environmental conditions of the Northern Caspian Sea) provides the description of the Caspian Sea environmental and ice conditions. To get a broad understanding of the problems related to the development of hydrocarbon fields in the region, distinctive features of the Northern Caspian Sea are determined such as sea states, water depth, sea level changes, etc.

Chapter 4 (Challenges in the Northern Caspian Sea) introduces challenges encountered in the Northern Caspian Sea. An analysis of these challenges is carried out in terms of activities required for the further field development.

Chapter 5 (Development concepts for the Northern Caspian Sea) discusses suitable development concepts for the Northern Caspian Sea. The main types of drilling and production platforms as well as factors affecting the selection of the development concept are identified. Ice mitigation measures and protection structures are introduced.

Chapter 6 (Ice action in shallow waters of the Northern Caspian Sea) contains the study of ice action in shallow waters, gives an overview of different semi empirical methods used for

ice loads calculations. This chapter covers somewhat the effect of ice rubbles in the vicinity of offshore structures resulting in reducing ice loads. Theoretical models for both vertical and sloping structures are presented.

Chapter 7 (The FEM Theory) introduces the background of the finite element method. Different numerical methods and approaches are overviewed. The general components of the finite element method combined with erosion technique are revealed. Issues related to the model realization and other parameters affecting the accuracy of the results are discussed.

Chapter 8 (The Finite Element Analysis of ice-structure interaction in shallow waters of the Northern Caspian Sea) provides the simulations results. Additionally, the comparison of loads obtained by the FEA and those obtained by the analytical approaches are carried out.

Finally, the acquired findings are summarized and suggestions for further research wrap up this thesis.

Chapter 2. Aspects of Sea Ice

Sea ice is a complex crystalline material mainly consisting of pure ice, brine and gas (air). Its properties are determined by the molecular structure, temperature, salinity, density and different impurities that take place within it. Moreover, sea ice properties significantly vary from one region to another one.

The ice properties determine the magnitude of ice loads on offshore structures and, therefore, it is of interest to discuss them in this thesis. Since this thesis relates to development concepts that are suitable in the Northern Caspian Sea, only aspects of sea ice, which are relevant for this region, are presented. It should be noted that only first-year ice takes place in the Caspian Sea, so multi year ice is beyond the scope of the thesis and not discussed.

This chapter reviews the main aspects related to the ice molecular structure, its physical and mechanical properties of sea ice and ice features with reference to Løset et al. (1998), Timco and Weeks (2010), WTO (1989), Sand (2008), Palmer and Croasdale (2012) and, partially, to lectures within the “Arctic Offshore Engineering” course delivered in Svalbard by Løset S. in 2014. The results of the field measurements carried out in the North Caspian Sea are presented in accordance with Terziev et al. (1992).

2.1 Physical properties

Some physical properties of sea ice that are mentioned in the preamble relate to such physical aspects as density and salinity of ice, its morphology and structure, grain sizes, ice thickness, porosity, etc.

Usually, an engineer does not need a detailed description of a microstructure and a crystallography of sea ice, so this section focuses only on a minimal required explanation of the molecular structure of sea ice and the physical properties that determine engineering decisions. However, the reader is referred to Løset et al. (1998), Timco and Weeks (2010) for more information regarding the topic of this section.

2.1.1 The structure of ice

There are several forms of ice existing under different temperatures and pressures, but only one of them, called Ih ice, takes place in nature. The crystal structure of Ih ice builds on a crystallographic arrangement of molecules of water, which have a repeating tetrahedral geometry with hexagonal symmetry (fig. 2.1). Besides, the ice structure has a series of parallel planes called “basal plane” and a major axis of symmetry, called c-axis, is normal to the basal plane. Note that basal-plane layers are not exactly planes and this is shown in fig. 2.1, b). In addition, three a-axis at 120° to each other are perpendicular to the c-direction.

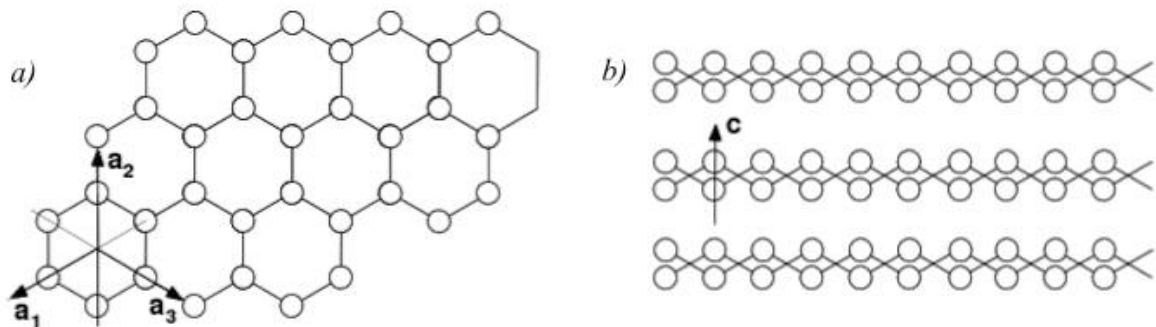


Figure 2.1: Idealized arrangement of atoms in Ih ice wherein oxygen atoms are presented in white circles and view of crystal lattice looking a) along the c-axis and b) along basal-plane layers (after Palmer and Croasdale, 2012).

The ice structure influences the ice formation process. It is easier to add atoms to an existing basal plane, i.e. perpendicular to the c-axes, so crystals growth in the a-directions. In addition, differences of the ice mechanical behaviour under different directional loads could be also explained in terms of the ice structure. Thus, an ice crystal has three hydrogen bonds

in the basal plane versus only one hydrogen bond along the c-axis. As a result, fracture along the basal plane requires rupturing two hydrogen bonds in the unit cell, while fracture of the unit cell along planes normal to the basal plane requires at least 4 hydrogen bonds to be ruptured. Also such ice properties as thermal conductivity, atomic diffusivity and elastic stiffness are also isotopically perpendicular to this c-axis (Løset S., 2014b).

However, in reality ice crystals might significantly vary in size. A group of ice crystals forming sea ice might have the c-axis randomly oriented. Moreover, sometimes we can distinguish the sea ice having nearly the same orientation of the c-axis and this depends on the ice formation conditions. As illustrated in fig. 2.2 ice is mainly an orthotropic material (columnar ice) with random orientated c-axes covered by the layer of granular ice. It should be noted that salinity and temperature are not constant and change through the ice sheet.

The reader interested in more detailed description of the microscopic structure of sea ice, its growth and formation is referred to Løset et al. (1998).

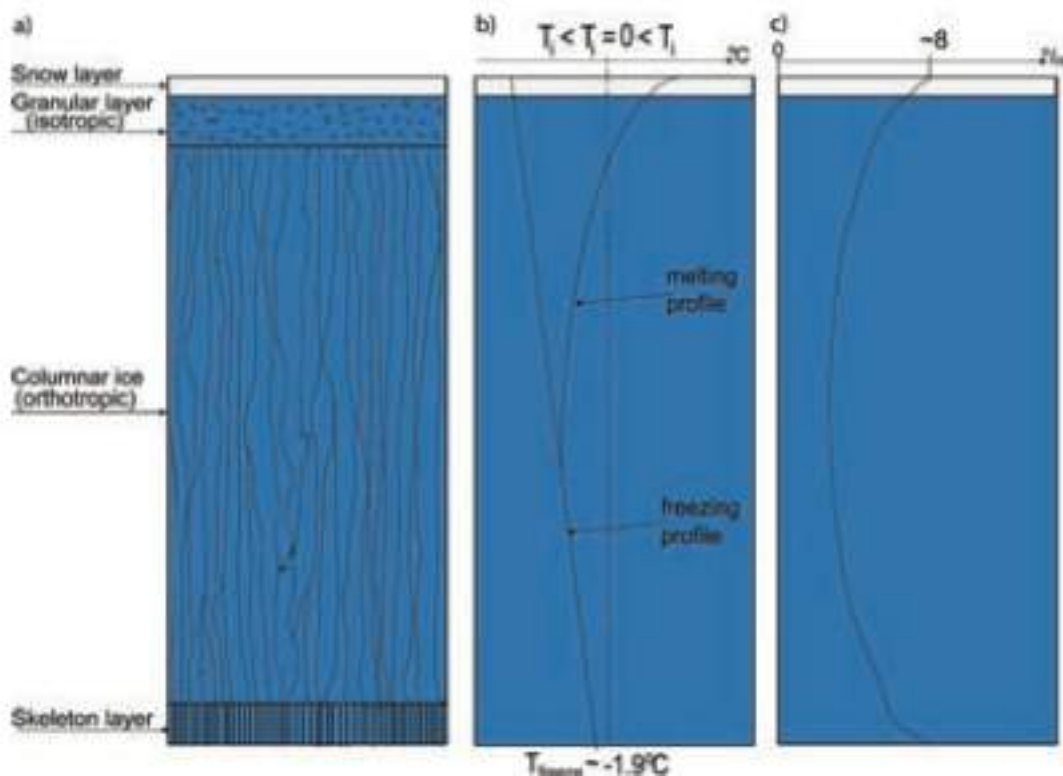


Figure 2.2: a) Typical morphology of a sheet ice layer; b) typical temperature profiles during freezing and melting, where T_{freeze} is the freezing temperature of the ice and T_i is the designates the ice temperature; and c) typical salinity profile (Gürtner, 2009).

2.1.2 Density

The density of sea ice mainly depends on the temperature and the salinity of seawater. This correlates with the Caspian field investigations presented by Terziev et al. (1992). Thus, sea ice density in the Northern Caspian Sea varies in the range between 630-968 kg/m³, while the probability of ice with the density that is higher than 900 kg/m³ is 85%.

2.2 Mechanical properties

Sea ice is an inhomogeneous, anisotropic and nonlinear viscous material (Sand, 2008). The ice mechanical properties including tensile, compressive, flexural, shear strengths coupled with Young modulus, Poisson ratio and friction coefficients are functions of the physical properties (the structure of ice, brine volume, porosity), temperature, the confinement of the ice sample, strain rate, etc.

The following section describes the mechanical properties that are important for the further discussion. Note that only results of the field measurements carried out in the North Caspian Sea are given although these ice properties could be derived from experimental correlations.

2.2.1 Compressive strength

Compressive strength is the maximal principal stress corresponding to failure beginning under ice compression (Løset et al., 2006). Generally, ice preferably fails in compression taking place when thick ice interacts with offshore structures (Timco and Weeks, 2010).

Ice is featured by two kinds of inelastic behaviours under compression (see fig. 2.3). On basis of the shape of the stress-strain curve, several zones can be determined: (i) brittle regime, (ii) ductile regime and (iii) transition zone.

Ice exhibits ductile behaviour when the stress-strain curve has a plateau and, on the other hand, the strain rate is lower than $\dot{\epsilon}_{D/B}$. The peak stress (or ductile compressive strength) increases with (i) increasing strain rate; (ii) with decreasing temperature and (iii) with decreasing salinity and porosity of the ice. According to Sand B. (2008) the grain size does not significantly influence on the peak stress.

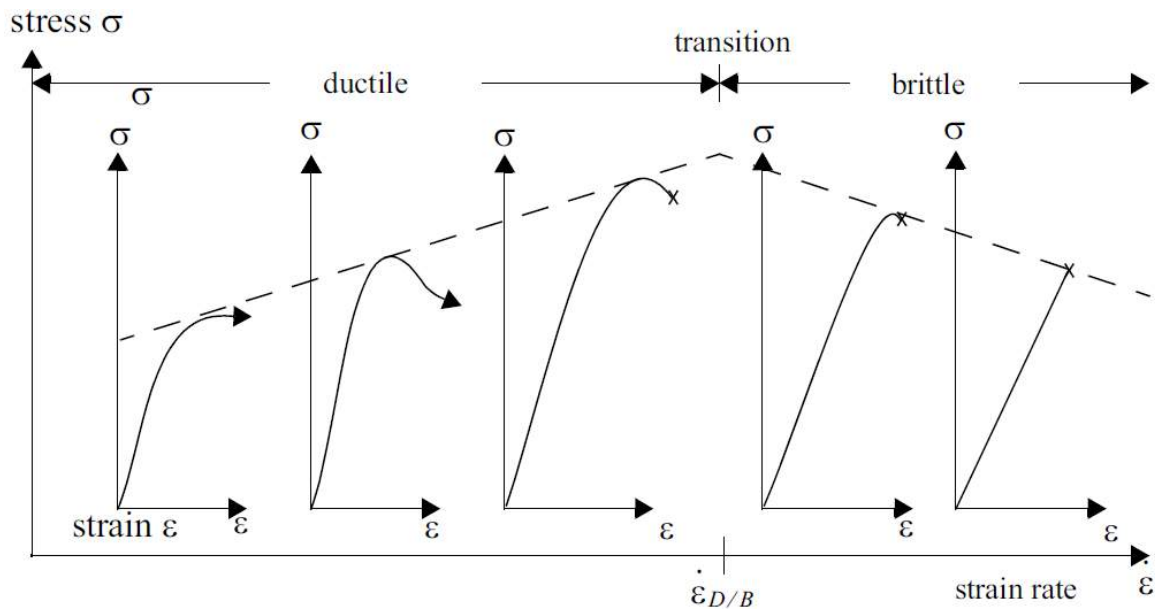


Figure 2.3: Schematic sketch showing the effect of strain rate on the compressive stress-strain behaviour of ice (Sand, 2008).

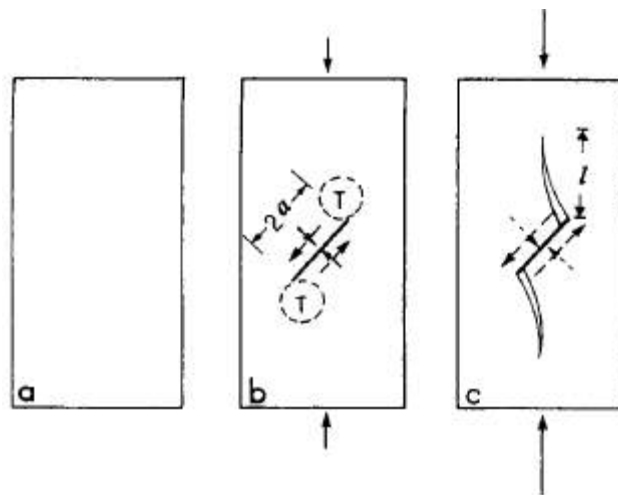


Figure 2.4: Development of the wing crack mechanism: a) Zero load. No cracks. b) Cracks nucleate at a critical compressive stress. Normal stress acts to close cracks and shear stress acts to cause sliding. T denotes tensile zone. c) Wings of length L nucleate in tensile zone at higher stress (after Sand, 2008).

Another important zone is the transition point, where the compressive strength reaches its maximum; hence, the ice loads on a structure will be maximal as well. The decreasing of the compressive strength after the transition might be explained by begetting of the crack propagation (see fig. 2.4): at strain rates lower than $\dot{\epsilon}_{D/B}$ (i.e. ductile ice behaviour) cracks form without propagation, while at strain rates above $\dot{\epsilon}_{D/B}$ (i.e. brittle ice behaviour) wing

cracks propagate from the cracks formed before. The transition rate $\dot{\epsilon}_{D/B}$ is in the range from 10^{-4} to 10^{-3} s^{-1} at temperatures from -40°C to -5°C .

Although the measured values of the compressive strength vary in wide range from 0.14 MPa to 6.0-8.0 MPa, the typical values for first-year ice in the North Caspian Sea do not exceed 4.5 MPa. It should be noted that these values of the compressive strength are comparable with the compressive strength of freshwater ice because of the low salinity of the Northern Caspian Sea. Thus, the compressive strength ranges from 5-25 MPa for freshwater ice (Petrovich, 2003), which is close to the compressive strength of the Caspian ice.

2.2.2 Tensile strength

Tensile strength is the maximal principal stress corresponding to failure begging under ice tension (Løset et al., 2006). Note that the tensile strength in vertical loading is three times higher than for horizontal one due to the ice structure and the ice growth direction. In addition, compressive and tensile strengths might vary significantly along different directions, but the compressive strength is normally 2-4 times larger than its tensile strength.

Typical values for first-year ice range from 0.13 MPa to 0.67 MPa (most of the Caspian measurements were carried out for the coastal zone). This is also close to the tensile strength of freshwater ice ranging from 0.7 to 3.1 MPa (Petrovich, 2003).

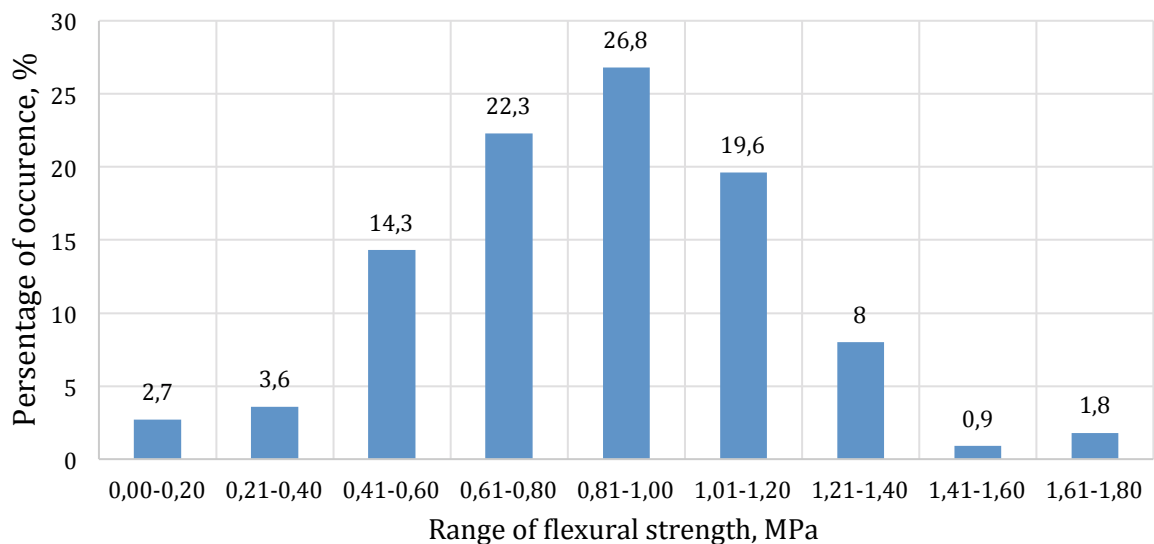


Figure 2.5: Flexural strength in the Northern Caspian Sea based on 112 measurements (after Terziev et al., 1992).

2.2.3 Flexural strength

Flexural strength is the ability of a brittle material to resist deformation under flexural loading conditions. In contrast to the compressive strength, the flexural strength of sea ice has not strict correlations with the loading rate. Since this parameter characterizes the material bearing capacity, the flexural strength is an important parameter for calculations of the ice action on sloping actions.

Typical values of flexural strength of sea ice measured in the Caspian Sea do not exceed 2.17 MPa while most of the results are in the range 0.41—1.20 MPa (see figure 2.5). However, the mean flexural strength based on 553 measurements in the North Caspian Sea is 0.78 MPa.

2.2.4 Shear strength

Timco and Weeks (2010) claim: “in engineering practice, the shear strength is not usually explicitly used. Since ice tends to fracture rather than to flow in a crack-free, volume-conserving manner, the shear strength is actually governed by the tensile strength of the ice. Since most ice engineering issues occur at higher loading rates (i.e. when ice exhibits brittle behaviour – the author’s note), the compressive strength is much higher than the tensile strength. Thus, ice loaded with a shear condition would fail in tension rather than in shear.”

However, the shear strength is an important material property to consider because the interaction between ice and structures is subjected to a biaxial stress state involving tensile stresses in addition to the compressive or shear stress. The author could found no reported measurements of the shear strength of the Caspian Sea ice, so the values of shear strength of columnar sea ice ranged from 550kPa to 900 kPa (Frederking and Timco, 1986) are proposed for the further discussion.

2.2.5 Young’s modulus and Poisson’s ratio

Elastic properties of ice are featured by an elasticity modulus and Poisson ratio.

Elasticity modulus, often called Young’s modulus, is defined as the ratio of the stress to the strain during elastic deformations (according to Hook’s law). One can notice that the total strain ε_{ij}^{total} is defined as a sum of the following strain components (the strains’ tensors (i j) are used because sea ice is considered as an anisotropic material):

$$\varepsilon_{ij}^{total} = \varepsilon_{ij}^{elastic} + \varepsilon_{ij}^{delayed} + \varepsilon_{ij}^{viscous} + \varepsilon_{ij}^{cracking} \quad (2.1)$$

where $\varepsilon_{ij}^{elastic}$ is the instantaneous elastic strain tensor; $\varepsilon_{ij}^{delayed}$ is the delayed elastic strain; $\varepsilon_{ij}^{viscous}$ is the viscous or permanent strain and $\varepsilon_{ij}^{cracking}$ is the cracking (tertiary) strain.

Note that in continuum mechanics of ice, it is not correct to call the elastic modulus as Young's modulus because any mechanical measurements involve the elastic and the viscoelastic components in Eq. (2.1), while the elastic modulus relates only to the elastic behaviour of ice. However, in this thesis the term Young's modulus is used.

The typical values of Young's modulus of ice in the Caspian Sea do not exceed $2.5 - 3.5 \times 10^9$ MPa and this is three times lower than for river ice.

Poisson's ratio is defined as the ratio of the lateral strain to the longitudinal strain in a homogeneous material for a uniaxial loading condition (Timco and Weeks, 2010). As Young's modulus, Poisson's ratio is an important engineering property of a material in terms of viscoelasticity effects in sea ice. However, it should be noted that measured values of the ratio would be more correct to call the Effective Poisson's ratio because the elastic response is mainly involved instead of purely viscoelasticity effects. Despite that there is no available data related to reported measurements of Poisson ratio in the Caspian Sea, its value is suggested 0.33 according to Timco and Weeks (2010).

2.2.6 Friction coefficient between ice and different materials

Friction forces are involved in problems associated with ice interaction with offshore structures. Due to static and dynamic ice-structure interaction conditions, static and kinetic friction coefficients are distinguished.

Friction depends on the ice temperature, roughness of interacting surfaces and relative velocity. However, temperature has not a strong influence on the friction coefficients. The friction coefficient decreases with increasing the relative velocity. The static and kinetic components of friction do not depend on the contact area. The values of the friction coefficients for the ice interaction with concrete, ice and ground are presented below.

The static friction of sea ice on rough concrete is equal to 0.13 and the corresponding kinetic friction coefficient is about 0.05 when the relative velocity is 30cm/s (Sand, 2008).

According to Frederking and Barker (2002) the friction coefficient for the ice-ice interaction is 0.03 at speeds greater than 0.1m/s and 0.09 at 0.01m/s.

The ice-sand/gravel friction coefficient (corresponding to sliding of a large ice block on the seabed) varies in the range of 0.2-0.6 and reduces with increasing relative velocity.

2.3 Ice features

In this section only the ice features that are relevant for the Northern Caspian Sea are presented. For additional information about other ice features the reader is referred to WMO (1989).

- *Level ice* is considered as sea ice that has not been subjected to deformation and has relatively uniform thickness.
- Rafted ice is defined as an ice feature formed when separate ice fields interact with each other. Due to currents and winds these ice fields override each other without a large amount of rubbles formation and eventually they adfreeze together.
- Ridges are formed when thick ice sheets interact with each other causing deformation of their edges and generate significant ice rubbles at the contact area.
- Stomukhas are grounded ridges that are usually form in shallow water where interaction between landfast ice and drifting ice exists.

More detailed information about these features observed in the Northern Caspian Sea is presented in Chapter 3.8.

2.4 Summary

Concentrating on the Northern Caspian Sea, the properties of first year ice that are applicable for later analyse in this report have been discussed. The magnitude of ice loads is a function of the ice properties, so it is of interest to properly determine each of them.

Ice is mainly an orthotropic material (columnar ice) covered by the layer of granular ice. It exhibits different behaviour depending on the strain rate of the load. It is important for the ice loads calculations to determine the transition point corresponding to the maximal compressive strength.

The results of the measurements carried out in situ have been also introduced. Generally, the analysis of the measurements' data shows a good correlation of the Caspian ice properties with the properties of freshwater ice. This is due to the low salinity of the Northern Caspian Sea and this is discussed in the next chapter. All properties presented in the chapter are summarized in Appendix A.

Chapter 3. Environmental Conditions of the Northern Caspian Sea

The Caspian Sea located at the crossroads of Europe and Asia is the biggest enclosed water body in the world. Being called a sea, the Caspian Sea is essentially a giant lake that is shared by Azerbaijan, Iran, Turkmenistan, Kazakhstan and Russia. The Caspian Sea covers 378 400 km² and the total volume of water is 78 100 km³. About 130 rivers feed it, but the most significant of them are Volga and Ural, which make about 90% of the total river discharge and which run into the sea in the northern part.

Traditionally, three main geographic areas are distinguished within the Caspian Sea: the northern, middle and eastern parts and the sea conditions within each of these areas significantly vary.

To get a broad understanding of the problems related to development of hydrocarbon fields in the region, the environment conditions only of the Northern Caspian Sea are introduced in this chapter. The data was taken from Terziev et al. (1992), Kuehnlein (2002), Dobrovolskyi et al. (1982), Lebedev et al. (2006, 2014) and Gürtner (2005, 2009) amongst others. Also observations of the Russian/Kazakh (former Soviet) stations located at the Kulaly, Pechnoy and Tyleniy islands (see fig.3.1) were used for the further analysis in this thesis.

3.1 Bathymetry

According to different sources (Kuehnlein, 2002, Kaltayev et al., 2007) the average water depth is about 4 m (fig. 3.1). However, the north-eastern part of the Caspian Sea is extremely shallow: the water depth within 25-30 km area from the shore doesn't exceed 2 m. (Sarybekova, 2004). The deepest part of the Northern Caspian Sea is the Ural furrow located in the center of the Kazakh sector, where water depth reaches 9 m. Nevertheless, due to the sea level changes discussed in detail in Chapter 3.7, the water depth and the countered shorelines specified in the bathymetry could be not accurate.

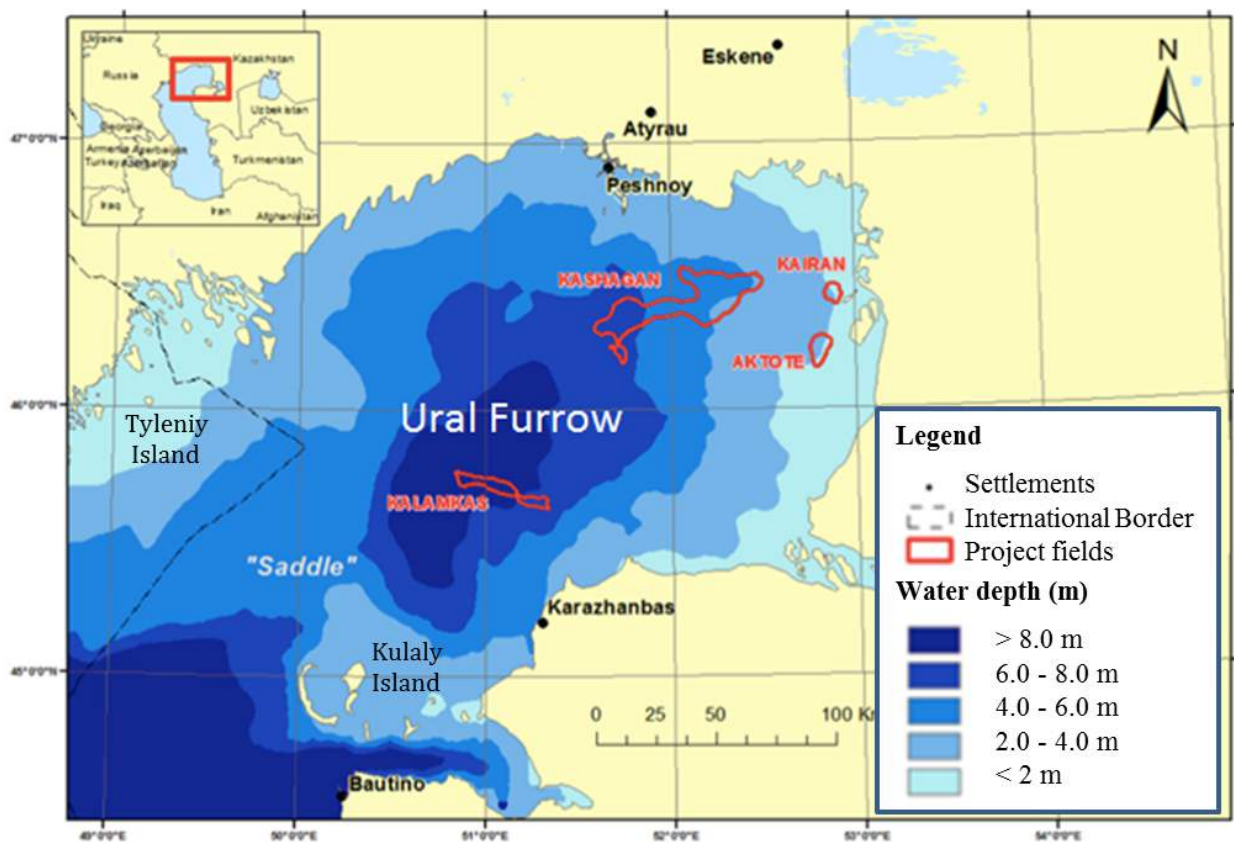


Figure 3.1: Bathymetry chart of the Northern Caspian Sea
(Based on Verlaan and Croasdale, 2011).

3.2 Air Temperature and Wind

The Caspian Sea is located in a zone of constant interactions between cold arctic and warm subtropical air masses. The main climatic feature of the sea is an air temperature difference between the northern and south parts of the Caspian Sea, which becomes significant only during winter seasons (Dobrovolskyi et al., 1982).

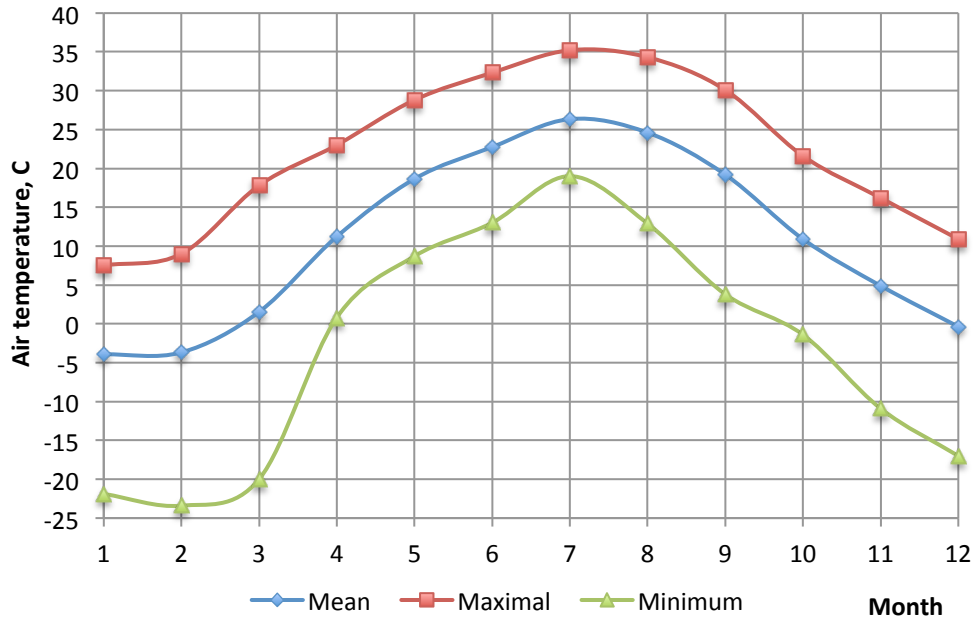


Figure 3.2: Monthly extreme and average daily air temperatures in Kulaly. The data derives from the period 1977-1985.

(Source: http://www.esimo.ru/atlas/Kasp/2_airtemp_station_97059_1.html, retrieved: 01/02/2015)

The number of days with temperature below 0°C is about 100 days in year. The average annual mean temperature for this part is 10°C, while the mean temperature in the coldest month, February, exceeds -4°C. The absolute registered minimum temperature was -38°C. (Terziev et al., 1992). This also correlates with air temperature measurements (fig.3.2) based on the observations from 1977 to 1985 at the Kulaly station.

Local air circulations are characterized by light winds with the general direction from the sea to shore. During spring-summer the SE wind prevails while the NW direction dominates in winter. However, the Northern Caspian Sea is featured by dust storms during summers. According to the observations from 1888-2006, the winds with speeds higher than 10 m/s (fig. 3.3) occur with about 14.9% frequency (Lebedev, 2014). The duration of 70% of the summer storms is less than 9 hours while the total number of days with the wind speed higher than 15 m/s is 40 days (Terziev et al., 1992).

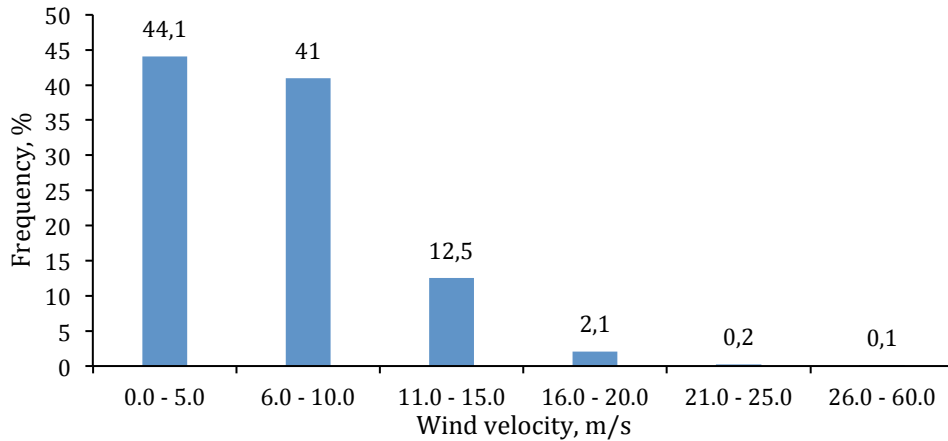


Figure 3.3: Frequency of the wind speed for the period 1888-2006.

(Source: http://www.esimo.ru/atlas/Kasp/3_windvelocity_waterarea_recurrence_0_13.html,
retrieved: 01/02/2015)

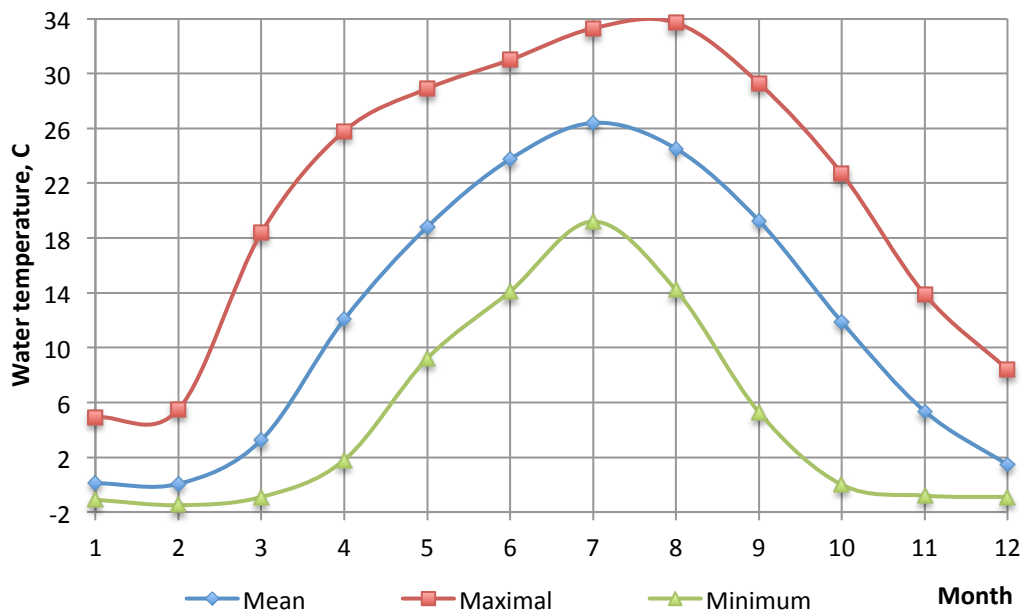


Figure 3.4: Monthly extreme minimum/maximal and average water temperatures at the Kulaly station. The data derives from the period 1977-1991.

(Source: http://www.esimo.ru/atlas/Kasp/2_watertemp_station_97059_1.html,
retrieved: 01/02/2015)

3.3 Water Temperature

The annual seawater temperature is equal to 0°C in winter and exceeds 25°C in summer. The coldest months are January and February with mean water temperatures of -1.1°C and -1.5°C, respectively (Dobrovolskyi et al., 1982). The annular mean water temperature is about

11°C while the absolute minimum water temperature was -1.9°C at the Tulenyi Island (Terziev et al., 1992). Fig. 3.4 presents the monthly extreme minimum/maximal and average water temperatures in the north of the Caspian Sea.

3.4 Water Salinity

In general, the Caspian Sea is a low saline water reservoir. The leading factors influencing on the Caspian salinity variations are (i) the Volga's runoff, which is one the most significant factors determining the water balance of the Caspian Sea, and (ii) water exchange with the Middle Caspian Sea.

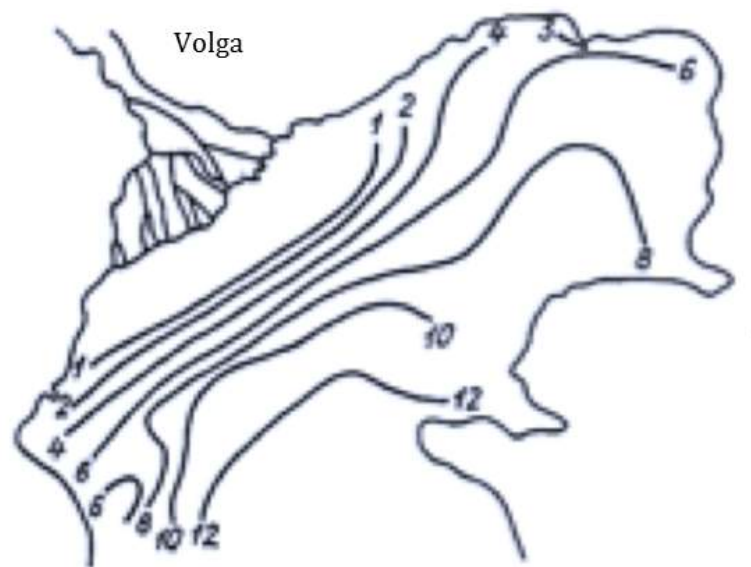


Figure 3.5: Salinity distribution (ppm) in April for the period 1940-1963 (Terziev et al., 1992).

The water salinity gradually increases from the delta of Volga to the middle part, i.e. in the direction of the propagation of the Volga's runoff (fig.3.5).

The seasonal changes of the water salinity are also controlled by the Volga runoff. Thus, annual variations of the water salinity have two seasonal peaks (fig.3.6). The first peak (in February) is explained by the fact that ice impedes spreading of the Volga runoff in winter, so this fresh river water drains to the Middle Caspian Sea. The second salinity increasing occurs when seawater of the Middle Caspian Sea enters and mixes with relatively fresh water of the northern part. In addition, the minimum salinity is observed in June, when the Volga river discharge is maximal.

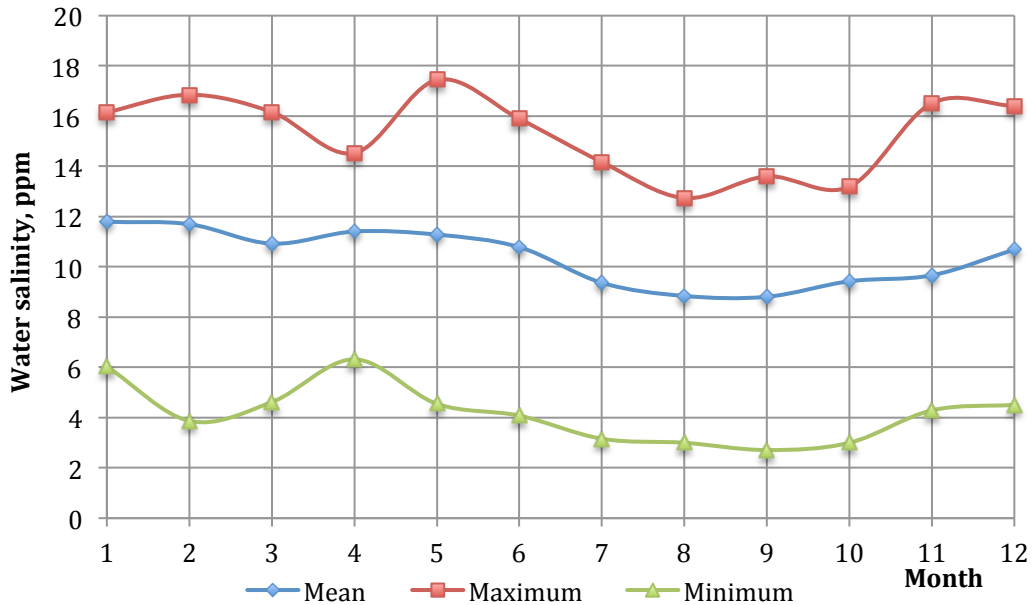


Figure 3.6: Monthly extreme minimum/maximal and average water salinity at Kulaly. The data derives from the period 1977-1991.

(Source: http://www.esimo.ru/atlas/Kasp/2_watersalinity_station_97059_1.html, retrieved: 01/02/2015)

3.5 Currents

Steady and wind driven currents of the northern part of the Caspian Sea are determined by (i) winds, (ii) the distribution of the seawater density in the sea and (iii) runoffs of Volga and Ural. The steady currents are regulated by the rivers' runoff and the difference in water densities between the northern and middle parts:

- The speed of the steady currents caused by the rivers discharge varies from 35 cm/s in summer to 150 cm/s in spring (when the rivers runoff are maximal) and these currents are observed in the deltas of Volga and Ural.
- The difference in water density of the northern and middle parts causes gradient currents. These currents generally occur in winter when the difference between water temperatures of the northern and the middle parts is maximal. The speed of the gradient currents is up to 20 cm/s.

One can notice that the wind driven currents dominate over steady ones. These currents are rapidly evolved (in 1-3 hours) and rapidly damped. The direction of these currents coincides with the wind directions (see Chapter 3.2). The maximal speeds of the wind driven currents during ice-free season are in the SW and NE directions because these wind directions have the

longest fetch. The speed of the wind driven currents can reach 30 cm/s. It worth mentioning that the currents direction can rapidly change due to the wind action (Terziev et al., 1992).

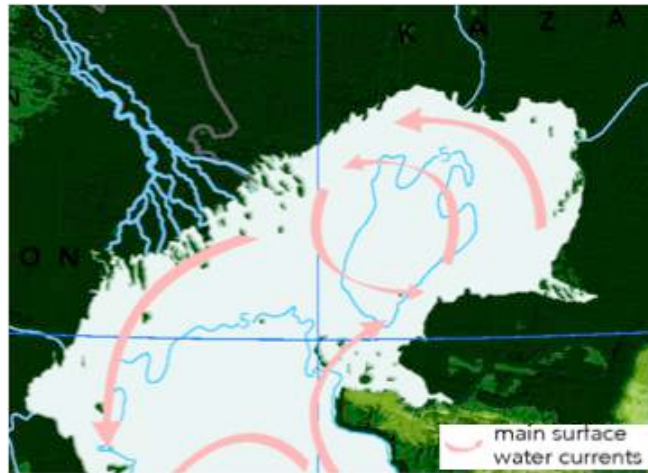


Figure 3.7: Main currents of the Caspian Sea (European Environment Agency, 2005).

All of these types of currents interact with each other so that the main current has a counter clockwise direction from north-to-south along the western shore (fig.3.7).

3.6 Waves

One of the distinct features of the Caspian wave regime is the presence of ice that controls the wave regime in winter and spring. The prevailing direction of waves is the same as the dominating wind directions – the SE and NW directions. The wave height, which depends on the fetch, decreases in the direction from the east to the north as the water depth becomes shallow. In summer the waves rarely reach 2-4 m due to the shallow water depth.

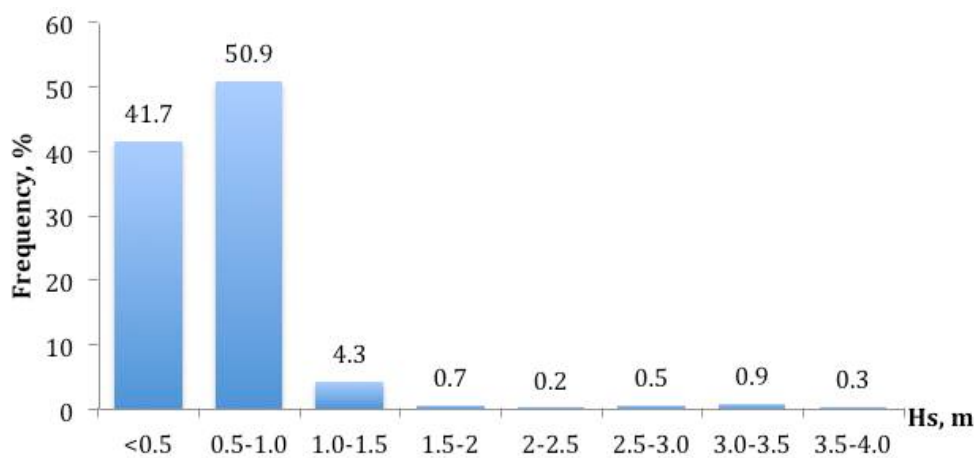


Figure 3.8: Distribution of the significant wave height in the Northern Caspian derived from salinity altimetry (October 1992- December 2005). According to Lebedev et al. (2006).

As reported by Lebedev et al. (2006) as much as 96,9% of waves has a height of 1.5 m, while the frequency of the waves with significant wave heights varying in the range 1.5-4.0 m is 2.6% during year (fig.3.8). The wave length reaches up to 85 m at the southern border of the Northern Caspian Sea (Shlyamin, 1954).



Figure 3.9: Significant and maximal wave heights for different return periods (Terziev et al., 1992):

- a) Significant wave height with $R_p=1$ year
- b) Significant wave height with $R_p=50$ year
- c) Maximal wave height with $R_p=1$ year
- d) Maximal wave height with $R_p=50$ year

According to Terziev et al. (1992) the 50-year extreme wave height (return period, $R_p = 50$ years) can exceed 7 m at the border with the Middle Caspian Sea. The significant wave height with the 50-year return period reaches 1.0 m in the north-eastern part while it is equal to 2.5 m at the border with the Middle Caspian Sea (fig.3.9).

3.7 Sea Level

The Caspian Sea is unique in that it is isolated from the world ocean and, therefore, its level is completely determined by changes in the water balance and by irregularity of the Volga runoff. Unfortunately, the Northern Caspian Sea is heavily exposed by these factors

due to its extreme shallowness. As a result short-term (seasonal) and long-term sea level fluctuations are observed.

3.7.1 Long-term sea level changes

The Caspian sea level significantly varies during its history (Gorelits, 1995). Only in the XX century two sea level changes with dramatic consequences were observed (fig.3.10):

- At the beginning of the XX century the level was relatively stable. Then it decreased by 3.0 m (1930-1977). This is considered as the lowest sea level for the past 400-500 years (Gorelits, 1995).
- For the past 30 years, the sea level has been increasing since 1978. Thus, the sea level increased by 2 m from 1978-1992 (Gorelits, 1995). The current sea level is -27 m regarding to the Baltic System (Karulin et al., 2002).

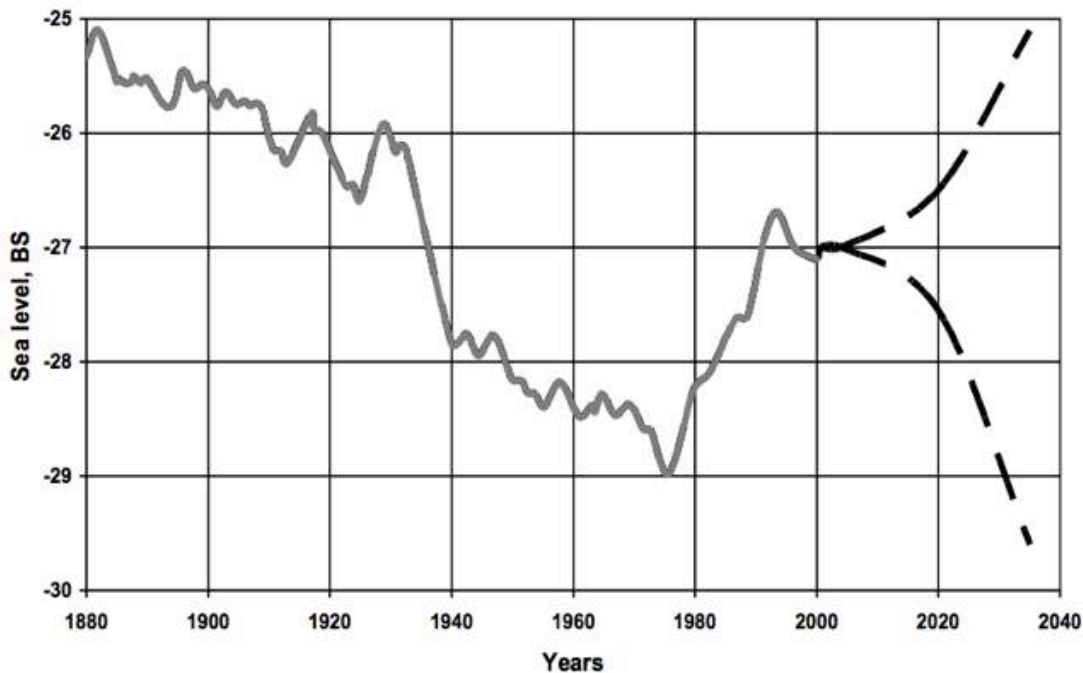


Figure 3.10: The Caspian Sea level variability over 1880-2005 and forecast up to 2035 (Karulin et al., 2002). Note that all values of the sea level are given in the Baltic System (BS).

Note that sea level fluctuations are caused by climate changes and an economic activity in the Volga drainage basin during the last 50 years (Gorelits, 1995). The main factors of the economical activities affecting the Volga river runoff include irrigation activities (including land reclamation), water supply for industrial and domestic purposes, construction of reservoirs. According to the report of Volga Ltd. (1992) the sea level without the human

activity would be 1.2-1.3 m above the current sea level and the decreasing could stop in the late 50s. The sea level rising, which has started in 1978, is a result of climatic changes caused by increasing precipitations and decreasing evaporation (Volga Ltd., 1992).

Several reports (Terziev et al., 2008, Imani et al., 2014, Polonskii et al., 2010, Lebedev, 2010, Volga Ltd., 1992) are dedicated to the forecasting problem of the multiyear sea level changes. However, today it might be concluded that sea level forecasts cannot provide either valid amplitudes or the direction of the sea level changes due to the complexity of the problem. Thus, the gap between these forecasts lies in the range from the sea level falling to -30 m by 2050 to its rising (to -26 m) by the mid of the XXI century (Volga Ltd., 1992).

One example is the design of the ice resistance platform for the Korchagin field development (the Russian zone of the Northern Caspian Sea) when two possible scenarios of sea level changes had to be considered:

- 1) increasing of the sea level will be 2.7 m regarding to the current position;
- 2) decreasing of the sea level will be 4.43 m regarding to the current position (fig.3.10).

However, Karulin et al. (2002) states that: “the normative documents or scientific publications failed to provide any proposals concerning summation of sea levels such as 100-year background sea level, 100-year high/low water and 100-year wave height.”

3.7.2 Short-term sea level changes

The short-term sea level fluctuations are caused by (i) seasonal changes of the water balance and (ii) storm winds. The seasonal changes are maximal in the period of June-July while the minimal sea level is observed in February. The amplitude of the short-term level variations is approximately equal to 35 cm (Terziev et al., 1992). This is clearly traced with observations at the Kulaly Island (fig.3.11).

The wind driven fluctuations occur across the sea so the shallow northern part is the most heavily exposed by this. The maximum surge level caused by the SE winds may rise up to 2.0-4.5 m and when the northern winds occur it can drop up to 1.0-2.5 m. The average duration of tides and ebbs in the most cases is 10-12 hours and, in rare cases, about two days (ESIMO, 2004). Furthermore, the wind-driven surges can shift the coastal line towards up to 10-15 km offshore and ebbs can shift the coastal line towards to 30 km inland (Sarybekova, 2004).

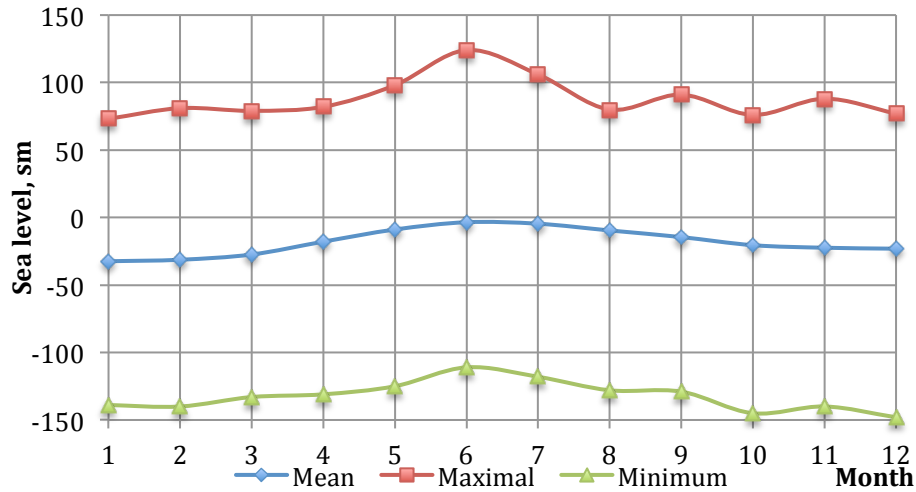


Figure 3.11: Monthly extreme minimum/maximal and average sea level at Kulaly. The data derives from the period 1977-1991.

(Source: http://www.esimo.ru/atlas/Kasp/2_waterlevel_station_97059_1.html, retrieved: 01/02/2015)

3.8 Ice Conditions

In contrast to the Middle and the Eastern parts, large areas of the Northern Caspian Sea are covered by ice in winter due to the shallow depth, harsh climate and low water salinity (see fig.3.12). On the other hand increased water exchange with the Middle Caspian, which is warmer, limits the ice development within this area. The presence of first-year ice is one of the futures of the Caspian Sea.



Figure 3.12: Satellite image of the North Caspian Sea taken by NASA’s Terra satellite, February, 2013 (MODIS, 2013)

In general, the ice formation begins in the shallow eastern part of the North Caspian Sea and then it develops to the west. The average duration of the ice season is up to 120 days (Kouraev et al., 2004). The ice season duration is determined by the type of winter (table 3.1). In severe winters ice can form in a very short period of time and cleaning of the sea takes place only in spring. In severe winters the ice cover reaches the warm northern part of the Middle Caspian, which is deeper as well.

Table 3.1. Ice periods for different types of winters (Terziev et al., 1992).

Type of winter	Beginning of ice formation	Clearing of the sea
Mild winter	mid of November	mid of March
Moderate winter	mid of November	early April
Severe winter	early November	mid of April

The main properties of sea ice have been described in Chapter 2. The following sections introduces three significantly different zones within the Caspian ice cover: landfast ice, drifting ice and shear zones.



Figure 3.13: Landfast ice zone (Terziev et al., 1992)

3.8.1 Landfast ice

About 70% of the sea surface is covered by ice during winters (again, see fig.3.12). Landfast fast ice forms quickly and it remains until February/mid of March. (Terziev et al., 1992).

The shallowness of the sea coupled with the harsh climate and the sea level fluctuations lead to interactions of ice with the seabed. The landfast ice zone normally extends to the 3-m depth areas (in severe winter – 7-10 m), but it is the most stable at water depths of 1-2 m (remains until spring). In addition, the extension of the landfast ice zone (see fig.3.13) reported by Terziev et al. (1992) is comparable with relevant satellite images shown in fig.3.15.

The ice thickness decreases in the direction to the Middle Caspian. The thickness of ice is maximal in January and exceeds 40-50 cm, but in severe winters ice thickness reaches up to 75 cm in the western part and 120 cm in the eastern ones (Kouraev et al., 2004, Terziev et al., 1992). At the same time the 100-return extreme ice thickness is equal to 96 cm (table 3.2).

Figure 3.14 presents ice thicknesses in different parts of the Northern Caspian Sea. One can notice that the ice conditions map presented by Kouraev et al. (2004) generally correlates with satellite images shown in figures 3.12 and 3.15. In this instance, according to satellite images of the Caspian Sea (fig.3.15) winter, 2015 could be classified as mild since the boundaries of the first zone in fig. 3.14 coincide to those specified in fig.3.14.



Figure 3.14: Ice condition of the Northern Caspian Sea: average duration of ice season, maximal ice thickness and boundaries of drifting ice in mild winter (1), in moderate winter (2) and severe winter (3). According to Kouraev et al. (2004).

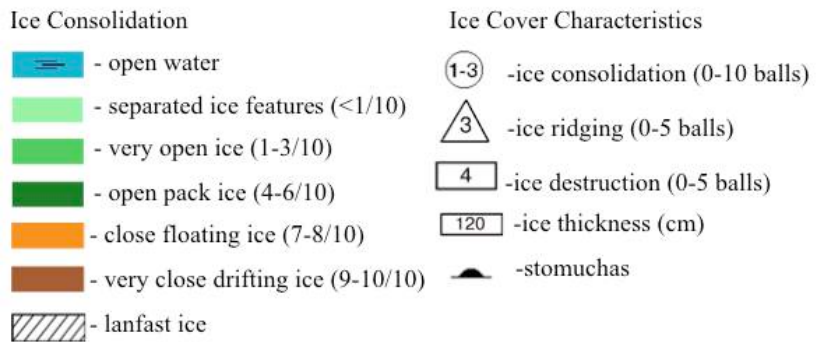
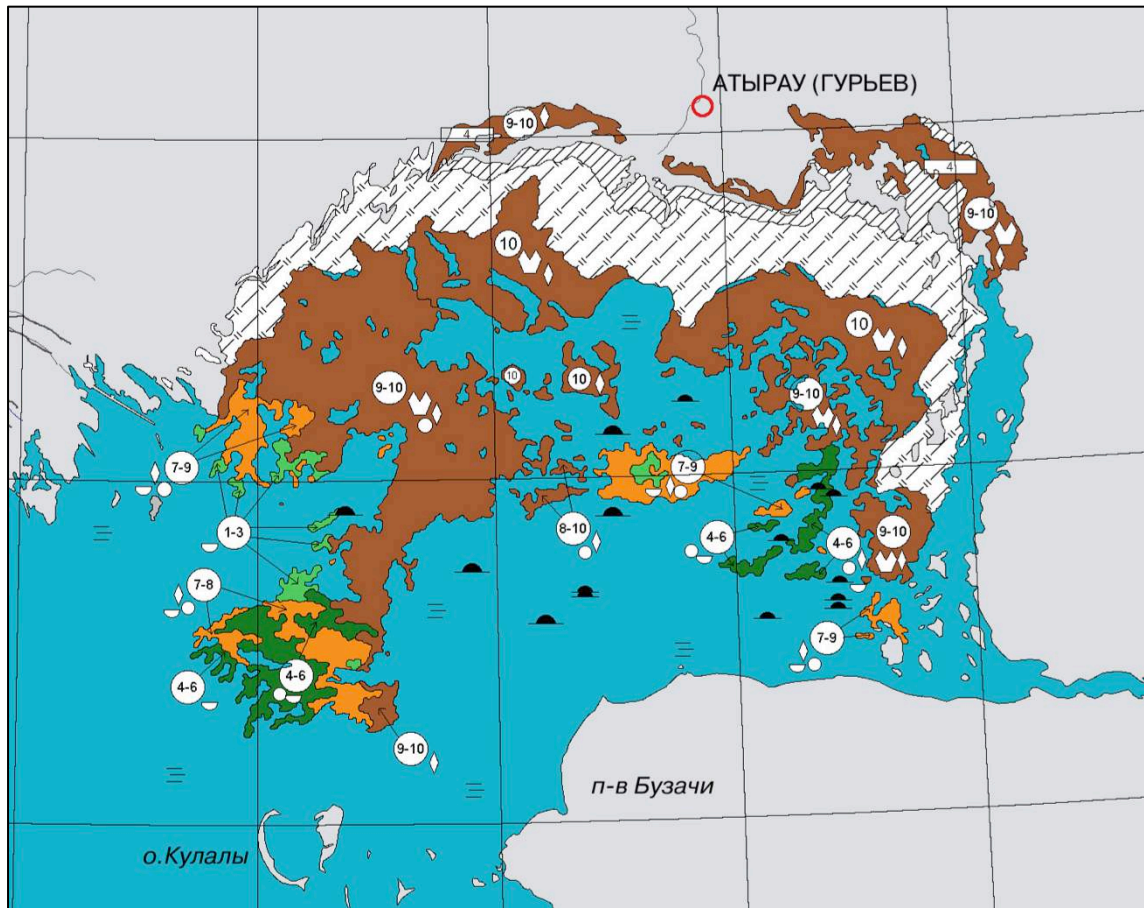


Figure 3.15: Chart-map of the Northern Caspian ice conditions based on the satellite images as for March 2015 (based on Planeta, 2015)

Table 3.2. The 100-return period ice thickness (Gürtner, 2005).

Parameter	Value
100-year ice thickness of:	
level ice	0.96 m
rafted ice	1.4 m

3.8.2 Drift Ice

The prevailing directions of ice drifts caused by winds are W and NW (fig.3.16). However, ice can come from any direction. The speed of ice drift is up to 0.5 m/s. In some parts of the sea the currents accelerate drift ice in addition to the winds (Verlaan and Croasdale, 2011). According to Terziev et al. (1992), the maximum average thickness of drift ice is up to 0.3 m. The boundaries of drift ice are shown in fig.3.14 for different types of winter.

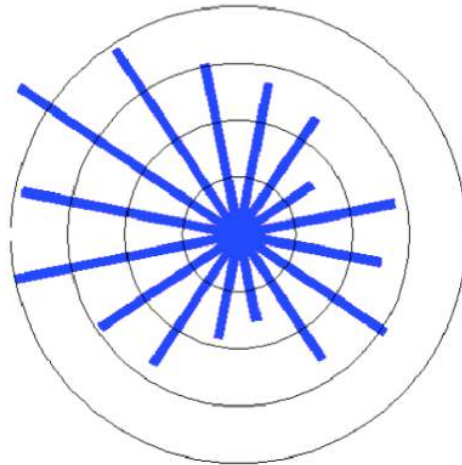


Figure 3.16: Rose plot of ice drift. Note that the directions are expressed “from”(Verlaan and Croasdale, 2011).

3.8.3 Shear Zone

Ridges, hummocks and stamuchas are formed in the shear zone, which is a zone of the most intensive interaction between the landfast and drifting ice fields. This zone can extend to kilometres. Strong winds lead to intensive ice deformation/rafting and to formation of hummocks and ridges.

3.8.4 Ridges and Stamuchas

In general, ridges intensity increases from the shore to the external landfast ice boundary, from the west to the east, and its intensity reducing begins from the shear zone. Moreover, ridges locate along the Ural furrow where water depth exceeds 8-9 m (fig.3.17, a). The maximum observed ridge height is 6 m, but normally sail heights vary in the range of 2-3 m. The ridge keel can exceed 12 m, while the average keel depth is up to 3-6 m.

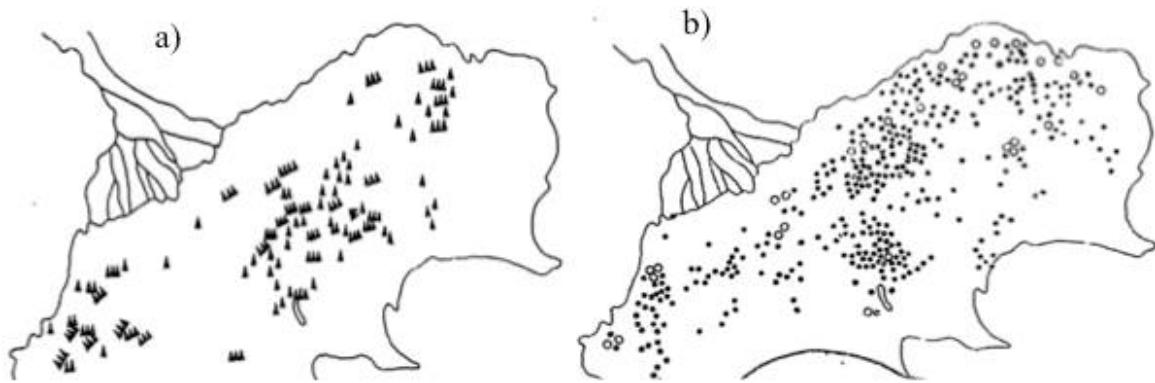


Figure 3.17: Location of ridges (a) and stomuchas (b) in moderate winters (Terziev et al., 1992).

In the Northern Caspian Sea stomuchas are also located along the Ural furrow at water depth of 2-5 m and might form a chain (fig.3.17, b). Being massive ice structures, grounded hummocks can reach a sail height of 10-12 m and a prevailing length of 100-300 m (up to 500 m). In moderate winters, the area with stomuchas is maximal in contrast to mild and severe winters (when the ice is more stable).

3.9 Summary

The chapter presents comprehensive description of the environmental conditions of the Northern Caspian Sea.

The data taken from the appropriate sources are compared with field measurements (including satellite images). The results obtained during the analysis of the Northern Caspian environment are used for the further study.

The next chapter somewhat summarizes all finding of this chapter in order to provide the harmony of the discussion.

Chapter 4. Challenges in the Northern Caspian Sea

The Northern Caspian Sea is treated as a region, which has similar conditions to the Arctic (Løset, 2014a). Along with great prospects of the fields, the Northern Caspian poses great challenges and risks. Namely, the following principal challenges associated with the development of the Northern Caspian Sea will be discussed in more detail below:

- Environmental sensitive area;
- Shallow water;
- Sea level fluctuations;
- Ice conditions;
- Ice Encroachment;
- Arctic codes;
- Evacuation of personnel in winter seasons;
- Undeveloped infrastructure;
- Logistical challenges.

Environmental sensitive area. A special status of the Northern Caspian Sea, which is specified as a nature preserve zone by the Kazakh government, strictly regulates all industrial activities and allows running only safe operations (Kuehnlein, 2002, Kaltayev et al., 2007). Thereby, the northern part of the sea is considered as a highly sensitive area and the environmental risks associated with the Caspian development are critical.

Furthermore, any serious accident could have dramatic ecological consequences and could result in tremendous social and political problems for the countries sharing the sea. Some

experts believe that the consequences of the oil spill caused by the Deepwater Horizon drilling rig explosion in the Gulf of Mexico in 2010 would be more disastrous in the conditions of the Caspian Sea. Note that more than 7,000 vessels and 47,000 people were involved in the Deep Horizons oil spill response activities (Ramseur, 2015) while in the Caspian Sea it would be extremely problematic to mobilize such amount of people and equipment due to the isolation/remoteness of the Caspian Sea. So only the Caspian emergency fleet would be there to cope with consequences of a similar accident.

It is worth mentioning that existing technologies for elimination of oil spills in the Arctic conditions are not sufficiently effective when oil spills especially occur in the presence of ice. An oil spill occurring in ice conditions is hard to be localized, collected, and dissolved because a thin layer of hydrocarbons can travel under the ice cover and contaminate large areas.

On the other hand special focus must be on the “zero discharge” policy that should be applied in order to achieve minimal impacts on the environment and a key issue for operating in this region is safety provision. Besides that this requires to minimize the emergency response.

Shallow water. The shallowness of the Northern Caspian Sea imposes restrictions to vessel draught and, therefore, limits the maximal deadweight of ships.

Furthermore, it is well known that “waves on shallow waters differ from waves at deep sea” (Zolotukhin, 2014b). This can be explained by the relationship of the water depth d to the wave length L , which is less than $1/20$ (i.e. $d/L < 1/20$) for shallow water conditions (Gudmestad, 2014). According to the environmental data described in Chapter 3.6 (the wave length is 85 m and the water depth corresponding to the deepest point in the sea is about 9 m) the North Caspian Sea can be really considered as shallow because this condition is met. This phenomenon could lead to the amplification of hydrodynamic loads due to the wave action or surges and might enhance erosion processes.

Sea level fluctuations. Another principal issue is sea level changes coupled with the extreme shallowness of the North Caspian Sea. As discussed in Chapter 3.7, the Northern Caspian Sea is featured by significant short-term sea level changes caused by the strong southern winds that can rapidly decrease the sea level up to 2.5 m and increase it up to 2-4.5 m.

On the other hand, the long-term sea level changes coupled with the wind driven sea level fluctuations lead to considerable shoreline shifts (Sarybekova, 2004). Thus, according to the Volga Ltd. report (1992) a possible flooding caused by rising of the Caspian sea level to -25 m (BS) would lead to flooding of 53 cities with population of 58,000 people, 61 rural towns with population of 41,600 people, 384.5 km of roads/energy communication installations, etc.

In addition to the social-economic consequences, the water depth and the countered shorelines specified in the bathymetry could be not accurate. That might be more challenging for planning of long-term operations (as production) rather for short-term ones (such as exploration drilling).

The uncertainties associated with sea level changes should be carefully analysed before the project execution. For instance, the caisson platform for the Korchagin field development (the Russian sector of the Caspian Sea) had to be designed for two different scenarios of long-term sea level changes and the amplitude of these fluctuations was taken 7.13 m (Karulin et al., 2007). It worth mentioning that the sea level changes should be constantly monitored in order to predict hazardous events and to avoid dangerous consequences associated with this phenomenon.

Ice conditions. A combination of shallow water, low water salinity with harsh weather conditions during winters lead to freezing of the Northern Caspian Sea, at least, for five months per year. As mentioned in Chapter 3.8, the 100-year thickness of level ice is assumed to be 0.96 m and the 100-year return period for rafted ice features is estimated to be 1.4 m. This causes significant ice loads acting on offshore structures and imposes operational limitations. On the other hand, the presence of ridges and shallow water depth imply another threat associated with plugging of the seabed (Zolotukhin, 2014b) so all pipelines, cables, flowlines between offshore structures should be designed with focus on it.

Finally, another issues related to the Caspian ice conditions are discussed below.

Ice Encroachment. Ice Encroachment is the term describing the phenomena when ice moves onto the surface of a structure. Traditionally, there are two ice encroachment types, namely, ice over-ride and ice pile-up.

Ice over-ride presented in Fig. 4.1 is a rare event, which could occur when continuous ice exerts on a wide structure with low freeboard and gentle slopes (Palmer and Croasdale, 2012). One example is an ice over-ride accident occurred in the North Caspian Sea when the 0.5-meter ice climbed over the freeboard across the island perimeter in a few minutes (see Fig.

4.2). Fortunately, it stopped without any damaged of the equipment and didn't cause further events associated with the ice over-ride. It is obvious that such ice over-ride might lead to severe consequences when potentially dangerous equipment is involved.

There are several design methods, which might be applied for the design of both an artificial island and a gravity based structure, including high freeboard, rough surfaces, a special geometry of a structure and the utilization of external ice barriers. Thus, steep slopes are favourable for ice pile-up rather than for ice over-ride. This phenomenon will be discussed in detail in the following chapters.

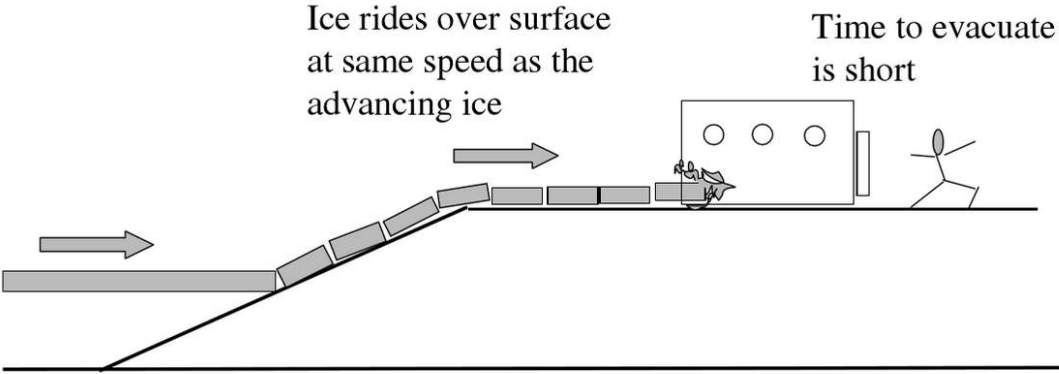


Figure 4.1: Ice ride-up on low freeboard structure (after Palmer and Croasdale, 2012).



Figure 4.2: Ice encroachment in the Caspian Sea (McKenna et al., 2011).

Arctic codes. Growing interest in development of the Arctic fields motivates a strong demand for specialized codes. Ghoneim (2011), Bruun et al. (2006), Løset et al. (2006) report that the results of ice load calculations considerably vary with the different code formulations (e.g. American API RP-2N (1995), European ISO 19906 (2010), Canadian CAN/CSA, Russian SNIP 2.01.07-85, SNIP 2.06.01-86, etc.).

In addition to the gap between these codes, there are still considerable uncertainties related to the calculation of ice actions in shallow water due to the effect of ice rubble grounded around the structures. The point is that the rubble accumulation intensified in the shallow water conditions will influence on the interaction between ice and a structure. Also, grounded ice rubble might partially dissipate the ice load into the environment. Palmer and Croasdale (2012) state that this phenomenon is not completely covered by ISO 19906 (2010) because the ice load on sloping structures calculated by the code is not correct.

An engineer should be aware of this issue while appropriate codes should be developed in order to provide a comprehensive guidance.

Evacuation of personnel in winter seasons. The hydrocarbon development always involves a possibility of an emergency situation that will require an effective evacuation of personnel. Poplin et al. (2013) states that “an ideal evacuation system for ice covered waters allows personnel to abandon the facility in response to an emergency under any ice or open water sea condition and proceed a safe distance from the disabled facility to await rescue”.

One can notice landfast ice and accumulated ice rubbles can surround offshore structures and this might complicate a fast evacuation. Conventional lifeboats used for emergency evacuations in ice-free offshore regions are not applicable due to the shallowness of the sea and the ice cover. However, the helicopter evacuation might require relatively long mobilization time. Moreover, sometimes the access to a landing area might be complicated and associated with additional risks. Note that this type of transport heavily depends on the weather conditions. One example is an accident that occurred in 13-15 December 2012, when the air transportation was totally blocked due to the storm. As a result two islands were totally isolated (Shahnazaryan, 2012).

According to the Barents-2020 program report (2012), all evacuation options that are available today for the Arctic evacuation can be divided in two groups:

- Concepts already used on the Arctic projects, e.g. special amphibious vehicles and icebreaker emergency evacuation vessels (IBEEV).

- New concepts adapted for the Arctic conditions, e.g. «Boat-In-A-Box» system, hovercraft, ships with Archimedean screws AST/TIT800, sea rescue vessel, hermetically sealed Arctic rescue capsule (TEMPASC), ice-resistant lifeboat (ISL), polar enclosed lifeboats, container landing "Ganymede".

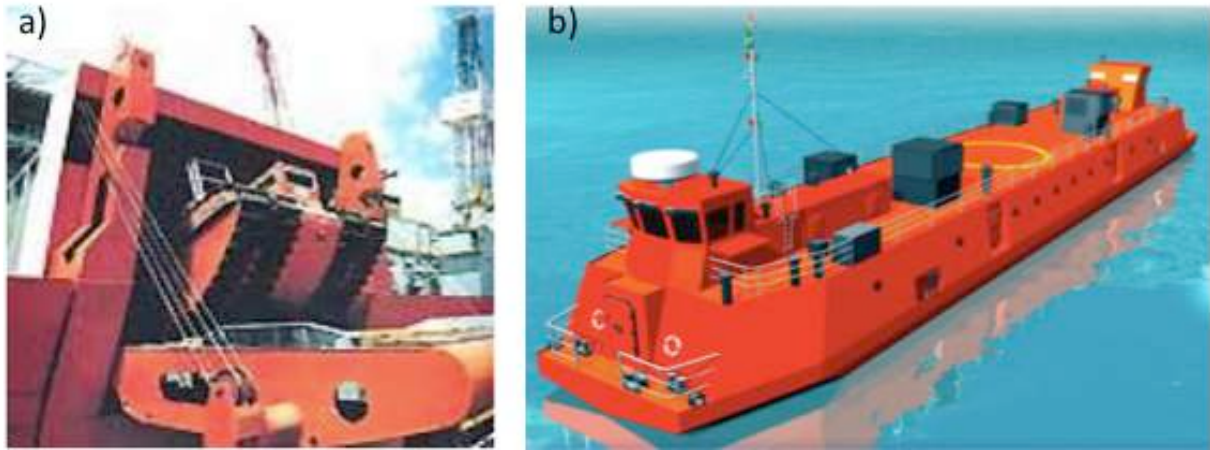


Figure 4.3: a) The Arctos special amphibious vehicles (Juurmaa and Wilkman, 2002) and b) Ice breaker emergency evacuation vessels (Remontowa Company, 2006).

It worth mentioning that only solutions from the first group have been already applied for the Kashagan field while other ones are under development. Thus, NCOC selected the utilization of special vehicles (fig.4.3), Arctos, which were deployed on the Sunkar barge and on the North Star Island (Beaufort Sea). It is an amphibian vehicle with combined chain drive on ice and water propulsion for ice-free conditions. However, this option has several drawbacks:

- Due to problems related to the ice bearing capacity the Arctos vehicle could capsize when ice is not stable,
- These vehicles have serious problems associated with their deployment, because massive ice rubbles accumulated around the structure might block it.

Several icebreaker evacuation vessels (DNV ICE-1B class) are currently applied for emergency evacuation from the artificial island 'D', where the field processing is carried out. The vessels (fig. 4.3), which draft is 2.1 m, can be safely operated in shallow water and in ice with maximal thickness of 0.6 m. Because of extreme shallowness of the operating area, the IBEEV cannot operate as a normal icebreaker so the nose of the IBEEV crushes ice in front of the ship while powerful engines allow the vessel to move through the ice. The technical design of these vessels, which are capable to evacuate up to 340 persons at time, includes

autonomous systems of life support within toxic environment, so the passengers breathe through autonomous air supply devices, and evacuation from the island is carried out through a special tunnel (Remontowa Company, 2006).

However, there might be several issues related to the evacuation by the IBEEV icebreakers:

- The further development of the Kashagan field will require a large amount of such vessels and that will lead to additional challenge for the project budget.
- Although these vessels are designed to break up 0.6-m ice, this is probably not sufficient because the value of the 100-year ice thickness is 0.9 m while the thickness of ridge formations reaches 1.4 m (chapter 3.8).



Figure 4.4: The Picture of D Island (Kashagan) wherein an ice wake can be observed behind the structure (Topaz Energy and Marine, 2015)

Even though no 100%-reliable evacuation methods in the Arctic exist, some measures could be implemented to reduce risks for personnel in case if a hazardous event(s) occurs:

- Keep evacuation water routes and the space required for vessel deployment free from ice rubbles. Another method to increase efficiency of the evacuation process is to take advantage of an ice free leeward area (called wake, see fig.4.4) formed behind a structure toward the direction of the ice movement, which might be used for the deployment of evacuation vessels (this is especially important for the Arctos vessels).

- Proactive HSE management, i.e. all employers should be trained how to behave if major emergency arises and etc.
- Another proactive measure that might reduce risks for personnel during evacuation is decreasing the number of personnel on the dangerous/remote or complicated for evacuation locations.

Undeveloped infrastructure. This challenge includes a poor developed transport system, a lack of electric and water supply. Shipbuilding and construction industries are limited and all important processing facilities/icebreaking vessels should be imported from another places.

In addition to the undeveloped infrastructure of the region, there are some requirements related to the governmental policy of the Kazakh content. According to it the Kazakh content of various components should be maximized and if an operator company ignores the law about the Kazakh content, it might be subjected to an administrative punishment (Sultanov, 2010).

Logistical challenges. The remoteness of the Caspian Sea from industrial centres coupled with the undeveloped infrastructure of the region is another factor that should be taken into account for the Northern Caspian projects. The region can be only supplied by the Volga Don Canal and Baltic Sea-Volga waterways (fig.4.5), which are navigable for six months due to the ice presence in winter.



Figure 4.5: the Volga Don Canal and Baltic Sea-Volga waterways (NCOC, 2011).

Moreover, the shallowness of the Volga transport system, as well as considerable constrains of bridges crossing the canals, limits the maximal weight/dimensions of the cargo that can be transported to the Caspian Sea via these routes. Hence, a large part of equipment fabricated in Europe or Asia cannot be transported to this location. All of these factors lead to increasing of transportation costs and complicate the project execution.

On the other hand winter supply (including requirements for regular supplies of materials and transfer of personnel to the location) is a crucial issue due to the presence of ice features. In severe winters navigation in the Northern Caspian is complicated, so icebreaker vessels should be used to support supply operations in ice seasons. Currently only one supply base located in Bautino exists but more supply bases should be developed in the future when more fields are explored. It also worth mentioning that a fleet of supply vessels has to be constructed from scratch.

In conclusion, these challenges encountered in the Northern Caspian Sea are not usually met in such combination in another regions. For instance, the shallowness of the sea is itself an issue challenging ship navigation, transportation, as well as installations of heavy structures. Moreover, shallow water depth combined with the ice conditions complicates winter supply and running of marine operations due to the conditions favourable for ice accretion. This makes the already complex problem of the emergency evacuation in winter even more complex. Not to mention the uncertainties related to the forecast of the sea level changes and the gap between the Arctic codes.

Therefore, each of these issues (together with harsh climate, wave and wind conditions) has to be adequately considered and managed before the realization of any project in the Northern Caspian Sea. In addition, the ice conditions should be carefully considered during design of structures, winterization, selection of appropriate materials, etc. In addition to the environmental conditions, such field characteristics as large reservoir extension, high H₂S content in the reservoir fluids affect the selection of the field development concept. This should be achieved in terms of high HSE standards that will provide environment, life and assets safety.

Chapter 5. Development Concepts for the Northern Caspian Sea

When the economical profitability of the field development has been proved, planning of production and the selection of an appropriate development concept begin. As demonstrated the Kazakh sector of the North Caspian Sea is a promising area, where many prospects including the giant Kashagan field have been explored. Therefore, an appropriate development concept should be selected in order to provide safe and effective development of oil and gas fields in the future.

A development concept includes a set of engineering solutions with respect to:

- Drilling system;
- Production system or a type of an appreciate offshore structure;
- Process system;
- Transportation system of hydrocarbons.

The development concept should take into consideration all challenges discussed in the previous chapter. Note that after starting of the project it is very challenging to change the development concept, while costs of any changes might dramatically increase the project budget and additional environmental risks might be involved as well. So the concept should be selected adequately and it should allow safe year-round drilling and execution of all required operations under the Caspian conditions. However, not every drilling system or type of a production structure can be utilized in the Northern Caspian Sea.

The coming chapter is dedicated to the discussion of suitable solutions in light of hydrocarbon field characteristics to develop a robust and optimal field development concept for the Northern Caspian Sea.

5.1 Production drilling systems

In contrast to the exploration stage, a drilling unit should withstand waves and ice loads (even in severe winters when the worst case occurs) but, on the other hand, it has to be mobile in order to allow extensive development of large areas and to keep the development progress. It should be mentioned that an alternative to the production drilling options providing year-round operability might be drilling during ice-free seasons, but the final decision to utilize either non ice resistant units or units for year-round drilling should be based on the economic/engineering analysis and requirements for the management of the project schedule.

On basis of the environmental conditions of the Northern Caspian Sea discussed in the previous chapters, the most optimal options for production drilling selected among traditional ones are listed below:

- Ice island,
- Drilling barge,
- Jack-up rig protected by ice barriers,
- Drilling rig installed on the production structure.

One can notice that drilling ships and semisubmersible platforms were not taken into account due to the sea conditions discussed above. The construction of artificial islands, as well as the utilization of grounded semisubmersible drilling platforms, only for drilling purposes will not meet the described above requirements and/or will lead to unnecessary increasing of the budget of a project.

This section is concerned with the discussion, on a technical feasible level, of these options in lights of the principles stated above.

5.1.1 Ice islands

After the analysis of the Beaufort Sea drilling experience, where ice islands were used in the end of 1990's, the possibility of applying of this type of islands was examined.

An ice island could be built by spraying of seawater or by using of an existing massive ice feature. Once a drilling rig and well control equipment are installed on the ice island, drilling can be carried out until melting of the ice island.

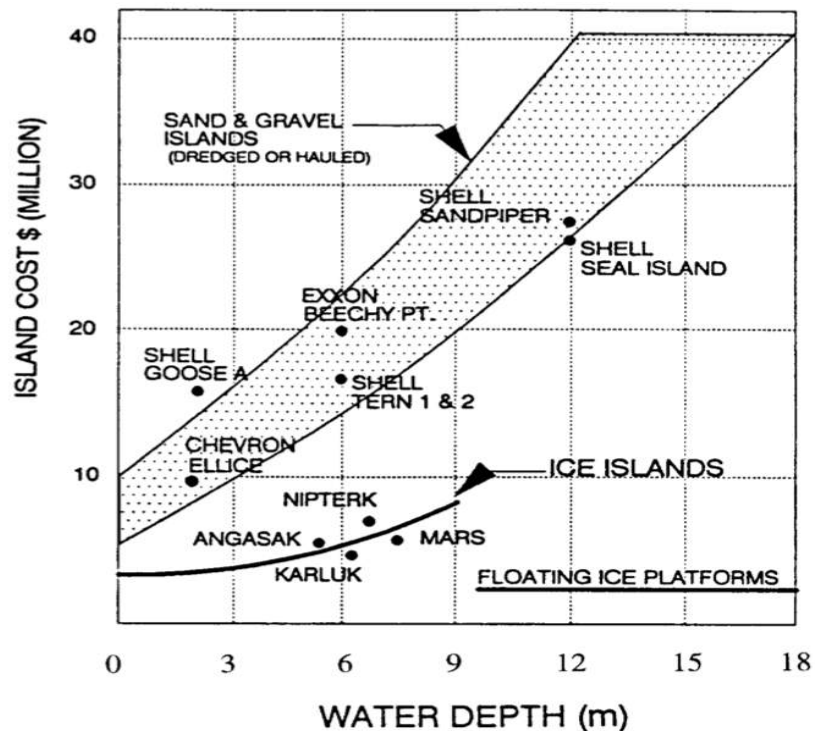


Figure 5.1: Island costs vs. water depth in the Beaufort Sea (Løset, 2014).

The basic idea of this drilling option is to take advantage of the combination of shallow water and low construction costs of such islands. The construction cost of an ice island is from $\frac{1}{4}$ to $\frac{1}{2}$ of the cost of gravel ones (fig.5.1) and they are more environmentally friendly than gravel islands (Brinker, 1980, Matskevitch, 2007).

Brinker (1980) specifies the following conditions required for safe application of grounded ice islands:

- The geographic area is very cold,
- Water depth is relatively shallow,
- Ice movement is small,
- Project can be completed before the ice breakup.

However, all required criteria somewhat meet in the Northern Caspian Sea except the last one related to the ice island operability time. The analysis of the realized projects shows that the construction time of grounded ice islands (Karluk, Imperial's Nipterk P-32), which were built at water depth of 7-8 m, varied in the range of 53-72 days (Brinker, 1980, Matskevitch,

2007). Taking into account the Caspian ice conditions, the time available after the island construction could be not sufficient to run a safe drilling operation, especially, if we deal with such complex reservoirs as Kashagan.

Generally, ice islands are recognized as an alternative for exploration drilling while production drilling from similar structures is considered as not practicable (Matskevitch, 2007). However, such structures could be applied for temporary operations and this mainly depends on the time required for a particular operation.

5.1.2 Drilling barge

Another option for production drilling in the Northern Caspian Sea is the utilization of a drilling barge. It is a big floating structure that is often employed in shallow waters (lakes, delta of a river, inner waters). The drilling barges provide insufficient characteristics for the wave conditions of the open sea. Since this option doesn't allow drilling in open sea conditions without implementing a bottom foundation, they should be ballasted on a prebuilt berm before drilling (Gudmestad et al., 2010).

Currently, two drilling barges, Sunkar and Caspian Explorer, are available in the North Caspian Sea. These barges were designed to allow year-round drilling in the Caspian conditions. The Sunkar barge, previously a swamp barge, was modified in order to improve its ice resistance and was equipped with ice deflectors installed on the sidewalls.

However, the main issue associated with the implementation of drilling barges in the Northern Caspian Sea is their insufficient characteristics to withstand ice and open sea actions (Granneman et al., 2001).

The most feasible options that might be used to avoid these challenges will be discussed below.

5.1.2.1 Barge foundation options

Since drilling barges show poor characteristics in open sea, the structures that would provide the required foundation stiffness of drilling barges should be utilized. There are two options that include the construction of either gravel or steel berms as the barge foundation.

A *gravel berm* is a man-made underwater island (ISO 19906, 2010) designed to resist the barge from the wave and ice actions. This type of foundation was selected by NCOC for drilling at Kashagan. The volume of berms used as a foundation for the Sunkar barge exceeded 44,000 t and the construction of the berms took 6 months (Granneman et al., 2001).

A schematic drawing of the barge counter ballasted on the gravel berm is presented in fig.5.2. The proper selection of a sloping angle of a berm can provide supplementary ice resistance of the entire system and can suppress ice over-ride discussed in Chapter 4.

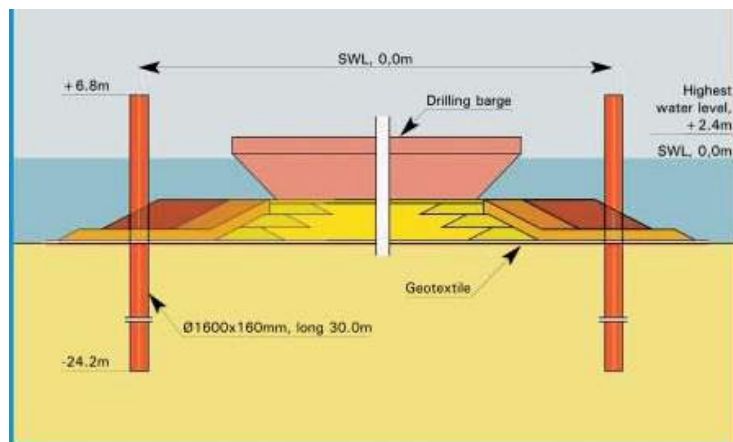


Figure 5.2: Gravity berm for the Sunkar barge (Granneman et al., 2001).

However, Granneman et al. (2001) report that the main issues related to the berm constriction in the Northern Caspian Sea are poor quality of the rock and logistic. Since such berms are constructed during ice-free seasons, the erosion process should be taken into account. It worth mentioning that construction of gravel berms contaminates the environment.

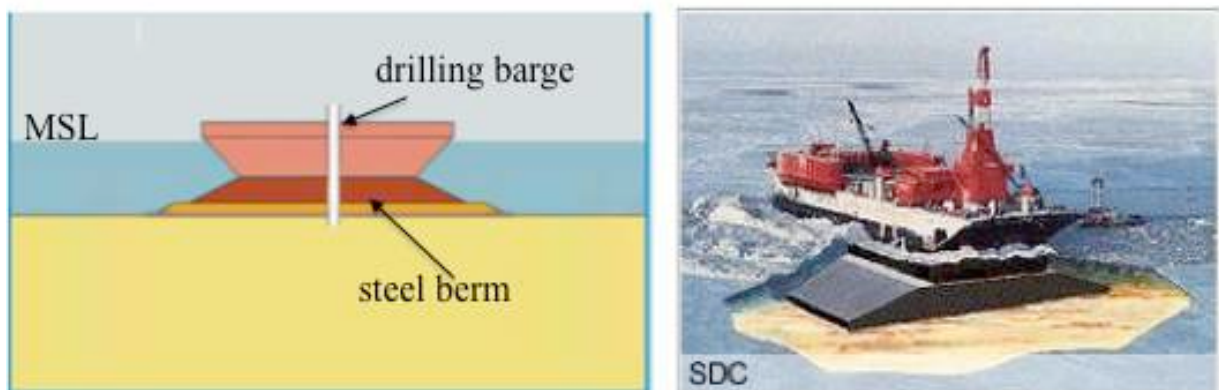


Figure 5.3: a) Steel berm foundation that can be used as a barge foundation (based on picture from Granneman et al., 2001) and b) existed example of the steel berm for the SDC drilling platform (Rigzone, 2015).

Another option is a *steel berm* that allows avoiding the drawbacks of a gravel foundation. Similar structure was successfully used for drilling in the Beaufort Sea. A steel berm can be

easily implemented for the drilling barges like Sunkar or Caspian Explorer. The concept of steel berms is presented in fig. 5.3. List advantages of this option:

- It optimizes the time required for the barge deployment;
- No problems related to the foundation erosion and gravel sticking to the bottom of the barge;
- A steel foundation can be used as a storage tank for drilling mud which is important especially when winter supply is complicated;
- A steel berm can be re-used;
- Utilization of a steel berm can significantly reduce the environmental contamination due to the construction of a gravel berm and, moreover, it can be easily abandoned.

However, the construction of a steel berm requires larger capital expenditures, but it might be more cost effective for the long-term utilization than the construction of a gravel berm each time before the barge deployment.

5.1.2.2 Ice protection barriers for the drilling barge

Additional modifying of the barge similar to the Sunkar barge modification is not sufficient to provide the total ice protection of the drilling barge against the ice action. Hence, special external structures taking ice loads should be used for these purposes.

There are several options that could be utilized for the ice protection in the Northern Caspian Sea and they will be discussed in detail in Chapter 5.3.

5.1.3 Jack-up protected by ice protection barriers

A jack-up drilling rig is a mobile drilling unit consisting a buoyant hull and long legs, which is used to raise the rig over the sea level. Traditionally, jack-up systems can't be used for the conditions, where ice exists, because its legs are not designed to withstand significant ice loads. According to Weihrauch et al. (2005) a formation of ice rubbles between the legs of the jack-up is critical because this leads to significant loads on its legs. Thereby, a conventional jack-up must be protected from formation of ice rubbles adjacent to the structure in the ice conditions.

There are several solutions based on an idea of using special external structures to in order to provide total ice protection:

- a concept of an ice protection system presented in fig.5.4,

- a concept with using of protection barriers (of different shapes) arranged so that they will form an inside area fully protected from the ice action.

These options are very attractive because of the high mobility of a jack-up connected with one of these structures (steel caisson or ice barriers). Such systems could be re-used and relocate during ice-free season. Furthermore, the drilling process could be carried out without the construction of an ice resistant drilling platform, which might be expensive. In addition to the technical aspects, a jack up protected by such protection systems has minimal environmental impact.

However, the implementation of only steel caisson might not provide the total ice protection because the steel caisson presented in fig.5.4 has vertical walls and, hence, high ice loads should be expected. Moreover, this structure is needed in additional fixation/protection because under the ice loads it can slide along the seabed and this can lead to damages of the legs.

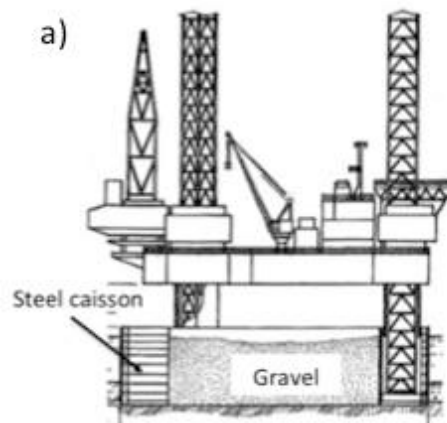


Figure 5.4: Concept of a jack-up with ice protection system (Dudik E., 2009)

The other way to provide the required ice tolerance is to deploy ice protection structures, i.e. ice barriers. Possible configurations of such ice barriers will be discussed in Chapter 5.3.

5.1.4 Platform drilling rigs

Drilling from production structures could be used both for drilling and for well service operations. Drilling rig might be installed stationary and then replaced by well servicing equipment when drilling operations have been completed. The total amount of wells drilled from a production structure is usually up to 40-50 (Gudmestad et al., 2010).

Drilling rigs installed on the production offshore structures could be implemented on a par with mobile drilling rigs to satisfy the drilling progress.

5.2 Production system

The production system is one of the main parts of the field development and it must be designed for safe operation during the whole field life.

The development scenario is mainly determined by such reservoir characteristics as its properties, extension, recoverable resources, etc. The development plan also regulates the number of offshore structures, their configuration required to develop the field recourses. Offshore production structures accommodate not only all production/drilling equipment, but also personnel. Hence, as well as drilling systems, the production structures should guarantee safe year-round production even under extreme wave and ice loads. At the same time, the chosen concept should provide the most optimal economical solution. The number of offshore structures required for the field development should be minimized. It should be noted that the chosen concept should consider development options for satellite/small fields, which might be discovered in the future.

An engineer has mainly two alternative concepts for such shallow water conditions:

- to construct a structure, which could withstand even the maximal environmental loads, or
- to construct a semi ice tolerant structure protected by special ice protection structures that will take the main ice action (Croasdale et al., 2011).

The first concept includes a “stand alone” platform while the second one implies a semi ice tolerant platform. The main types of production platforms as well as factors affecting the selection of the development concept will be identified in this section.

5.2.1 Technical solutions

The selection of a suitable platform type is controlled by different requirements including operational and engineering aspects. Thus, operational aspects relate to the work area required for the installation of drilling/production/processing units, a number of wells, the supply concept, evacuation requirements, while the engineering factors are governed by water depth, wave and ice actions, soil conditions, construction needs, etc.

The environmental conditions in the Northern Caspian Sea favour to only limited options that could be integrated into these concepts. Primary, the analysis of the water depth and ice conditions of the region indicates a fairly beneficial environment for islands and platform developments rather than for subsea development, because floating systems are not realistic

due to the draught limitation and capacity of mooring (or dynamic positioning) systems, which cannot effectively withstand ice loading.

The following section discusses only the options regarded as the most feasible based on ISO 19906 (2010) and the experience of the Beaufort Sea development, which is given in accordance with Hewitt (2014) and Matskevitch (2007).

5.2.1.1 Artificial Islands

According to Bailey (2009) artificial islands that have been successfully implemented in the Beaufort Sea for over 40 years are one of the most effective solutions for the Arctic shallow waters.

Although there are five types of the man-made islands only some of them can be applied for the given conditions. The main criteria of their applicability in light of economical feasibility are the availability of a suitable construction material, water depth and the construction season limitations (Hewitt, 2014).



Figure 5.5: Sheet pile island built at the Kashagan field (Nymo, 2010).

Thus, *sacrificial beach islands* are usually built when a large borrow source of ‘clean’ sand is located near the location. However, the utilization of this type of man-made islands as an offshore structure in this region could lead to supplementary challenges due to the poor quality of the rock in the Caspian Sea (Granneman et al., 2001). Additionally, such structures

are significantly affected by wave actions. *Slope protected islands* require costly armor units to protect the island's fill while these units cannot provide full ice protection. Hence, sheet piled and caisson retained islands could be identified as the most suitable options among others.

A *sheet pile island* (fig.5.5) is an island, which is retained by sheetpiles (regular, cofferdam or cellular sheetpiles) to protect the island fill from the wave action. A sheet pile island is essentially a vertical structure so there are no sloping walls within the structure to reduce ice loads. A key consideration for the design of such islands is local ice action and the integrity of the sheetpile assembly during the whole design life.

Note that this type of islands should be adapted for the Caspian conditions in light of the ice encroachment protection (see Chapter 4). Since the construction of an island with steep slopes or high freeboard protecting from ice over-ride might be challenging from an economical point of view, so the islands might have a special shape design to avoid these potentially hazardous accidents. This includes some protection area without any equipment since this perimeter will be subjected to the ice encroachment as shown in fig.5.6 (McKenna et al., 2011, Palmer and Croasdale, 2012, ISO 19906, 2010). However, the ice protection barriers might partially hade off risks associated with ice over-ride.

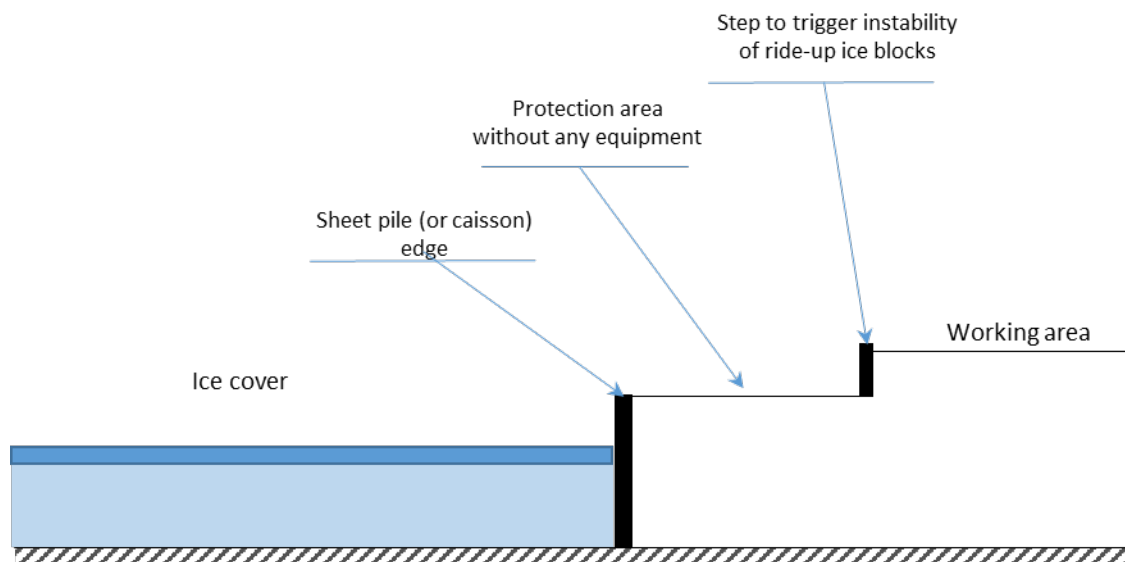


Figure 5.6: Special shape of a sheet piled island to avoid ice over-ride (not to scale, according to Palmer and Caroadale, 2012).

The relevant experience has proved that these structures could not be used as a fully ice resistant ('stand alone') platform in the conditions of the North Caspian Sea. However, a sheet

pile island is a possible option for a semi tolerant platform with the ice protection provided by external structures.

It should be also noted that the volume of the fill material would exponentially increase with increasing water depth, so at deeper locations the construction might take several seasons with all consequences appearing due to this.

Since island construction activities will be more sensitive to wave actions in deeper waters, the second option includes a *conventional caisson-retained island* (CRI). Caisson-retained islands are similar to sheet pile islands discussed above but they are retained by pre-built caissons (steel or concrete) so that they form a retaining ring filled with the fill material (fig.5.7). This island type has been successfully implemented in such projects in the Beaufort Sea as: Kaduluk O-07 (water depth is 13.6 m), Kaubvik I-43 (17.9 m), Tarsiut (22 m), Amerk O-09 (26 m) (Matskevitch, 2007). The main driver of such islands construction is reduced requirements for the fill volume comparing to the other island types (fig.5.8).



Figure 5.7: Tarsiut Island during construction (after Britner-Shen Consulting Engineers Inc.)

Unlike to the other island types a CRI occupies a smaller footprint. A CRI might be constructed in one year and its caissons could be fabricated on the available construction capacities or, at least, the transportation/installation of each pre-constructed caisson is less challenging in shallow waters in contrast to a GBS. The retaining caissons serving as slope protection against waves and ice (ISO 19906, 2010) could be used for the further development activities. Moreover, they provide an “instant” protection against the erosion for the retained

fill (Comyn, 1984) and minimize impact on the environment. Finally, potentially scour of interior infill due to the susceptibility to waves should be avoided.

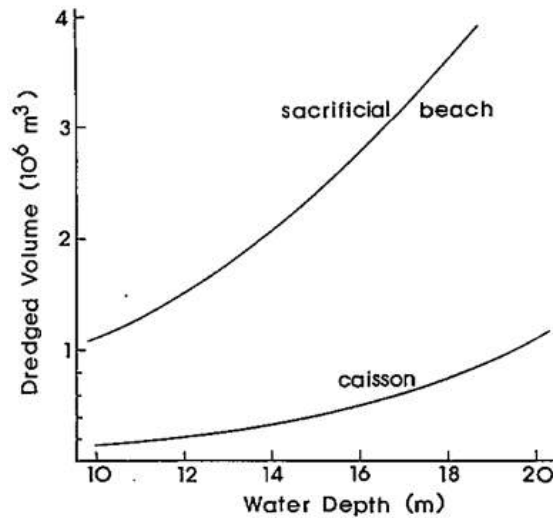


Figure 5.8: Fill requirement for sacrificial, beach and caisson-retained islands (Comyn, 1984).

It should, however, be mentioned that the CRI utilization might face the same challenges as GBSs and this is discussed in the next section.

5.2.1.2 Gravity based structures

Gravity based structure (GBS) is a heavy structure designed to resist severe conditions of shallow and intermediate water depth. These structures can be constructed of steel or concrete and can have storage tanks. Normally, such structures provide full ice resistance and no additional ice protection is required. One example is the Priralomnaya ice resistant platform (fig.5.9) using in the Russian Arctic conditions.

However, even though GBSs have been using in the Arctic for decades, this option has several weaknesses related to construction/transportation/installation of such structures in extreme shallow waters. For the most of the areas of the Northern Caspian Sea gravity based structures are not applicable due to the water depth, because these platforms are suitable for water depths greater than 20-25 m due to the transportation and economical issues (Mirzoev, 2009). However, the final decision should be based on economical and engineering analysis.

In conclusion, the selection of an appropriate offshore structure should be based on the analysis of the local conditions, the availability of construction capacities and transportation of a pre-built structure to the location.



Figure 5.9: Ice resistant platform at the Prirazlomnaya field (Noyonews.net, 2013).

5.2.2 Concept of a Semi ice tolerant platform

As discussed in the preamble of this section, there are two alternatives wherein the ice protection is provided either by the structure itself or by external structures.

Primary, the concept includes the adjustment of non-fully ice-tolerant platforms protected by ice barriers, which will take the main ice loads. The basic idea is to simplify the design of a structure (where it is reasonable) with high reliability of the whole system. A properly designed arrangement of barriers might significantly decrease the ice load on a leeward placed platform; therefore, this might reduce the cost of the project without any risks for the system. Moreover, evacuation/supply vessels might be deployed within the inner leeward area protected by ice barriers. Hence, adjustment of one of the barriers described in Chapter 5.3 could be more practicable.

This option chosen for Kashagan by NCOC (fig 5.10) considers production and service operations carried out from conventional sheetpile-retained islands used as non-fully ice-tolerant platforms, because these islands are the most cost-effective among the structures described above. Together with this, GBSs or CRIs will provide superfluous ice protection resulting in rising of the project budget.

In order to maintain the development progress, this concept can be optimized by implementation of two island types depending on its sizes and functions:

- Large hub-islands (protected by ice barriers) where all field processing facilities are installed. These islands could be used as gathering hubs where all oil and gas are treated before transportation to onshore. In order to achieve optimal drilling progress drilling rigs could be installed together with processing facilities, but, of course, all risks associated with drilling while production must be evaluated and all necessary measures to reduce these risks should be considered. A self-evaluating barge with required production modules might be also deployed within the ice-protected zone in order to reduce the required working area of the sheet pile island. Finally, the barges with pre-installed modules might be re-usable to provide flexibility of the project schedule.
- Small islands (protected by ice barriers) could be used for production drilling and then they could be easily converted for production by retrieving drilling equipment and installing of production facilities. In order to reduce capital expenditures, these islands should be tied back to the main hub-islands and all fluids to be transported to the hub islands for the further processing. In addition these islands might be unmanned in order to reduce risks for personal during production.



Figure 5.10: Semi-ice tolerant platform built in the Kashagan field (after Atyrau-city.kz, 2011).

The experience of the Kashagan development shows that this concept can be successfully implemented in the future projects and the main driver of using this concept is the ability to provide relatively cheap development of large fields located at shallow water depths (like Kashagan). This concept is flexible in terms of extension of islands if it is required in the future, while its construction can be realized during one season.

Even though sheet pile islands are cheaper comparing to other structures, a volume of the fill material grows exponentially with water depth (Hewitt, 2014). So this option is suitable for shallow water, because construction of protection barriers/sheet pile islands in relatively deep waters of the Kazakh sector of the Caspian Sea might be not feasible. In addition, the overturning stability of ice barriers required for protection of semi ice tolerant platform becomes challenging with increasing water depth.

5.2.2 Concept of a Stand-alone platform

The concept includes a platform, which will accommodate all required equipment and personnel. Stand-alone platforms can be presented by bottom-founded structures (GBS or CRI) that are designed to withstand wave and ice loads without the utilization of external ice barriers.

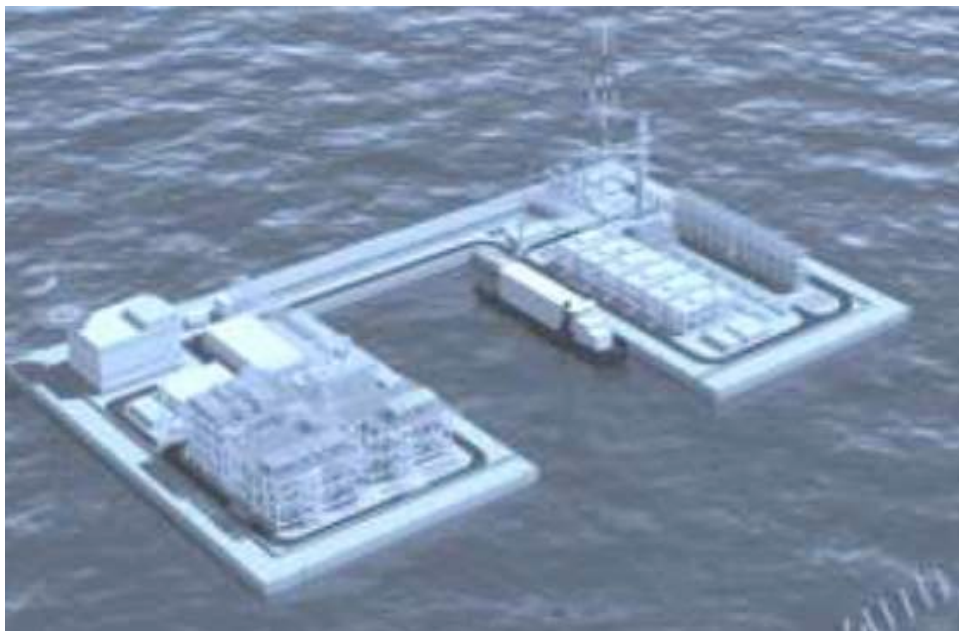


Figure 5.11: A stand-alone platform (CRI) for the Kalamkas field development (NCOC, 2013).

Stand-alone structures might be implemented to develop fields located in relatively deep locations of the Northern Caspian Sea where semi-tolerant structures protected by barriers are

not economically feasible. A platform (GBS or CRI) might have sloping walls in order to reduce ice loads. The freeboard of the platform should be sufficient to avoid wave or ice overriding. As discussed such structures will be likely surrounded by ice rubble in winter so the supply and evacuation would be complicated. In order to avoid this an ice management system should be considered. In order to optimize the project schedule a drilling rig might be installed on the platform, but risk-mitigating measures should be done.

One can notice that stand-alone structures might be implemented for the fields located in relatively deep locations of the Northern Caspian Sea (the Ural furrow, see fig.2.1) where semi-tolerant structures protected by barriers are not so economically feasible. Due to this a stand-alone platform (CRI) has been selected by NCOC for the development of the Kalamkas field located 8 m water depth (fig.5.11).

In general, it should be noted that this concept is one of the most common for the industry and the considerable experience has been gained. The Beaufort Sea production activity might be used as an example where several structures (GBS and CRI) with full ice resistance were successfully applied.

5.2.3 Wellhead platforms

One of the major issues related to the Northern Caspian development is the design of cost-effective options for the development of small fields, where construction of special platform is not commercially feasible.

A wellheads platform tied back to the main structure (e.g. a hub island) can be used as an option both for production from such fields and to improve a drainage strategy of extended reservoirs (fig.5.12).

Given that a wellhead platform is properly designed to provide safe production, this option could be a cost-effective solution for small field development and could improve the drainage strategy resulting in high ultimate oil recovery. In addition, such structures have the following advantages:

- They might be re-usable in order to improve their economical efficiency;
- They have a small footprint coupled with low environmental impacts;
- They provide easy abandonment, etc.

Finally, these platforms are considerably small in comparison to GBSs and thus might be built on existing construction facilities. However, a wellhead platform should provides total

ice and sliding resistance to prevent sliding of the structure along the sea bottom, even more such accident occurred with ice barriers. It should be taken into consideration that, as discussed above, the access to the structure in winter might be complicated so the emergency response time could be long. Thereby service works should be normally carried out during ice-free seasons in order to mitigate risks associated with the intervention.

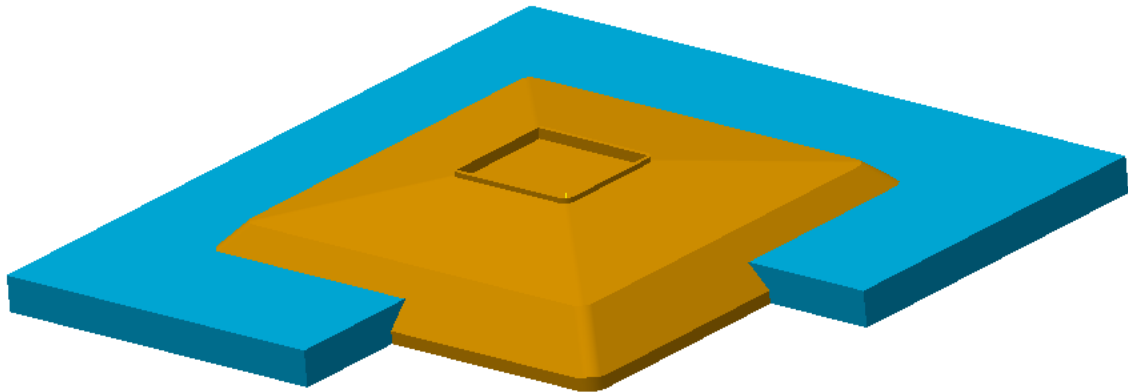


Figure 5.12: Wellhead platform with increased ice generating capability (based on the SIB concept).

Despite that there are no experience of operating of such structures in the North Caspian Sea, this option implies unmanned structures, which are remotely controlled, so risks of human injury are significantly reduced comparing to other solutions.

5.3 Ice barriers

Increasing development activities in the shallow waters of the Northern Caspian Sea raise needs for cheap and robust solutions that could provide ice protection both for drilling units and for production platforms. Ice barriers deployed in close vicinity to such offshore structures can significantly reduce ice loads on the structure and can protect from the hazards associated with drifting ice.

Hence, the proper design of ice barriers arrangement might provide the maximal mobility of a project because of their re-usability and simplicity of construction/installation of individual modules. This might result in high progress of the project realization while the environmental impact could be significantly minimized. Since protection barriers are expected to take ice encroachment, a freeboard of a structure might be reduced which will also

favourable for different operations. Also ice protection systems will have a positive effect on winter supply or emergency evacuation since ice rubbles will likely accumulate at external barriers rather than adjacent to the protected structure.

It should be noted that although protection barriers are used for the protection from both ice and wave action, the ice protection seems to be more foreground in the North Caspian Sea due to high ice loads. An ice barrier must withstand the ice loads by drifting ice and/or accumulating ice and, at the same time, it should be stable during all time of its deployment at different locations. It is of interest to discuss this issue before discussion of other aspects.

The term ‘stability of an ice barrier’ means that no sliding and overturning are allowed (optionally, the geotechnical stability should be taken into consideration for rock mound barriers). One can notice that in such extreme shallow conditions as the North Caspian Sea the sliding becomes more likely rather than overturning failure, so this should be taken into account. The sliding resistance of an ice barrier is a function of the seabed properties and the geometry of the barrier. If the seabed consists of a cohesive material as clay, the footprint area of the barrier is a dominating factor determining the bottom stability of the barrier so the increase in the barrier’s footprint could provide the required stability. In case when the seabed consists of such materials as sand, gravel, etc. possessing less cohesion characteristics; the weight of the barrier controls the sliding stability of the barrier rather than its footprint area. An approach how to take advantage of this phenomenon during design of ice barriers will be discussed in the next sections.

In the previous sections various scenarios of the ice barriers utilization have been described. The main factors governing the efficiency of a protection system, in general, are the geometry of barriers and spacing between the barriers and a structure. So the following section discusses different types of ice barriers and other design aspects of such structures for the Northern Caspian Sea conditions.

5.3.1 Breakwaters

Breakwaters known from harbour protection against waves can be used in the conditions of the Northern Caspian Sea as well. In general, the construction of rock mound barriers is similar to that of man-made islands and rock berms described in the previous chapters. Currently rock mound barriers (see fig.5.10 and fig. 5.18) are used for the ice protection of artificial islands at the Kashagan field, though the results of their using have never been

reported. The main drivers of such structures construction of are the availability of the required construction material, water depth and the construction season limitations.

Furthermore, breakwaters initially designed to withstand the wave action should additionally provide ice resistance in ice-infested seas. One can notice that the interaction of ice with such structures is still needed in investigation; however, the global ice action can be calculated by using of the approaches described in Chapter 6.

Longkeek et al. (2003) suggest the design of such barriers to counterbalance the edge failure due to the ice action by selecting the crest height. The minimal crest freeboard should be 2 times the ice thickness. However, due to ice encroachment a higher freeboard of the structure might be required, although it is not effective in terms of preventing the edge failure.

Together with the design issues, different sources give varying values of the rock size required to provide the geotechnical stability of the barrier subjected to ice loads. According to Lengeek et al. (2003) the rock size should be equal to half of ice thickness, while Sodhhi et al. (1996) states that the diameter of rocks should be 2-3 times the thickness.

It should be noted that the application of rock mound barriers might be challenging for relatively deep locations within the Northern Caspian Sea because their construction might take several seasons with all consequences that come due to this. Also the utilization of riprap as protection structures might results in problems related to the breakwater maintenance because of losing of the rocks during storms (or interaction with ice) due to the absence of their interlocking ability.

Another type of barriers used for harbour protection is concrete armour blocks of various shapes (such as Kolos, Dolos, tetrapods, etc.) forming together an assembly protecting against the wave action. However, the implementation of such structures in ice-covered areas is not feasible since the blocks could be damaged by ice because the stability of the assembly of such modules relying on a gravity force of an individual module is not sufficient. Sulatabayev and Gudmestad (see Appendix B) proposed a concrete interlocking armor block with improved interlocking ability in order to avoid these drawbacks by improvement of their shape. One can notice that even though the presented design provides a high interlocking capability in situ, which is beneficial for the protection against hydrodynamic forces, this might be still not enough to withstand the action.

Finally, as reported a key issue for construction of rock mound barriers is a poor quality of rocks available in the Caspian region (Granneman et al., 2001), so this might face significant challenges and another type of ice barrier might be required.

5.3.3 Grounded satellite barges

Generally, the deployment of such structures includes ballasting with seawater at the drilling location to increase the weight of the system (to increase the sliding resistance).

Grounded barges were used to provide the ice protection at the Kashagan project. Due to the lack of information about the experience related to the barges application in the Northern Caspian Sea, it is difficult to analyse the efficiency of this type of ice barriers. According to several pictures of the Sunkar barge protected by the grounded barges (fig. 5.13 and fig. 5.19), one can conclude that some barges had vertical walls while some of them had sloping walls. Since the geometry of barriers affects on the ice-structure interaction mechanisms, a vertical barge will be likely subjected to higher ice loads than a sloping one; therefore, it might be beneficial to utilize the barges with sloping face. The advantages of sloping structures in terms of ice loads mitigation are discussed in Chapter 6.



Figure 5.13: Grounded barge in the North Caspian Sea (Bastian et al., 2004).

However, high ice loads on these structures of a simple shape might lead to deformation of the barges and might complicate the maintenance. In addition some negative experience associated with insufficient sliding stability of the barges has been gained. In February 2002 an accident involving the application of barriers occurred, when one of the grounded barges

was moved to 120 m by drift ice, but, fortunately, the Sunkar barge wasn't damaged. Nevertheless, no official reports of the incident analysis have been presented. However, currently the adjustment of the grounded barges was refused to apply (Kouraev et al., 2003). It is likely that the barge lost the sliding resistance.

As mentioned in the preamble of this section, the sliding resistance of barriers deployed on pre-built berms (consist of cohesive type of the material) is mainly controlled by their weight. Thereby, the main measure to avoid such incidents is to increase the overall weight of barriers both by ice spraying and by triggering the ice rubbles accumulation on the barrier.

Finally, it is likely that grounded ice rubble in front of the barge deployed in shallow water will reduce the global ice loads on it and will increase the effective diameter of the barge, i.e. protection radius of the barge.

5.3.4 Rubble generators

An ice rubble generator is a structure of a special shape that induces the ice failing in a predefined manner. After some time, the ice rubble accumulated in front of the structure becomes grounded, whereby it dissipates the ice loads into the seafloor and the environment. Hence, it is beneficial to initiate the ice rubble generation in terms of ice loads mitigation in shallow waters of the Northern Caspian Sea, which is favourable for accumulation of fragmented ice in front of wide structures.

On the other hand, the stability of ice barriers on non-cohesive type of soil (for instance, when underwater berms are used as a foundation for the barriers) mainly relies on their weight, so ice rubbles accumulated on the barrier will increase sliding resistance of the system. In this case, the sliding resistance will proportionally increase with increasing pressure on the contact surface between the bottom of the barrier and the upper layer(s) of the seabed. Hence, ice barriers with enhanced ice-generating characteristics might be used for the protection of semi-tolerant structures described in the previous section. Therefore the main structure will be subjected to lower ice loads so its design can be simplified in terms of ice resistance requirements. However, there are a limited number of studies dedicated to the barrier design considering this phenomenon. The following discussion will present only concepts of ice generators considered as most feasible.

Gürtner et al. (2006) introduced an innovative concept called the shoulder ice barrier (fig. 5.14, a). A shoulder ice barrier (SIB) provides effective ice breaking-up because of the changes of sloping angle accelerating ice breaking-up and resulting in increased ice rubble

generation adjacent to the barrier. Gürtner (2009), Repletto-Llamazares et al. (2013) presented comparison of a SIB with ice barriers with different inclination of the second slope (the first sloping angle is 45 deg). The tests successfully proved the role of the second slope in generating of ice rubbles and a SIB demonstrated better characteristics of ice generation in comparison with a barrier without the second slope (fig.5.15).

One can note that the SIB concept, *ceteris paribus*, will be more stable than barriers of other shapes. In addition since a SIB is concrete, its individual weight will be greater than the weight of a barge of the same length/height/width filled with seawater and, hence, this will promote enhanced bottom stability.

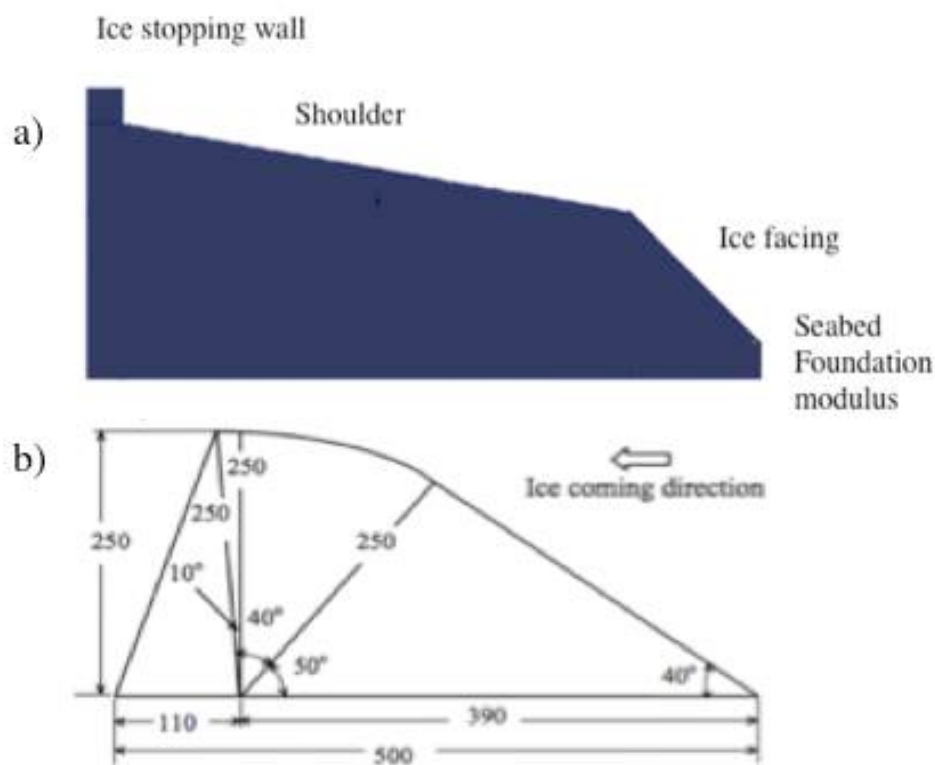


Figure 5.14: a) a Shoulder Ice Barrier (not to scale) and b) a curve surface barrier proposed by Li et al., 2006.

An alternative to the SIB concept might be curve surface barriers (CSB, fig. 5.14, b) initially proposed for the protection of a jack-up from ice loads (Li et al., 2006). Although no results of CIB tests has been reported, it could be expected that the CSB concept, which bases on the same principle as the SIBs, will provide less effective ice breaking capability. In addition the design of the CIB does not include any deflector to trigger instability of coming ice rubbles and this will lead to ice over-riding rather than the ice accumulation.

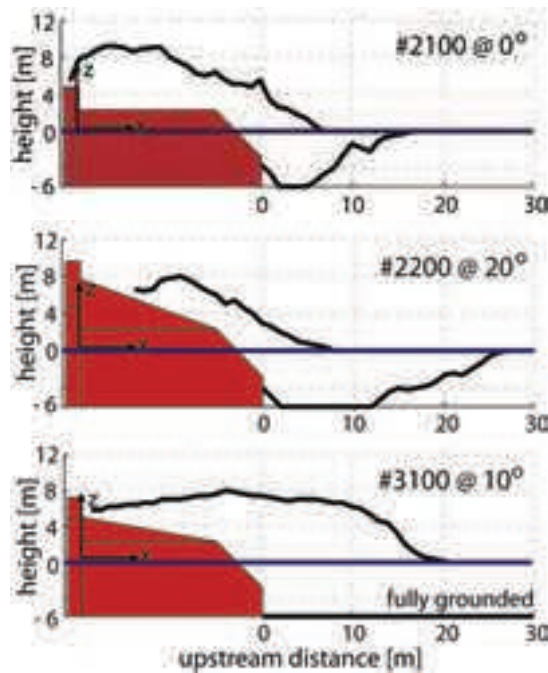


Figure 5.15: 2D plots of ice rubble profiles at the centre of the SIB (Gürtner, 2009).

However the benefits of ice rubble adjacent to the structure might be diminished when the ice rubble is mobile due to the sea level changes and winds. Furthermore, a poor design of the barriers alignment might complicate the access to the leeward located structure or emergency evacuation from it. The arrangement of barriers is discussed in section 5.3.6.

5.3.2 Ice Protection Piles

Note that piles with different spacings and diameters have contrasting scenarios of ice interaction (fig.5.16, b) and they can be implemented as an ice protection system (Løset et al., 2006). Vertical or sloping piles are hammered into the seabed in order to get sufficient resistance.

The pile diameter and the spacing between piles are selected so that the pile arrangement promotes the ice rubble generation in front of the protection structure. It should be noted that the broken pieces of the ice might bypass the piles toward the leeward area without ice piling-up. This scenario should be avoided by using of additional barriers or the central structures should have some level of ice resistance, i.e. should be semi ice tolerant.

Although the ice load reducing piles are installed around of the Sunkar barge (fig.5.16, a), the results of instrumentation of the piles have not been reported. It was further confirmed by investigations of Gürtner (2009) that piles with specially selected spacing could be used as rubble generators. The main recommendations for the IPPs design are (Gürtner, 2009):

- An optimal spacing between the piles are three diameters of the piles and should not be larger than six diameters of the piles;
- Higher ice loads on the IPPs should be expected due to increasing of the contact area with ice;
- Actual piling depth should be carefully selected to provide resistance of the piles;
- Pile dynamics cause liquefaction of the soil so particular attention should be given to this potentially hazardous phenomenon.

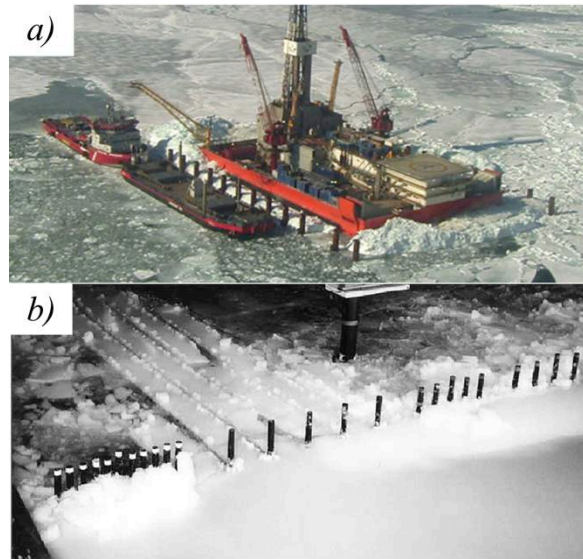


Figure 5.16: a) The Sunkar Barge is on the location (IMPac, 2011) and b) Model-scale testing of piles with different spacings (Weihrauch and Gürtner, 2006).

The IPPs can reduce the barge deployment time and might be more cost-effective than other types of ice protection systems. However, Gürtner (2009) reports that the IPPs concept are not a self-sufficient barrier system and it can be used only as an additional ice protection system to reduce ice loads on the structure. However, the IPPs design is a wide topic and it is beyond the scope of this thesis. The reader interested in more details is referred to Gürtner (2009).

5.3.5 Grounded ice as an ice barrier

Although the adaptation of ice islands faces significant challenges in the Northern Caspian Sea (see Chapter 5.1.1), ice protection barriers built by ice spraying might be an alternative to other ones (fig.5.17, b). It should be noted that massive ice rubble fields observed in the Northern Caspian Sea could alone resist large ice floes exerting on it (see fig. 5.17, a).

These barriers might be implemented for additional ice protection of structures by generation of ice built-up adjacent to the structure. The main advantages of this option are low costs and high mobility. However, this option might be suggested only for temporary ice protection and doesn't protect a structure from waves during ice-free seasons. One can notice the sliding stability of a sprayed barrier should be taken into consideration.

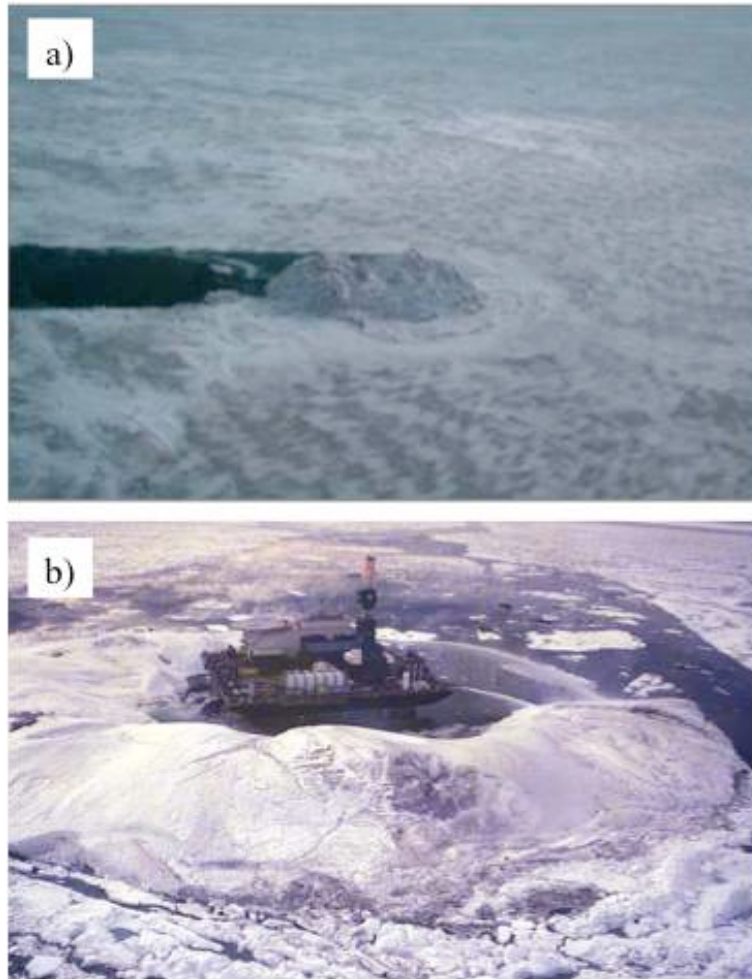


Figure 5.17: a) Stomukha resisting moving ice in the Caspian Sea (Lengeek et al., 2003) and b) Spray ice protection barrier around CIDS during its deployment at Antares in the US Beaufort (Matskevitch, 2007).

5.3.6 Ice barriers arrangement

Different types of ice barriers have been described in the previous sections. However, together with their shape, dimensions, etc., their alignment is a key issue.

The arrangement of ice barriers should exclude extreme ice loads acting on the leeward lying structure. The distance between barriers and the structure as well as the configuration of

the protection arrangement should be selected properly in order to avoid potentially dangerous situations. The following section presents possible options for barriers arrangement.

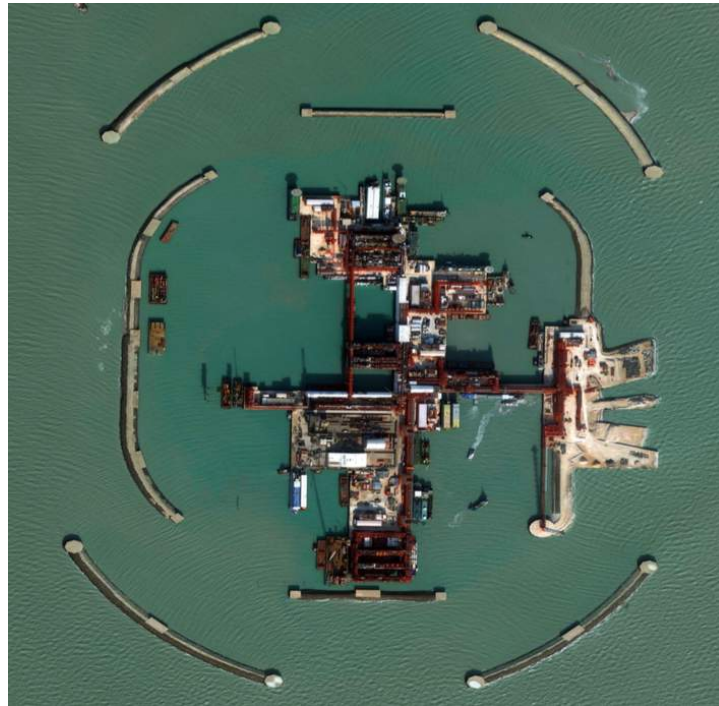


Figure 5.18: Top view of a sheet pile island protected by rock mound ice barriers at Kashagan (SpartialEnergy.com, 2010).

Primary, ice barriers assembled at some distance from the platform could be continuous or intermittent, however, the arrangement of intermittent barriers (see fig. 5.18) is more reasonable in terms of providing access for supply or emergency evacuation vessels.

It should be noted that the ice resistance of a leeward located structure somewhat governs the design of the barriers arrangement. The protection system might allow the ice loads acting on a central structure in a predefined manner so that the structure can withstand them without any risks. Hence, the design of the protection arrangement will become simpler with increasing the ice resistance of the leeward lying structure. For instance, ice protection systems for sheet pile islands or jack-ups (non ice resistant structures) should be more intensive (fig. 5.18) while the ice protection arrangement for the Sunkar drilling barge might be simpler so that ice barriers should be deployed only in the main direction of ice drift (see fig. 5.19).

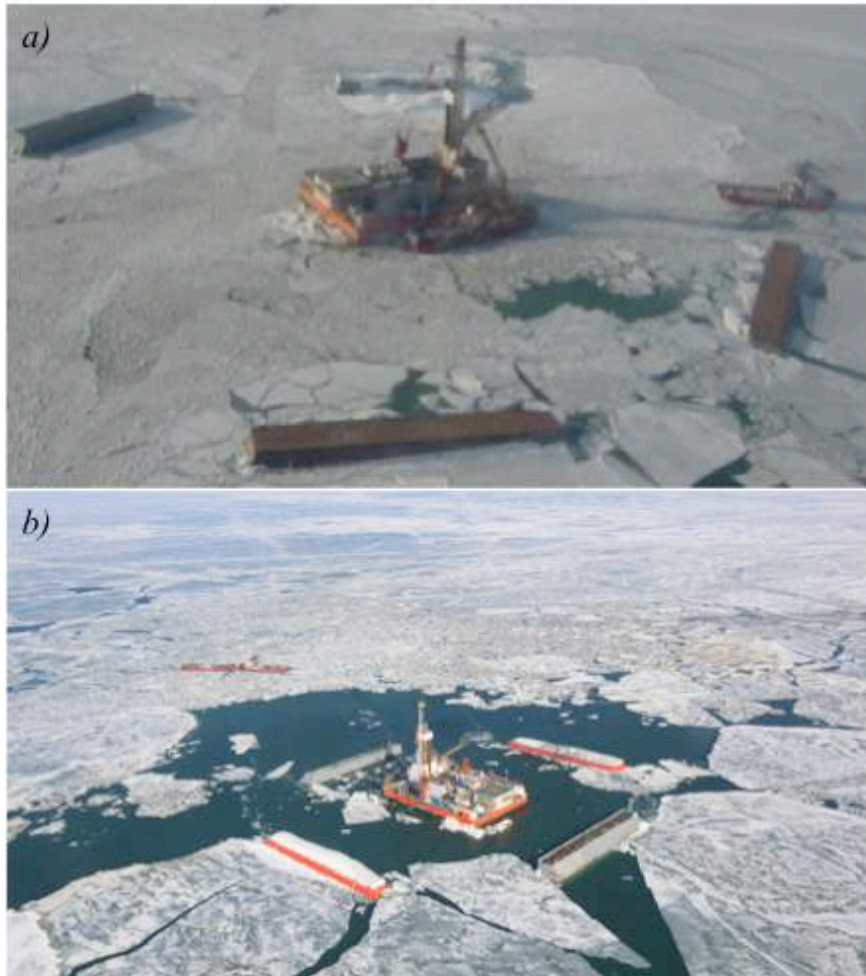


Figure 5.19: The Sunkar drilling barge protected by submerged barges. After a) McKenna, 2012, and b) CDE, 2015.

Jochmann et al. (2003) discussed a system with two ice barriers on each side of the Sunkar barge as shown in fig. 5.20. It has been proved during the tests that a structure protected by barriers is subjected to lower ice loads than a structure without any ice barriers alignment. The ice loads (horizontal) on the barge without the ice barriers arrangement vary in the range about 80-60 MN depending on the direction of the ice drift, while the results for the protected structure are more impressive: the ice load varies from about 5 MN to 30MN (see fig. 5.21). Hence, the ice loads could be reduced from 80MN to ca. 5MN by the employment of ice barriers.

Along with the impressive results, these tests show that a critical issue for the barriers alignment is the main direction of the ice drift. In case when the approaching ice acts from the unexpected direction, the leeward structure is subjected to undesired loads (fig.5.20, a and b).

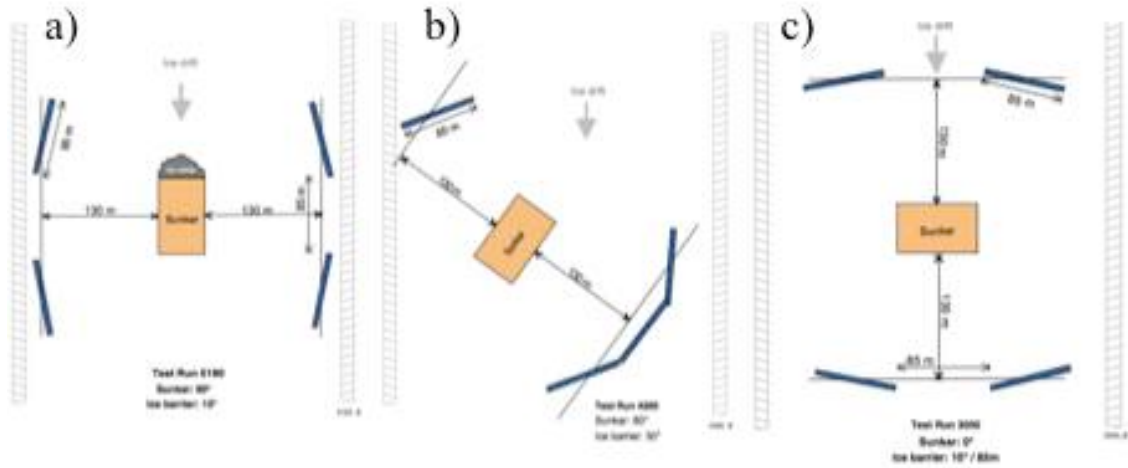


Figure 5.20: Different scenarios of ice action on the central structure as the Sunkar Barge (Jochmann et al., 2003)

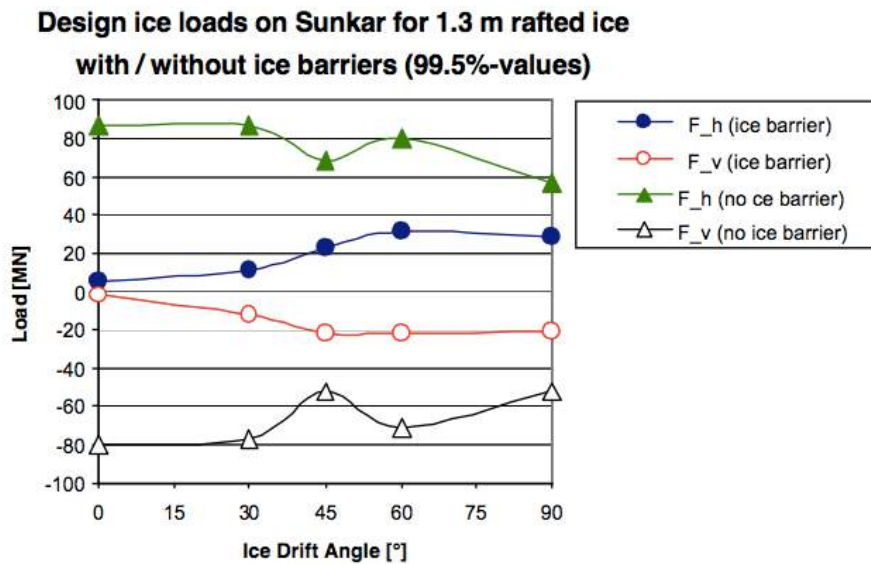


Figure 5.21: Ice loads on the barge with and without external ice protection (Jochmann et al., 2003).

Additionally, one can conclude that the sliding resistance of an ice barrier in such arrangements is crucial because if a barrier is moved by ice due to the low sliding resistance, it can potentially damage the leeward structure. Hence, in order to provide barriers with enough sliding resistance they can be supported both by piles (IPPs) and by ice spraying in order to increase the weight of the system and to form grounded ice rubble in front of it. However, it is more beneficial to use barriers with enhanced ice generation in order to avoid the accidents involved the barge sliding due to the ice action in 2002 (section 5.3.3).

Finally, the separation distance of barriers from the central platform is another key factor. It is important to keep a balance during the design of the separation of ice barriers. A large separation will provide a larger inner area protected from ice action wherein supply/emergency evacuation vessels might be safely depleted. In addition, such arrangement will provide time to react to potentially dangerous hazards (such as sliding of a barrier) and the time of emergency evacuation will be longer as well. On the other hand, too large distance might be inefficient from the ice protection point of view while additional ice loads mitigation measures might be required within the protected area.

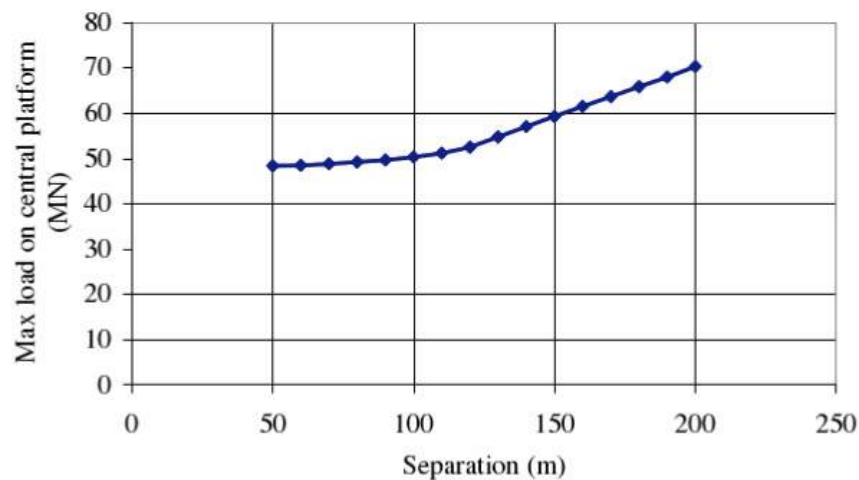


Figure 5.22: Maximum ice load on a central platform varying with separation of barriers from the platform (Palmer and Croasdale, 2012).

Palmer and Croasdale (2012) presented calculations of the maximum ice load for various separations (fig.5.22). As shown the separation might be increased from 50 m to 100 m without significant increasing the maximum ice load. However, this is determined by several factors (such as the design ice action, the soil conditions at the location, the geometry of the barriers and the platform, the ice properties, the angle of the ice drift, the arrangement of the ice barriers, the velocity of the ice drift) and it should be proved by model tests in order to design the most optimal option for the separation.

5.4 Processing system

As a rule, well flow producing from the reservoir is a mixture of oil, gas, water and other byproducts, which necessitates its further treatment and processing in order to meet the oil/gas specifications. So a development concept of offshore fields should include a process system

for produced oil and gas in order to get the products that are suitable for storage, transportation and sale.

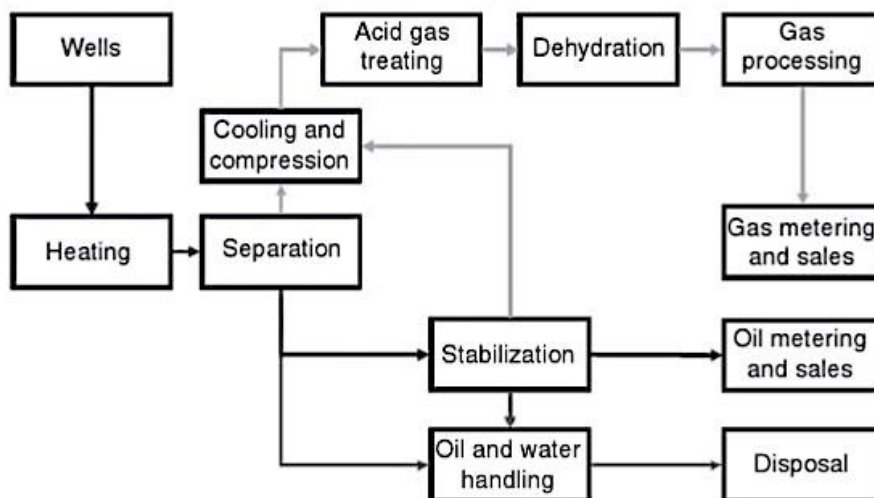


Figure 5.23: Processing facility block diagram (Gudmestad et al., 2010)

A processing scheme commonly consists of several components presented in fig. 5.23, but its arrangement varies depending on the composition and the properties of the well stream flowing from the reservoir and the technical specifications for oil and gas. On the other hand, in most cases, water and/or gas injection are simultaneously carried out with oil production, hence, these injection fluids should satisfy to the technical requirements as well.

There are several options depending on the type of the hydrocarbons producing from the reservoir:

Oil and gas condensate. The processing equipment might be installed either on shore or on offshore. In the first case, the well flow is fully transported to the shore processing facility and then oil/condensate is treated in order to satisfy to the sale specifications. Other option is a processing cycle implemented in several stages: the primary treatment could be realized on the offshore location and after the stabilized oil/condensate could be transported to the shore, where these products are treated in order to satisfy to the sale specifications, because often it is not economically suitable to realize the final oil and gas processing on the offshore location. The Kazakh laws strictly prohibit the flaring of associated gas and one of the effective solutions is re-injection of this gas into the reservoir. This necessitates additional compressor systems causing the project budget rising, but, on the other hand, this approach increases oil recovery factor. In addition, sometimes H₂S (and/or CO₂), which is highly

corrosive, is presented in the well flow and this fact should be considered during the material selection for the processing/flowlines/pipeline design.

This option was chosen by NCOG for the Kashagan development. Primary, oil processing is carried out on the offshore location and then stabilized oil is treated on the offshore processing facility located near Atyrau. All associated gas is planned to be re-injected.

Gas. For gas processing system the same options could be implemented. Nowadays gas liquefaction is realized in addition to gas separation and traditional pipeline transportation, but in the conditions of the North Caspian Sea, it is not economically feasible due to obvious reasons.

5.5 Transportation system

Hydrocarbons should be delivered to buyers and consumers to get profit from it. There are two options for hydrocarbon transportation including either pipeline transportation or utilization of special ships (so-called tankers). In general, both options can be applied for oil and gas depending on the processing system. The main factors governing the transportation system selection are the distance to users and volumes of hydrocarbons that should be transported.

However, due to shallowness and remoteness of the Northern Caspian Sea, tanker transportation is complicated, especially in ice seasons. Furthermore, the tanker transportation requires some storage capacity on the place and offloading equipment, while for pipeline systems stabilized hydrocarbons directly transported to the shore. Hence, the pipeline transportation is more effective for the field development in the Northern Caspian Sea while this option will provide hydrocarbons transportation that does not depend on weather/ice conditions. It worth mentioning that this options has been currently applied for the development of the Kashagan field.

The pipeline transportation is characterized by high initial capital and low operating expenditures. The pipeline capacity is determined by its diameter and by operation pressure (power of pump/compressor stations). The main drivers for pipeline design that should be considered are (Karunakaran, 2014):

- Pipeline route
- Pipeline design
 - Flow issues – Pipe size

- Pressure and temperature – Wall thickness
- Corrosion protection
- Coatings (thermal insulation, impact protection, etc)
- Linepipe selection
- Installation issues
- On-bottom stability
- Upheaval and lateral buckling
- Freespan and correction.

It should be noted that pipeline routing is a crucial activity, because a route chosen poorly may lead to unnecessary increasing of the project expenditures. On the other hand, flow assurance has to be considered in order to prevent such challenges as slugging, hydrate formation, wax buildup, corrosion and erosion, scale formation, asphaltene deposition. This is a critical issue because the production on the Kashagan field has been stopped since 2013 due to H₂S corrosion of the main pipeline connecting the field and onshore. Unfortunately, no reliable information is currently available about on-going works.

Another challenge in the Northern Caspian Seas related to a pipeline transportation system is seabed gauging by ice ridges, which is compounded by the shallowness of the sea. Ice ridges scouring the seabed might damage flowlines/pipelines either by direct contact of the ridge with the pipeline or by soil deformations below the ridge's keel. One of the most effective methods of pipeline protection against ice gouging is trenching and burial. Pipelines should be buried below the seabed to the depth that is larger than the depth of the deepest scour (Barrette, 2011, Been et al., 2013). However, this is beyond the scope of this thesis and is not discussed.

5.6 Summary

This chapter gives an analysis of each system of a development concept and options that can be utilized in the Northern Caspian Sea.

Production drilling. Ice islands could be implemented for temporary operations depending on the time required for a particular operation. Since drilling barges have poor open sea characteristics, one of the discussed foundation options should be implemented. Although the utilization of conventional jack-ups with ice protection might be beneficial, the success of their employment is determined by the efficiency of the ice protection system. Finally, a platform rig can be installed in order to provide high development progress.

Production systems. The analysis of the Northern Caspian conditions shows that island or platform development is advantageous. The most effective technical solutions are sheet pile islands, caisson retained islands and gravity based structures. Being the cheapest option among them, a sheet pile island has worse ice resistance. In addition, the main advantage of it, low construction costs, is diminished with increasing water depth. Therefore, this option might be incorporated into the concept of a semi ice tolerant platform protected by the external system. One can notice that this is the first solution extreme shallow water of the Northern Caspian Sea.

A concept of an ice tolerant platform, in turn, imposes utilization of a structure that can singly withstand ice and wave loads. A CRI or a GBS might be used as a platform; though a CRI is more beneficial.

A concept of a wellhead platform is presented. Although there is no experience of such structures implementation, they can improve the reservoir drainage strategy and ensure the development of small fields. In conclusion, the selection of an appropriate offshore structure should be based on the analysis of local conditions, the availability of construction capacities and transportation options of a pre-built structure to the location.

Finally, processing and transportation systems are discussed and the most feasible options are presented.

Chapter 6. Ice action in shallow water

In general, the magnitude of ice loads is governed by several factors that are partially related to the ice properties and, on the other hand, to the structure (see fig. 6.1).

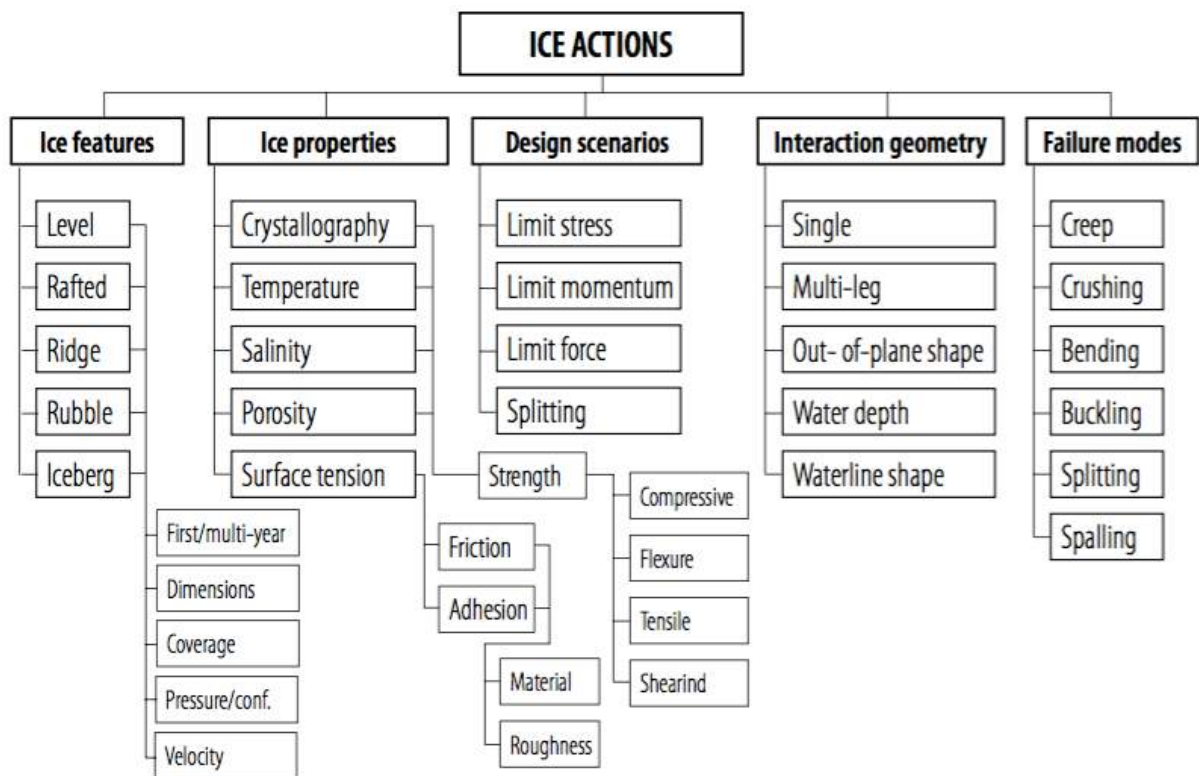


Figure 6.1: Illustration of factors influencing ice actions (Løset et al., 2006).

Different types of the ice features observed in the Northern Caspian Sea and the ice properties have been discussed earlier, in Chapter 2 and, partially, in Chapter 3. Since the

movement of ridges is constrained in shallow waters, it is more probable that ridges will not be a controlling ice feature for ice loads so a structure will be protected from ridges by grounded ice rubble accumulated in front of it (Palmer and Croasdale, 2012). So only ice loads caused by interaction of first-year level ice with structures in shallow water are taken into the further consideration. The following chapter presents other aspects related to the ice action on structures in shallow water.

6.1 Design scenarios

According to ISO 19906 (2010) there are several factors that limit the maximum ice load and the next limiting scenario corresponding to the situation when one of parameters exceeds the greatest value are regarded (fig.6.2):

- Limit stress is expected when ice fails adjacent to the structure and the ice strength determines the maximal force applied to the structure by the ice. This limiting scenario involving crushing of ice against the structure often governs the maximum force on the structure.
- Limit force is when the force applied on the structure is determined by driving force, while the environmental action applied on the ice feature halted in the vicinity of the structure (e.g. wind and currents) is not sufficient to initiate the ice failure against the structure. Note that this scenario also corresponds to an ice floe failing against the ridge fixed in front of the structure.
- Limiting momentum is the limiting mechanism when the kinetic energy (momentum) of the ice determines the ice action. The kinetic energy of the ice floe is not sufficient to initiate the ice penetration into the structure and the ice floe slows down in reaction to the contact force.

Additionally, Løset et al. (2006) distinguishes limit splitting when the propagation of cracks occurs during the interaction of a relatively small ice sheet with a structure.

However, the limit stress scenario will likely govern the ice action in the North Caspian Sea because in such shallow water conditions as Northern Caspian Sea ice rubble built-up adjacent to structures will affect the ice action. One can notice that the limit force scenarios will likely control the design ice load in deeper locations within this region where the drift of ridges is not so restricted.

In some cases the combination of these mechanisms should be considered. ISO 19906 (2010) recommends “if more than one limiting mechanism can occur simultaneously, the one that gives the lowest ice action should govern the design”.

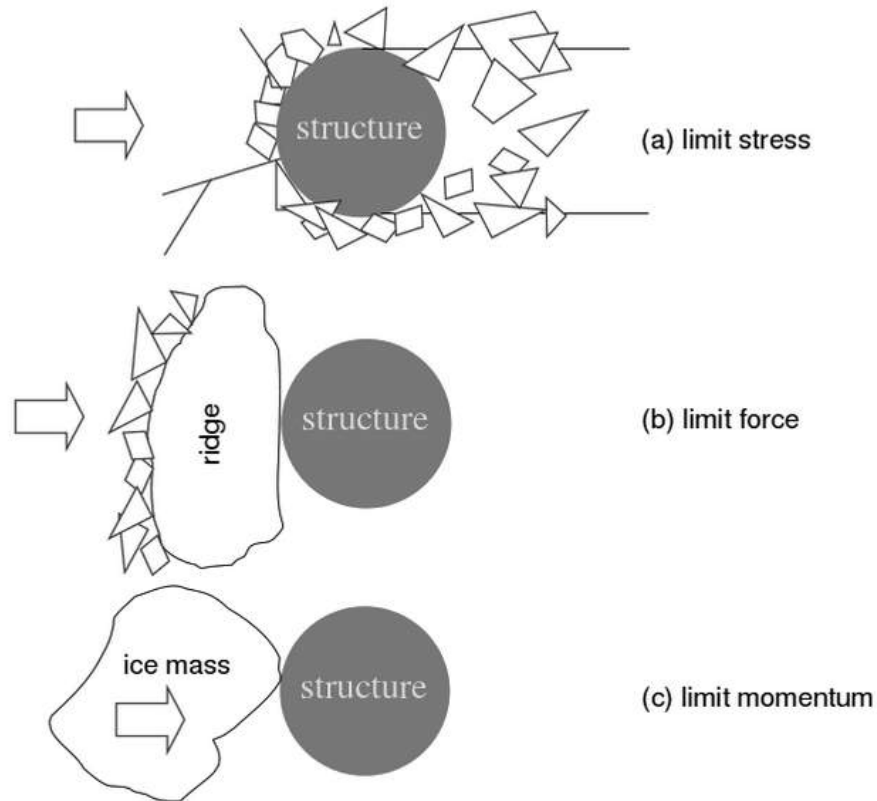


Figure 6.2: Design scenarios (Palmer and Croasdale, 2012).

6.2 Interaction geometry

Along with the limiting mechanisms the geometry of the structure interacting with ice controls the ice action. This encompasses such parameters as the size of the structure, the number of supports, its out-of-plane shape (sloping or vertical) while the cross-section at the waterline area is less important except certain situations.

Structure size is one of the most important parameters regarding the interaction geometry when the ice loads are to be determined. The effective diameter of the structure (including the diameter of each support with spacing between legs) at the waterline influences the ice action as well, see figure 6.3.

The cross-section shape of the structure at the waterline area is also a key factor. Higher ice actions are expected on a vertical faced structure rather than on a sloping one. A structure

with vertical walls might pose a higher risk of vibrations induced by the ice action. In this thesis, the further discussion of the ice loads calculation will be focused on the main structures of interest that are:

- Vertical faced structures (ice barriers, barges, sheet-pile islands, etc.),
- Sloping structures (ice barriers or other structures).

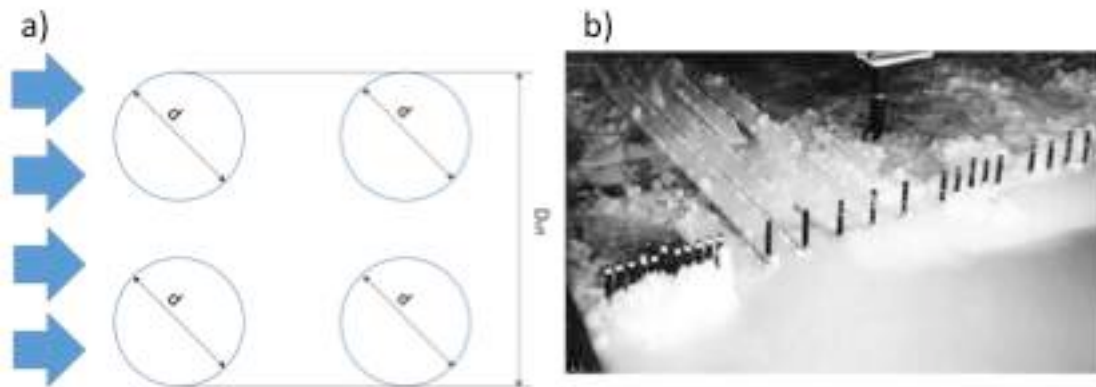


Figure 6.3: a) Effective diameter of a multiple legs structure and b) Model-scale testing of piles with different spacing (Løset, 2014c).

6.3 The effect of Ice Rubbles in shallow waters

In reality, the interaction process might be complex due to the shallowness of the Northern Caspian Sea favouring ice rubble built up adjacent to structures (see fig.6.4). It should be noted that this phenomenon was firstly noticed during the Canadian Beaufort Sea development and then it was revived in the Northern Caspian Sea.

In order to evaluate the effect of ice rubble it is crucial to know the ice rubble properties and the process of loads transmission to the structure. Kry (1977) reports that in the shallow Beaufort Sea ice rubble becomes soon grounded during its formation process. The process that took place prior the ice rubble grounding is similar to the formation of pressure ridges in thin ice (Weeks et al., 1971). Thus, the consolidation of broken ice blocks begins as they become stable, i.e. case to move. Then freezing of the seawater filling the pore volume of the rubble's keel leads to the further ice rubble consolidation. Note that the ice rubble consolidation in shallow water is controlled by its initial temperature, its initial pore volume of the keel, the height of the rubble sail (see fig. 6.5), the presence of snow, the sea level changes, air temperature and wind speed. On the other hand, due to the weight of the sail and the action of the coming ice sheet, the higher level of consolidation should be expected at the

waterline of the ice rubble. This phenomenon characterizes the ability of the ice rubble to transmit the ice loads from the coming ice sheet to the structure.



Figure 6.4 :Ice rubble built up in front of a wide structure in the Caspian Sea (Loset et al., 2006 with reference to Evers and Kühnlein, 2001).



Figure 6.5: Air temperature at which it would be possible for rubble of porosity γ to completely consolidate. Note that the initial temperature distribution in the ice sheet is assumed as linear and equal to the air temperature on the top surface (Kry, 1977).

Together with the consolidation issue, the sliding resistance of the grounded rubble determines the effect of ice rubbles in shallow water. The main physical and mechanical properties of the ice rubble keel should be determined from in situ measurements, because

they determine how the ice loads are dissipated to the seabed (or underwater berm). The friction force between the rubble keel and the seabed is created due to the weight of the sail that is not compensated by the buoyance force on the keel. In addition, the topography of the seabed might contribute to the process of the ice rubble grounding.

There are a small number of researches dedicated to this phenomenon in the North Caspian Sea (McKenna et al. 2011, Croasdale et al., 2011, Barker and Croasdale, 2004). Observations and measurements that were carried out in 2001 show the predominant thickness when ice freeze-up occurs is about 0.15 m. Also, Palmer and Croasdale (2012) with reference to Timco et al. (2000) offer the next correlation between the average maximum sail height h_s of the ice rubble and the ice thickness h_i :

$$h_s = 3.7h_i^{-0.5} \quad (6.1)$$

Such parameters as the cohesion and the friction angle of the ice rubble are not well studied. Wong et al. (1988) reviewed shear box tests on broken ice and made practical recommendations. The cohesion varies in the range from 1.7 kPa to 3.4 kPa while the friction angle is 11°-34° when the porosity of the saline ice rubbles ranged from 0.19 to 0.50 (Wong et al., 1988 with reference to Weiss et al., 1981). However, caution is recommended when using of these Mohr-Coulomb parameters, because no peak or ultimate shearing resistance was detected during these tests (see Chapter 7.2.2).

On the other hand, ice rubble adjacent to the structure will complicate the access to the structure and, hence, it will hamper winter supply operations as well as emergency evacuation (see fig. 6.5). However, the ice rubble field in the vicinity of an offshore structure might be difficult to clear it if it is grounded.

Finally, ice rubble grounded in the vicinity of structures affects the ice action on both vertical and sloping structures so that the process of the ice-structure interaction will change. It should be expected that ice loads on a structure with grounded ice rubble filed would be subjected to lower ice loads. This is discussed in detail in the next sections. However, it should be taken into consideration that sometimes the ice rubble field might be removed by operations, especially, at the earlier stages when it is not stable.

6.4 Ice loads on vertical structures

Although the interaction between ice and a vertical structure seems to be simple to analyse it, in reality, it is not. The interaction process involves such failure modes as creep, buckling,

crushing. However, the maximal ice load on a vertical structure is expected when ice fails in crushing (Croasdale et al., 2011). This failure mode is inherent for the ice interaction with vertical structures and loads caused in such case might dominate in the design action.

Crushing develops at sufficiently high indentation rates of the ice. In contrast to the creep failure mode, this mode is characterized by the non-simultaneous partial contact and local pressure concentrations over the entire contact area. So, in reality, the ice acting on a vertical structure will fail due to the compression failure as presented in fig. 6.6. The ice is pulverized upward and downward. This leads to the occurrence of high-pressure zones and the no-pressure (or low-pressure) zones along the contact area. These zones are not constant and vary in time and in space, the ice loads are irregularly transmitted to the structure. Because of this there are two types of ice loads considered for structural design - the local pressure and the global ice action. The global ice action is the action on the system at any instant time while the local pressure is the pressure on a limited area of the contact zone corresponding to the crushing mechanism described above.

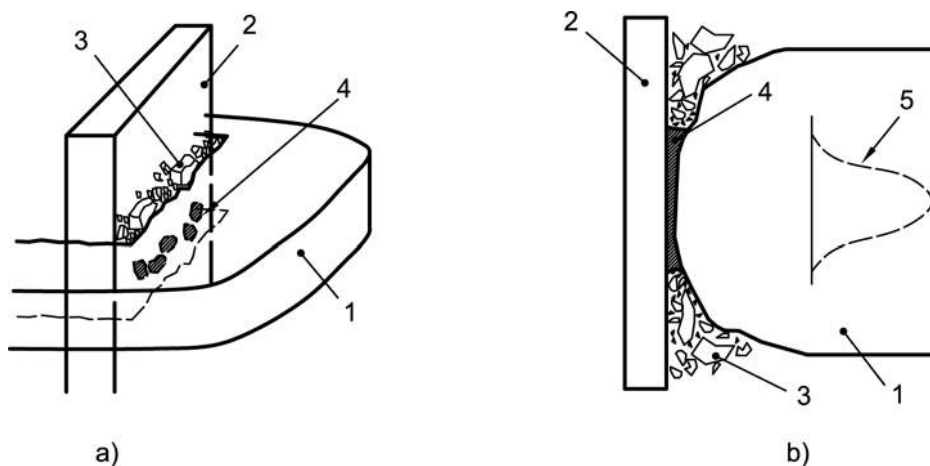


Figure 6.6: Schematic showing localization of action in compressive ice-structure interaction: a) ice sheet interaction with the flat surface of a narrow vertical structure and b) profile of ice sheet interaction with vertical structure: 1 - ice sheet, 2 - structure, 3 - spalls and extrusion, 4 - high pressure zones in a), layer of crushed ice of high pressure zone in b), 5 - pressure distribution over the contact surface (after ISO 19906, 2010).

It should be noted that ice rubbles built-up adjacent to the structure might result in dominating of the rubbing mode rather than crushing (Croasdale et al., 2011). Thus, the ice failure mode will be changed from crushing to rubbing for a vertical structure. Even though ice rubble accumulated in front of a vertical structure might reduce the ice loads, in this thesis,

only a limit stress scenario is discussed further, because the maximum ice loads acting on the structure are expected during the initial interaction stage when ice fails in crushing (see fig. 6.7, a).

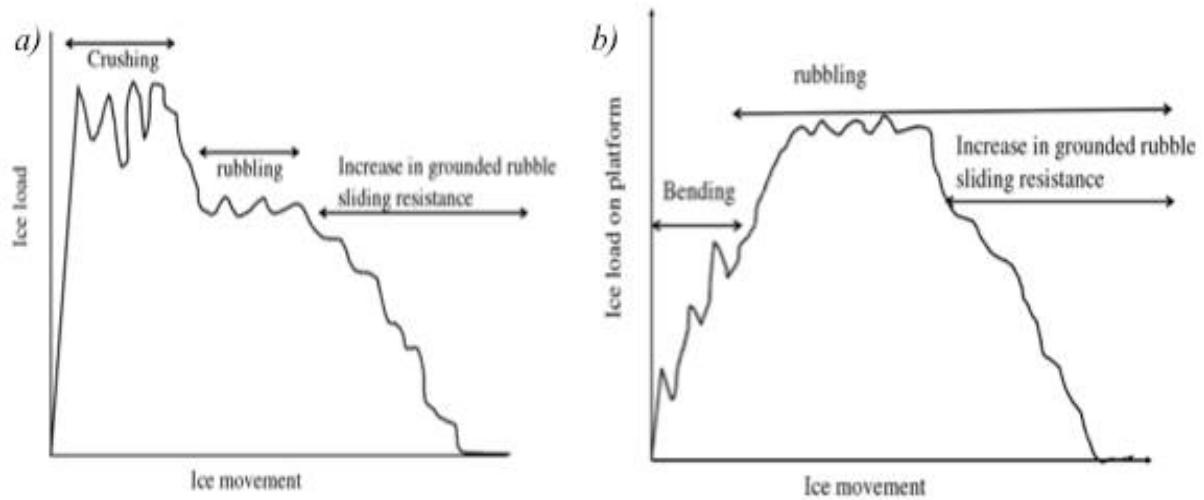


Figure 6.7: Ice loads during different stages of ice interaction with a vertical structure (a) and a sloping structure (b) in shallow water (Palmer and Croasdale, 2012)

Note that even though the magnitude of ice loads is considered as a constant, in reality it is not. Instead of it, a quasi-static design load equal to the maximal peak ice force is used. The following sections introduce the main empirical methods to estimate ice loads on vertical structures.

6.4.1 Simple equation of the global ice action

The global actions can be determined by the next equation (Løset S. et al., 1998):

$$F = h \int_{-\frac{\pi}{2}}^{\frac{\pi}{2}} \sigma_c \cos \varphi R D \varphi = h \sigma_c 2R = \sigma_c D h \quad (6.2)$$

where σ_c is the unconfined compressive strength of the ice; D is the diameter of the structure and h is the ice thickness.

However, Eq. 6.2 is not practically applicable for engineering investigations due to the next assumptions:

- The load is assumed as distributed uniformly on the structure's face and the ice properties are homogenous while in fact the compressive strength varies across the contact.
- In addition the equation doesn't consider ice drift velocity, geometrical properties of the structure, roughness of the material etc.

6.4.2 Korzhavin's approach

These factors that aren't considered in Eq.6.2 were included in Korzhavin's formula:

$$F = I \cdot K_1 \cdot K_2 \cdot \sigma_c \cdot D \cdot h \quad (6.3)$$

where

I is the indentation factor including stress-strain distribution within the ice field. This factor is determined by the ice crystallographic structure and takes into account the difference between the unconfirmed- and real stress distributions. This coefficient depends on the internal structure of ice (columnar or granular) and such factors as the aspect ratio, strain rate, etc. According to Korzhavin (1962), the indentation factor I is equal 2.47, when the ice width is greater than $15D$.

K_1 is the contact factor representing incomplete contact between the ice edge and the structure. It is assumed to be between 0.4-0.7 when the diameter of the structure is in the range of 3-10 m.

K_2 is the shape factor depending on the structure cross-section form (it is 1.0 for flat structures and 0.9 for circular ones).

σ_c is the unconfined compressive strength,

D is the structure's diameter and

h is the ice thickness.

This formula is based on analysis of river ice actions and according to Korzhavin (1962) this equation holds for vertical structures (slope angle is in the range 75° - 90°). However, Løset et al. (1998) reports that Korzhavin's equation significantly overestimates the loads on big structures and the main causes of this are:

- Scale effect. Korzhavin's experiments were carried out on piles of small diameters, which were several times less than the diameters of offshore structures. Moreover, the ice strength decreases when scale increases and these phenomena weren't covered by the measurements.
- Non-homogeneous ice field and non-simultaneous ice failure. In reality ice fields are not homogeneous which results in failures developing from the impaired areas. It leads to non-simultaneous ice failure and incomplete contact.
- The unconfined compressive strength σ_c doesn't represent the total stress distribution around the structure.

6.4.3 Michel and Thussaint approach

Michel and Thussaint (1977) presented a modified formula based on Korzhavin's approach. The variation of the unconfined compressive strength σ_c is defined as a function of the strain rate $\dot{\epsilon}$. The strain rate is defined as $\dot{\epsilon} = v/(4D)$, where v is the rate of indentation, D is the effective diameter.

Korzhavin's formula (Eq.6.2) is valid for strain-rates from 10^{-3} to $10^{-2} s^{-1}$, where ice exhibits brittle behaviour and the ice strength decreases (see fig. 2.3). Michel and Thussaint's approach covers all zones, i.e. the ductile regime, the transition zone and the brittle regime. Michel and Thussaint (1977) presented the following correlations (note that the notations are similar to that of Korzhavin, 1962):

$$F = I \cdot K_1 \cdot K_2 \cdot \sigma_c \cdot D \cdot h \cdot \left(\frac{\dot{\epsilon}}{\dot{\epsilon}_0}\right)^{0.32} \quad \text{for} \quad 10^{-8} \leq \dot{\epsilon} \leq 5 \cdot 10^{-4} s^{-1} \quad (6.4)$$

$$F = I \cdot K_1 \cdot K_2 \cdot \sigma_c \cdot D \cdot h \cdot \left(\frac{\dot{\epsilon}}{\dot{\epsilon}_0}\right)^{0.32} \quad \text{for} \quad 5 \cdot 10^{-4} \leq \dot{\epsilon} \leq 10^{-2} s^{-1}$$

$$F = I \cdot K_1 \cdot K_2 \cdot \sigma_c \cdot D \cdot h \quad \text{for} \quad \dot{\epsilon} > 10^{-2} s^{-1}$$

The reference strain rate $\dot{\epsilon}_0$ is $5 \cdot 10^{-4} s^{-1}$, other values of the coefficients in Eq. 6.4 are introduced in Table 6.1.

Table 6.1: Comparison of Korzhavin's formula with Michel and Thussaint approach

Approach's author	Indentation factor, I	Contact factor, K_1	Shape factor, K_2
Korzhavin (1962)	2.47	0.4-0.7 ³⁾	1.0 ⁵⁾ 0.9 ⁶⁾
Michel and Thussaint (1977)	2.97 ¹⁾ 3.0 ²⁾	1.0 ⁴⁾ 0.3 ³⁾	1.0 ⁵⁾ 0.9 ⁶⁾
1) For $\dot{\epsilon} \leq 5 \cdot 10^{-4} s^{-1}$. 2) For $\dot{\epsilon} > 10^{-2} s^{-1}$. 3) For incomplete contact or continuous crushing. 4) For full contact. 5) For rectangular cross-section structures. 6) For circular cross section structures			

However, this approach might predict incorrect results because in reality the strain rate is not constant as presented in Eq. 6.4 due to the non-simultaneous ice failure (see fig.6.6). The

actual strain rate will vary along the contact area and the components of the strain rate in different directions might exhibit different behaviours. Again, the unconfined compressive strength σ_c doesn't represent the total stress distribution around the structure.

6.4.4 Empirical correlation based on field measurements

Despite that there are several approaches to estimate ice loads on vertical structures, the design should be based measurements on real structures. Some guidance might be given by ISO 19906 (2009) where empirical correlations for the global pressure on a vertical structure are given. A more simplified equation is applied to characterize the ice action:

$$F = pA \quad (6.5)$$

where p is the average effective pressure acting on the nominal contact area A .

According to Løset et al. (1998) this formula is more suitable because the average effective pressure in the experiments could be expressed F/Dh and it should consider all aspects that have not been covered by Korzhavin's equation.

6.5 Ice action on sloping structures

Sloping structures are considered to be effective for ice loads reducing because the ice flexure strength is lower than its compressive strength. Therefore, level ice acting on a sloped surface is likely to fail in bending rather in crushing mode that is typical for a vertical structure. It should be noted that crushing could take place locally as a part of bending failure or this failure mode might replace bending at high velocities of the coming ice. For an upward sloped structure the ice sheet's bottom will be subject to tension, while its top will be subject to compression and versus versa for a downward sloped structure. Usually, radial-and circumferential cracks form due to the high stress levels during bending of the ice sheet. However, sometimes the ice thickness, velocity, etc. might result in reversing of the ice failure pattern for the same structure. It should be noted that structures with the sloping angle that is greater than 80 degrees are practically considered as vertical in terms of forces.

Traditionally, the interaction process might be divided into such substeps as (i) failure of intact ice, (ii) ride-up of broken ice pieces, (iii) ice rubbles accumulate on the slope and (iv) clearing of the ice rubble accumulations (ISO 19906, 2010).

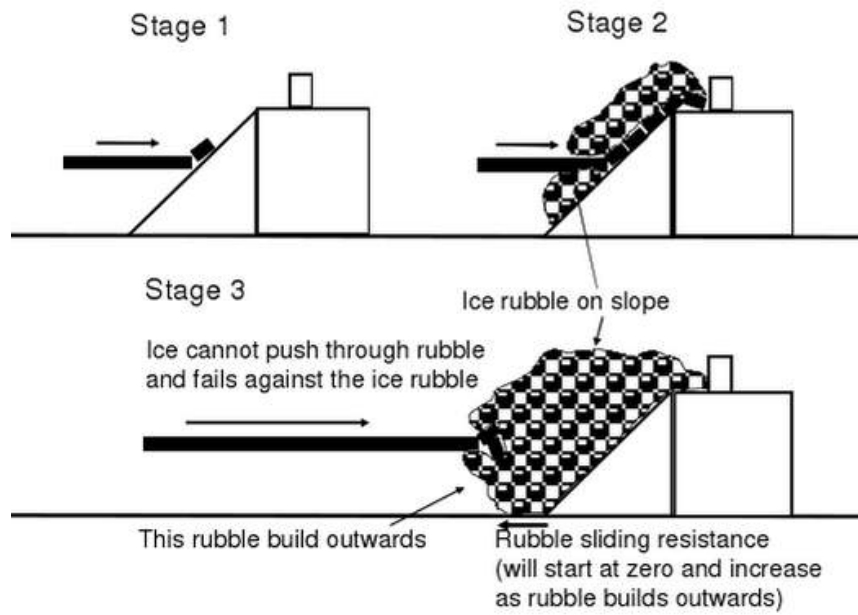


Figure 6.8: Phases of ice interaction with a sloping structure in shallow water (Palmer and Croasdale, 2012)

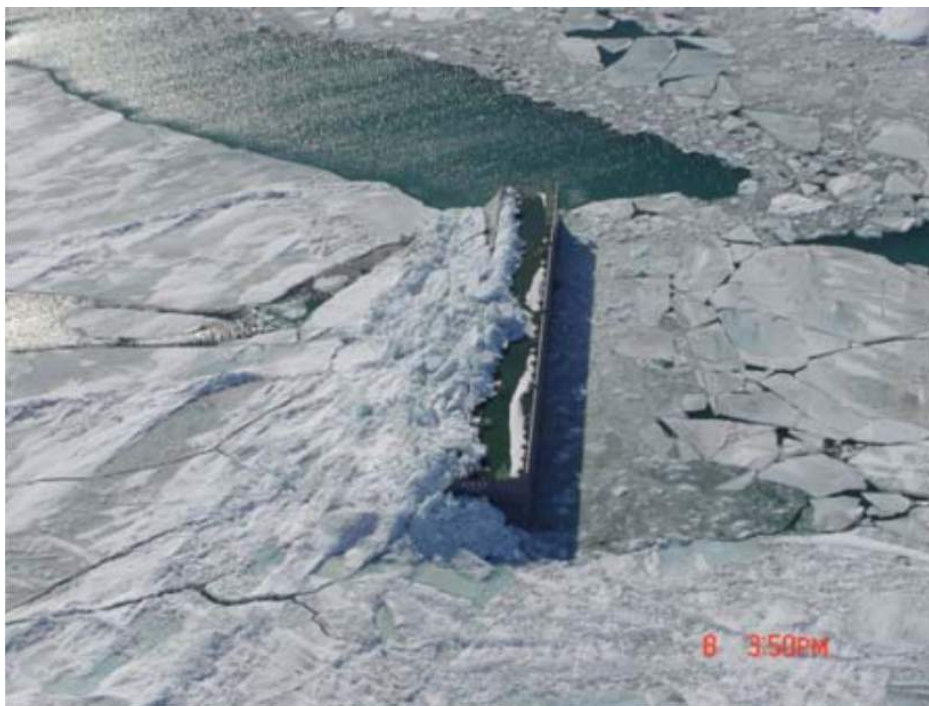


Figure 6.9: Ice rubble in front of a barrier in the North Caspian Sea (Croasdale et al., 2011).

As discussed above the ice rubble accumulating process affects the ice interaction with both sloping and vertical structures in shallow waters. Hence, the ice interaction will be

somewhat different (see fig.6.8) because clearing of ice rubble doesn't occur. The process of the interaction is the next:

- The first stage corresponds to the ice failing in bending and riding up to the top of the inclined face. Some ice rubbles start to accumulate on the inclined face of the structure.
- Then, in the second phase, ice pushes through the ice rubble and it still fails in bending. Together with this, the vertical force coinciding with the weight of the ice rubble on the slope results in increasing the rubble sliding resistance.
- Finally, in the third stage when ice can't push through the ice rubble due to high sliding resistance, the ice fails in rubbing against the grounded ice rubble.

This fully correlates with the results of model tests of the SIB presented by Repetto-Llamazares et al. (2013) and could be observed from pictures of structures in the North Caspian Sea (see fig. 6.9).

When ice rubble is grounded, the ice loads are partially dissipated due to the sliding resistance of the ice rubbles (fig.6.7, b). Although this makes beneficial the ice rubble generation (described in Chapter 5.3), the effect of the ice rubble in the vicinity of structures is difficult to consider due to a complex nature of this phenomenon.

The following sections introduce the main approaches used for calculations of ice loads on sloping structures.

6.5.1 Croasdale's approach

Generally, the global ice load on vertical structures is a sum of the vertical F_V and horizontal F_H force components, which are related by the next relationship:

$$F_V = \frac{F_H}{\xi} \quad (6.6)$$

where

$$\xi = \frac{\sin\alpha + \mu\cos\alpha}{\cos\alpha - \mu\sin\alpha} \quad (6.7)$$

where μ - the ice-structure friction coefficient and α is the slope of structure face from horizontal.

The horizontal component could be derived from a model based on a semi-infinite beam on an elastic foundation (Løset et al., 2010):

$$F_H = C_1 D \sigma_f \left(\frac{\rho_w g h_i^3}{E} \right)^{\frac{1}{4}} + C_2 D z h_i \rho_i g \quad (6.8)$$

where

C_1 is a coefficient given as:

$$C_1 = 0.68 \frac{\sin\alpha + \mu \cos\alpha}{\cos\alpha - \mu \sin\alpha} \quad (6.9)$$

C_2 is a coefficient calculated as:

$$C_2 = (\sin\alpha + \mu \cos\alpha) \cdot \left(\frac{\sin\alpha + \mu \cos\alpha}{\cos\alpha - \mu \sin\alpha} + \cot\alpha \right) \quad (6.10)$$

E – Young's modulus,

D – the width of the structure,

σ_f – the ice flexural strength,

ρ_w and ρ_i – sea water and ice density, respectively

h_i – the ice thickness,

z – the vertical distance the ice up the inclined face,

g – standard acceleration.

The first term in Eq. 6.7 presents the braking force due to flexural failure of the ice sheet and the second term is the ride-up force. However, due to the characterized interaction process in shallow waters of the North Caspian Sea this practice might be not correct. Croasdale (1988) suggested adding a correction factor c defined as:

$$c = \left(1 + \frac{\pi^2 L_c}{4D} \right) \quad (6.11)$$

where D is the effective diameter of the structure and L_c is the characteristic length given as:

$$L_c = \left(\frac{E h_i^3}{12 \rho_w g (1 - \nu^2)} \right)^{\frac{1}{4}} \quad (6.12)$$

where ρ_w is the seawater density, ν is Poisson's ratio of ice.

This correction coefficient is multiplied to the first term in Eq.6.8 in order to account 3D effects.

6.5.2 ISO approach

Palmer and Croasdale (2012) offered a modified model that takes into account 3D effects and the presence of ice rubbles on the sloping surface of the structure subjected to ice action. This model also idealizes the ice sheet as an elastic beam on elastic foundation and assumes that the fracture occurs when the bending stress exceeds a critical strength.

The horizontal component of the total force according to this method according to ISO 19906 (2010) is given as:

$$F_H = (F_B + F_P + F_R + F_L + F_T) \cdot \frac{1}{1 - \frac{F_B}{\sigma_f l_c h_i}} \quad (6.13)$$

where the breaking force component F_B is given by:

$$F_B = 0.68 \xi \sigma_f \left(\frac{\rho_w g h_i^3}{E} \right)^{\frac{1}{4}} \left[D + \frac{\pi^2 L_c}{4} \right] \quad (6.14)$$

The last term in Eq. 6.14 involves the characteristic length L_c of an ice beam on an elastic foundation and considers ice fracturing near the structure's corners given in Eq.6.12.

The term F_P considering load required to push the ice sheet through the ice rubbles that is determined by:

$$F_P = D h_r^2 \mu_i \rho_i g (1 - e) \left(1 - \frac{\tan \theta}{\tan \alpha} \right)^2 \left(\frac{1}{2 \tan \theta} \right) \quad (6.15)$$

where h_r is the rubble height, μ_i is the ice-ice friction, e is porosity of ice rubbles, θ is the angle of the rubbles inclination to the horizon.

The horizontal load component F_R needed to ice blocks up the slope through the ice rubble:

$$F_R = DP \frac{1}{\cos \alpha - \mu \sin \alpha} \quad (6.16)$$

where

$$\begin{aligned} P = & 0.5 \mu_i (\mu_i + \mu) \rho_i g (1 - e) h_r^2 \sin \alpha \cdot \left(\frac{1}{\tan \theta} - \frac{1}{\tan \alpha} \right) \cdot \left(1 - \frac{\tan \theta}{\tan \alpha} \right) \\ & + 0.5 (\mu_i + \mu) \rho_i g (1 - e) h_r^2 \cdot \frac{\cos \alpha}{\tan \alpha} \cdot \left(1 - \frac{\tan \theta}{\tan \alpha} \right) + h_r h_i \rho_i g \cdot \\ & \cdot \frac{\sin \alpha + \mu \cos \alpha}{\sin \alpha} \end{aligned} \quad (6.17)$$

The additional force F_L that is necessary to lift the ice rubble on top of the advancing ice sheet prior to breaking it:

$$\begin{aligned}
F_L = & 0.5Dh_r^2 \rho_i g(1 - e)\xi(\cot\theta - \cot\alpha) \cdot (1 - \tan\theta \cot\alpha) \\
& + 0.5Dh_r^2 \rho_i g(1 - e)\xi \tan\varphi(1 - \tan\theta \cot\alpha)^2 \\
& + D\xi ch_r(1 - \tan\theta \cot\alpha)
\end{aligned} \tag{6.18}$$

where c and φ are the cohesion and the friction angle of the ice rubbles, respectively.

The force F_T required to turn the ice block at the top of the slope due to the interaction with the top of the structure is:

$$F_T = 1.5Dh_r^2 \rho_i g \cdot \frac{\cos\alpha}{\sin\alpha - \mu\cos\alpha} \tag{6.19}$$

Note that the vertical component of the global force is calculated as in the mathematical relationship given in Eq. 6.6.

The model is sensitive to the friction coefficient μ , the height of the ice ride-up h_r , so these parameters should be carefully considered with the following recommendations of Palmer and Croasdale (2012):

- The rubble angle θ is practically lower to 5-10° than the slope of the structure. However, the angle of repose is determined by the ice thickness, its strength, velocity, friction and the waterline diameter. Note that, the angle of repose equal to the slope angle is equivalent to a single layer of ice riding up to the slope such as in the model described above. The selection of the angle should be based on observations from similar structures in the region of interest.
- The height of ice rubbles is a key issue because as described in Chapter 6.3 a wide structure arranged in shallow-water conditions is more likely to generate high-rubble accumulations in front. According to ISO 19906 (2010) the height of ice rubbles might exceed 12-20 m.

In conclusion, the high interaction velocity might inverse the bending failure mode to shear (for sloping structures), which can result in increasing the global ice forces. The velocity effect is complex to be accounted while ISO 19906 (2010) can provide limited guidance. One can note that the slope angle, roughness of the surface being subjected to ice loads, the ratio between the ice thickness, the structure's width should be considered in order to estimate the effect of the velocity of the interaction.

Thus, Palmer and Croasdale (2012) report that this approach is not correct for shallow water conditions when ice build-up exists and at some specific cases the gap between the ice loads calculated by the ISO 19906 (2010) approach and the real loads might be significant. Løset et al. (2006) reports that the model described in ISO 19906 (2010) “does not take into account a situation where the thickness of the rubble on the ice sheet near the structure reaches a level at which the ice sheet breaks in shear or flexure and then the rubble submerges. This may happen before the maximal action as predicted by Croasdale’s formula is reached. Therefore at some particular conditions, this method can overestimate the actions”.

6.6 Summary

The chapter deals with the theoretical approaches used for calculations of ice loads on vertical and sloping structures.

The governing design scenario in the North Caspian Sea is likely the limit stress scenario, while in deeper locations the limit force scenarios will likely control the design.

Semi-empirical approaches for vertical structures assume that the strain rate is constant and the unconfined compressive strength σ_c is used to account the total stress distribution around the structure.

The models for sloping structures idealize the ice sheet as an elastic beam on elastic foundation and assume that the fracture occurs when the bending stress exceeds a critical strength. One can conclude that the approaches either for vertical or sloping structures are highly sensitive to their parameters, the values for calculations input should be accurately determined.

Finally, these models do not consider the effect of grounded ice rubble in front of the structure, when the appearing ice sheet will failure against the ice rubbles and the global ice load is decreased by the sliding resistance of the grounded ice rubbles (Chapter 6.3). Hence, the considerable scatter of the loads calculated by using of these formulas is expected.

Chapter 7. The FEM Theory

The Finite Element Method (FEM) has been developed into a key method for modelling of various structures and systems. Being initially invented for engineering problems related to mechanics of solids and structures, the FEM has been intensively adopted for simulations of the ice-structure interaction and for calculations of ice loads on structures.

This chapter provides description of the FEM theory that is required to solve problems described in the previous chapters, so approaches that are relevant for modelling of the ice-structure interaction process will be closely looked upon. It should be noted that this chapter is aimed to be informative enough within the used FEM while for more detailed information the reader is referred for specialized literature sources.

The FEM theory is mainly given with reference to Liu and Quek (2003), Lu et al. (2012), Gürtner, (2009) and Sand (2008) amongst other, while references about Ansys Inc. (2009a, 2009b) is taken from a tutorial course dedicated to the Explicit Dynamics system.

7.1 State-of-the-Art: Computational Methods for the ice-structure interaction modelling.

Nowadays, two fundamental numerical techniques depending on a solution approach of the general boundary value problem are used for simulating of problems related to the complex interaction processes described above. Namely, there are:

- Continuum methods including the Finite Element Method (FEM),
- Particle methods such as the Discrete Element Method (DEM).

In the DEM the material model is assumed as a set of rigid bodies interconnected to each other by rheological models (e.g. springs, dashpots). Each discrete element of the assembly is characterized by own solution of Newton law of motion with respect to the corresponding contact formulation.

On the other hand, the FEM applies the material with defined constitutive properties (e.g. stress, strain, etc.) and it is based on the next fundamental conservation laws (Gürtner, 2009):

- Conservation of mass:

$$\frac{D\rho}{Dt} + \rho \cdot \text{div}(v) = 0 \quad (7.1)$$

- Conservation of linear momentum:

$$\nabla \cdot \sigma + \rho \cdot b = \rho \dot{v} \equiv \frac{Dv}{Dt} \quad (7.2)$$

- Conservation of energy:

$$\rho \cdot w^{int} = D : \sigma - \nabla \cdot q + \rho \cdot s \quad (7.3)$$

- Conservation of angular momentum:

$$\sigma = \sigma^T \quad (7.4)$$

where ρ is the mass density, v is the velocity field, \dot{v} is the acceleration field, t is the time, D/Dt is the total differential, σ is the stress tensor; σ^T is the transposed stress tensor σ , b is the body force, w^{int} is the internal rate of energy per unit volume, D is the rate-of- deformation tensor, $(:)$ denotes a scalar product between second order tensors, q is the heat flux and $(\rho \cdot s)$ is the heat source per unit volume.

One can notice that different approaches within these methods might be applied for simulations of different engineering problems related to modelling of the transition from

continuum to discontinua. Some of these computational methods have been successfully implemented for the ice indentation problem. Namely, such approaches are:

- the Discrete Element Method (DEM) with cohesive contacts,
- the Cohesive Zone Element (CEM or CZM),
- the Extended Finite Element Method (XFEM) and
- the conventional FEM combined with element erosion technique.

Despite that these methods use different techniques, all of them are based on the continuum approach coupled with the pre-failure process, which means that an ice element is assumed to be failed when a certain failure criterion is reached during the simulation. Therefore, the failure of the material is an output of the simulation.

The DEM with cohesive contacts combines the FEM and the DEM in order to simulate the ice-structure interaction and rubble accumulation. Thus, when ice rubbles have been produced during the interaction, the DEM comes up to simulate the ice accumulation and clearing processes. To attain this, discrete elements follow to a cohesive law for the damage initiation and evolution, so when the crack initiation criterion is exceeded, the degradation of the contact stiffness begins.

The CEM applies similar cohesive elements that are implemented into the model as inter-elements between two adjoining finite elements (bulk elements). The cohesive elements inserted between the bulk elements ensure the material separation along the boundaries of these finite elements according to the traction separation law. Additionally, the mass of the cohesive elements is negligible in comparison to the bulk elements. Since the CEM is mainly based on the cohesive elements providing the material separation, a simplified fashion can be used for modelling of these finite elements. Lu et al. (2012) reports that the main challenge of the CEM implementation is the convergence issue.

It should be emphasized that both methods allow only cracks propagation along the finite elements in a predefined discrete manner. Hence, this imposes the mesh dependence of these schemes. The XFEM, in turn, avoids this drawback, e.g. it is theoretically a mesh free method (Lu et al., 2012). Even though this method allows incorporation of such discontinuities as cracks, fractures into the FEM model, the crack initiation and propagation should be still implemented into the model. There is a set of reports dedicated to the implementation of the XFEM, the CEM, etc. For more detail the reader is referred to Lu et al. (2012) who carried out a comparison of these numerical techniques.

However, these approaches require significant computational capacities (such as clusters). For instance, Gürtner (2010) ran a cohesive element model by using the NRCan cluster in Canada while the study carried out by Lu et al. (2012) involved the cluster technology with 12 CPUs. Hence, if the available computational capacity is limited, the conventional numerical approach combined with erosional technique could be applied.

Being rather simple approach, the FEM with erosion technique is a computationally effective method to simulate the ice indentation process. The following discussion will be done with respect to the main features and challenges related to the implementation of this method in this thesis.

7.2 The conventional FEM combined with element erosion scheme

The procedure of computational modelling using the FEM broadly consists of four steps (Liu and Quek, 2003):

- Modelling of the geometry.
- Meshing (discretization).
- Specification of material property.
- Specification of boundary, initial and loading conditions.

Generally, all of these steps are typical for the realization of any numerical model. But the main feature of the FEM with erosion technique lies in the specification of the material property, because the success of its implementation heavily depends on a constitutive model that has been applied. Therefore, the model of the material must provide a correct stress/strain relationship at its failure while the failure mechanisms must follow to the mechanisms that are observed during experiments. There are several substeps that must be implemented within this item (Lu et al., 2012):

- 1) the constitutive model with the stress-strain relationship, yield criteria and the flow rule (if the material properties include plasticity);
- 2) the damage initiation criteria and the damage evolution law.

When a failure criterion has been exceeded, a degraded element of the material is removed from the calculations and from the mesh. The degradation evolution law is defined by the user and explicitly modelled.

However, since this thesis focuses on specific points of the FEM realization for the ice-structure interaction, the following sections will present some of these aspects instead of

describing all of them, but, first of all, the discussion starts with a brief description of the chosen FEM system.

7.2.1 Analysis system

To get a broad understanding of this method background, it is useful to start the description with the analysis system applied for the finite element simulation. The finite element model has been implemented into the “Explicit Dynamics” system within Ansys 15.0 Workbench. “Explicit Dynamics” (i.e. explicit solver) can be applied for dynamic simulations wherein large deformations and strains, non-linear material behaviour, complicated contacts between modelling geometries are expected. However, this system is normally used for short-time processes, which demands energy error control during the simulation. One more reason to use this system is the ability of the erosion implementation into the simulation.

The Explicit Dynamics system defines the solution of the problem by expressing the conservation of mass, energy and momentum in Lagrange coordinates coupled with initial and boundary conditions, material model, etc. The density of material at any time might be defined from the current volume of the zone and its initial mass (ANSYS Inc., 2009a):

$$\frac{\rho_0 V_0}{V} = \frac{m}{V} \quad (7.5)$$

The conservation of momentum, which relates to the acceleration of the stress tensor σ_{ij} , is described by the next partial differential equations (ANSYS Inc., 2009a):

$$\rho \ddot{x} = b_x + \frac{\partial \sigma_{xx}}{\partial x} + \frac{\partial \sigma_{xy}}{\partial y} + \frac{\partial \sigma_{xz}}{\partial z} \quad (7.6)$$

$$\rho \ddot{y} = b_y + \frac{\partial \sigma_{yx}}{\partial x} + \frac{\partial \sigma_{yy}}{\partial y} + \frac{\partial \sigma_{yz}}{\partial z} \quad (7.7)$$

$$\rho \ddot{z} = b_z + \frac{\partial \sigma_{zx}}{\partial x} + \frac{\partial \sigma_{zy}}{\partial y} + \frac{\partial \sigma_{zz}}{\partial z} \quad (7.8)$$

The conservation of energy is defined as (ANSYS Inc., 2009a):

$$\dot{e} = \frac{1}{\rho} (\sigma_{xx} \dot{\epsilon}_{xx} + \sigma_{yy} \dot{\epsilon}_{yy} + \sigma_{zz} \dot{\epsilon}_{zz} + 2\sigma_{xy} \dot{\epsilon}_{xy} + 2\sigma_{yz} \dot{\epsilon}_{yz} + 2\sigma_{xz} \dot{\epsilon}_{xz}) \quad (7.9)$$

These equations are solved for each time step for each mesh element within the model based on input values at the end of the previous time step (ANSYS Inc., 2009a). Note that only the energy conservation is constantly displayed in order to show the accuracy of the solution, while the mass and momentum are constrained by the numerical solver.

The system uses the explicit scheme based on half-step central differences. When forces due to internal stresses, boundary conditions and contacts are defined at the nodes of the elements, the nodal accelerations are calculated by dividing the forces by the mass (ANSYS Inc., 2009a):

$$\ddot{x}_i = \frac{F_i}{m_i} + b_i \quad (7.10)$$

where \ddot{x}_i are the components of the nodal acceleration ($i=1,2,3$), F_i are the forces acting on the node, m_i is the mass of the node and b_i are the components of the body acceleration.

With the accelerations at time $n-1/2$ determined, the velocities at time $n+1/2$ are found from:

$$\ddot{x}_i^n = \frac{\dot{x}_i^{n+1/2} - \dot{x}_i^{n-1/2}}{\Delta t^n} \text{ or } \dot{x}_i^{n+1/2} = \dot{x}_i^{n-1/2} + \ddot{x}_i^n \Delta t^n \quad (7.11)$$

Finally, the positions are updated to time $n+1$ by integrating the velocities:

$$\dot{x}_i^{n+1/2} = \frac{x_i^{n+1} - x_i^n}{\Delta t^{n+1/2}} \text{ or } x_i^{n+1} = x_i^n + \dot{x}_i^{n+1/2} \Delta t^{n+1/2} \quad (7.12)$$

To summarize, these equations are the basis of the explicit method because only knowledge of the input values at the end of the previous cycle is required to calculate x_i^{n+1} and $\dot{x}_i^{n+1/2}$. One of the main features that could be concluded from these equations is that the integration time step should be small enough to attain an accurate solution. Note that implicit methods, in turn, perform large time steps than explicit schemes, so more computational capacities are required within each cycle. However, an implicit solution might be used for transient simulations, but for models involving high non-linearity. Furthermore, this approach meets convergence issues because required time steps must be small enough otherwise the simulation time becomes unacceptable. Hence, explicit schemes perform greater accuracy accompanying less computational efforts than implicit ones.

A drawback of the described explicit solutions is that all elements follow the deformation of the body and cannot be displaced out of the body's boundaries. This results in the possibility of the accumulation of large energy errors. Again, it should be noted that the principle of the conservation of energy is used to monitor the accuracy of the solution and the energy error at each cycle (time step) is defined as:

$$\text{Energy error} = \frac{|(\text{Current energy}) - (\text{Reference energy}) - (\text{Work done})|}{\text{Max}(|\text{Current energy}|, |\text{Reference energy}|, |\text{Work done}|)} \quad (7.13)$$

In this thesis, the energy error has been set 10%, which means that if the energy error reaches 10%, the solution is treated as unstable and, hence, stops. Nevertheless, the Explicit Dynamics system can provide reasonable results upon condition that the energy error is acceptable.

7.2.2 The constitutive model

As described in Chapter 6, ice exhibits both brittle and ductile behaviours while its failure modes depending on the strain rate, temperature, grain size, loading direction, etc. include crushing, buckling, creep, rubbing. Ice might fail if the stress exceeds its tensile strength and the material cannot sustain this tensile because of the formation of cracks. Under increasing compressive loads, in turn, the formed cracks coalesce and lead to the ice crushing. The described processes relate to the transition state from a continuum to discontinuous material. Due to that ice cannot be treated as a purely continuum elasto-plastic material.

However, the classical yield conditions (such as von Mises, Tresca) broadly applied for metals are not valid for ice due to the next factors:

- The compressive strength of ice depends on hydrostatic pressure,
- The compressive strength of ice is greater than its tensile strength.

Hence, a constitutive model with the stress-strain relationship, yield criteria that complies the pressure dependency of ice is crucial for the numerical simulation. This is considered in the models borrowed from geophysics for Mohr-Coulomb and Drucker-Prager criterion (see fig.7.1).

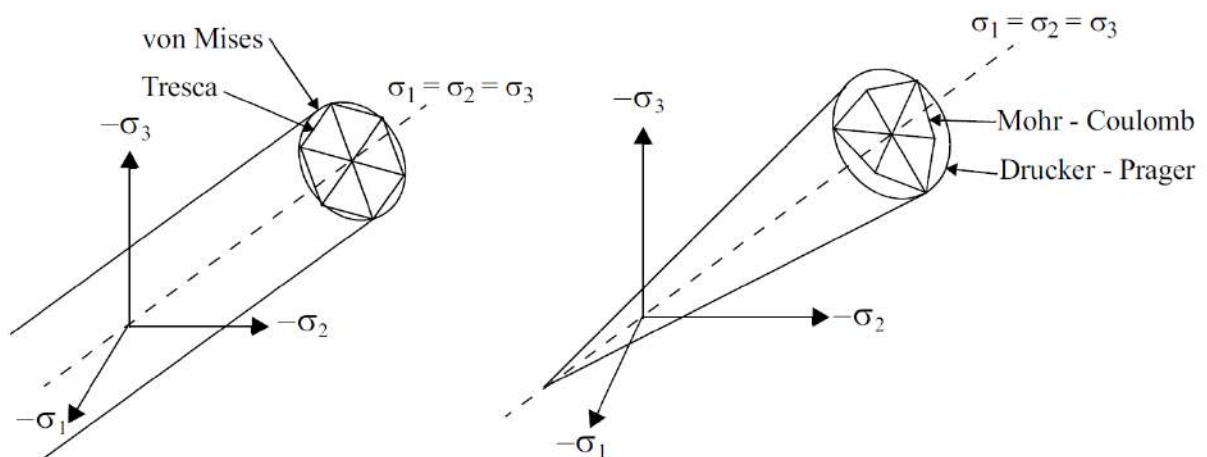


Figure 7.1 Representation of a) Tresca's and von Mises yield criteria and b) Mohr- Coulomb and Drucker-Prager yield criteria. (Sand, 2008)

The Mohr-Coulomb (MC) plasticity model is applied for granular materials that are under monotonically loaded:

$$\tau = c + \sigma \tan \varphi \quad (7.14)$$

where τ is the shear stress of the material, c is the cohesion of the material and φ is the angle of internal friction.

On the other hand, Drucker-Prager (DP) model smoothly approximates the Mohr-Coulomb hexagonal surface into the cone (fig 7.1, b) that coincides with the outer corners of the Mohr-Coulomb surface. The linear model is defined as (Lu et al., 2012):

$$F = t - p \tan \beta - d = 0 \quad (7.15)$$

where d is the cohesion of the material, β is the friction angle, $p = \frac{tr(\sigma)}{3}$ is the hydrostatic part of the stress tensor σ and $t = \sqrt{\frac{3}{2}S:S}$ is the equivalent Mises stress with S being the deviatoric part of the stress tensor σ .

In this thesis, a modified form of Drucker-Prager model called a hyperbolic model has been implemented into the FEM code by using of a tension cut-off p_t (see fig. 7.2).

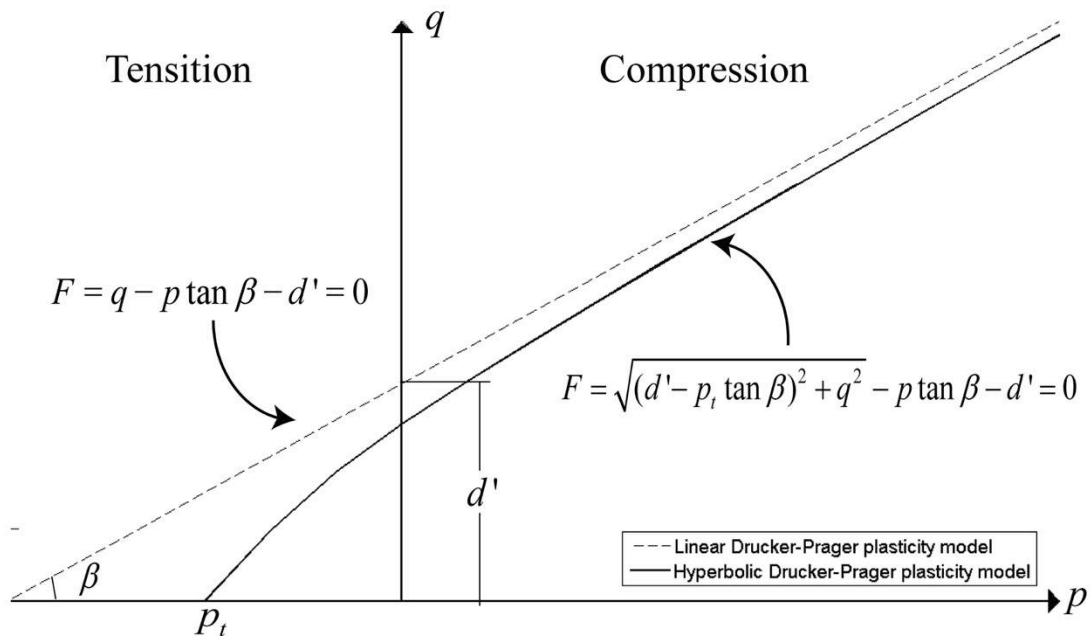


Figure 7.2: The hyperbolic Drucker-Prager plasticity model (Lu et al., 2012).

Note that the parameters of DP model correlate with the MH model parameters. Weizhi (2014) defined the relationship between these plasticity models (see table 7.1). Thus, the

difference between parameters of these models decreases with increasing friction angle φ of MC model. The required parameters of DP model have been calculated based on this relationship, because the parameters of MC model are commonly used for the description of ice.

Table 7.1. Parameter differences between associated and non-associated flow (after Weizhi, 2014).

Friction angle of the MC model φ	Associated flow		Non-associated flow	
	Friction angle of DP model β	d/c	Friction angle of DP model β	d/c
10°	16.7°	1.70	16.7°	1.70
20°	30.2°	1.60	30.6°	1.63
30°	39.8°	1.44	40.8°	1.50
40°	46.2°	1.24	48.1°	1.33
50°	50.5°	1.02	53.0°	1.11

However, these yield conditions (MC and DP) consider unlimited increase in material strength with increasing hydrostatic pressure, which is not fully correct for the anisotropic behaviour of ice. Furthermore, caution is recommended when using of the parameters of either MC or DP models, because the no peak or ultimate shearing resistance might be detected during tests. In addition to this, there are still significant uncertainties associated with constitute models that could perfectly describe ice rubble (see Chapter 6.3).

It should be noted that some researches try to adopt material models such as the Crushable Foam model, the Brittle damage model, Holmquist-Johnson-Cook Model, etc. (Nisja, 2014) that were initially formulated for concrete or ceramics, i.e. are initially inappropriate for such materials as ice. However, caution is strongly recommended for accurate defining of appreciate parameters of such models because the results obtained during the simulations based this approach might be not realistic or might not comply the physical processes taking place during the ice-structure interaction.

To summarize, along with the DP model parameters, the isotropic elasticity parameters (such as Young's modulus, Poisson ratio) have been implemented into the material model. These parameters describe the linear elastic material behaviour until the yield criterion is reached. The software programme automatically derives shear modulus G and bulk modulus K as (ANSYS Inc., 2009c).

$$G = \frac{E}{2(1 + \nu)} \quad (7.16)$$

and

$$K = \frac{E}{3(1 - 2\nu)} \quad (7.17)$$

where E is the effective Young's modulus, ν is the Poisson's ratio (see Chapter 2.2).

7.2.3 The damage initiation criterion and the damage evolution law

When the yield criterion defined in the constitutive model is exceeded, the material is considered to have a plastic behaviour according to a plasticity flow rule until the damage initiation criterion is reached. One can notice that the numerical realization of the ice fracture mechanics theory within the FEMs has not been reviewed in this section since this topic is wide and is especially important for the CEM, the XFEM, etc. For more details about the fracture mechanics theory the reader is referred to Gürtner (2010), Løset et al. (2006) and Løset et al. (1998).

In this thesis the tensile pressure failure model has been implemented into the finite element analysis. Thus, the maximum tensile pressure of the material introduced in the numerical algorithm is limited by:

$$P < P_{min}(1 - D) \quad (7.18)$$

where P_{min} is the maximum tensile pressure of the material and D is the damage coefficient varying from 0 to 1.0.

The failure initiation takes place if the pressure is lower than the maximum tensile pressure. This corresponds to instant failing of the material. In addition, the coefficient of the damage (varying from 0 to 1.0) provides scaling of the maximum tensile pressure when a damage evolution law is set by the material definition. It should be noted that this failure model could be implemented only for solid bodies.

7.2.4 Meshing

Meshing is a numerical process discretizing the geometry into elements using a set of nodes. The solution for an element can be approximated very easily by using simple functions such as polynomials. The solutions for all of the elements, thus, form the solution for the whole problem domain (Liu and Quek, 2003). In this thesis Lagrange mesh based on quadrilateral element meshes has been applied to all bodies involved into the finite element model. It should be noted that quadrilateral element meshes are more complicated to generate but the simulation results are expected to be more accurate than for triangulation element meshes.

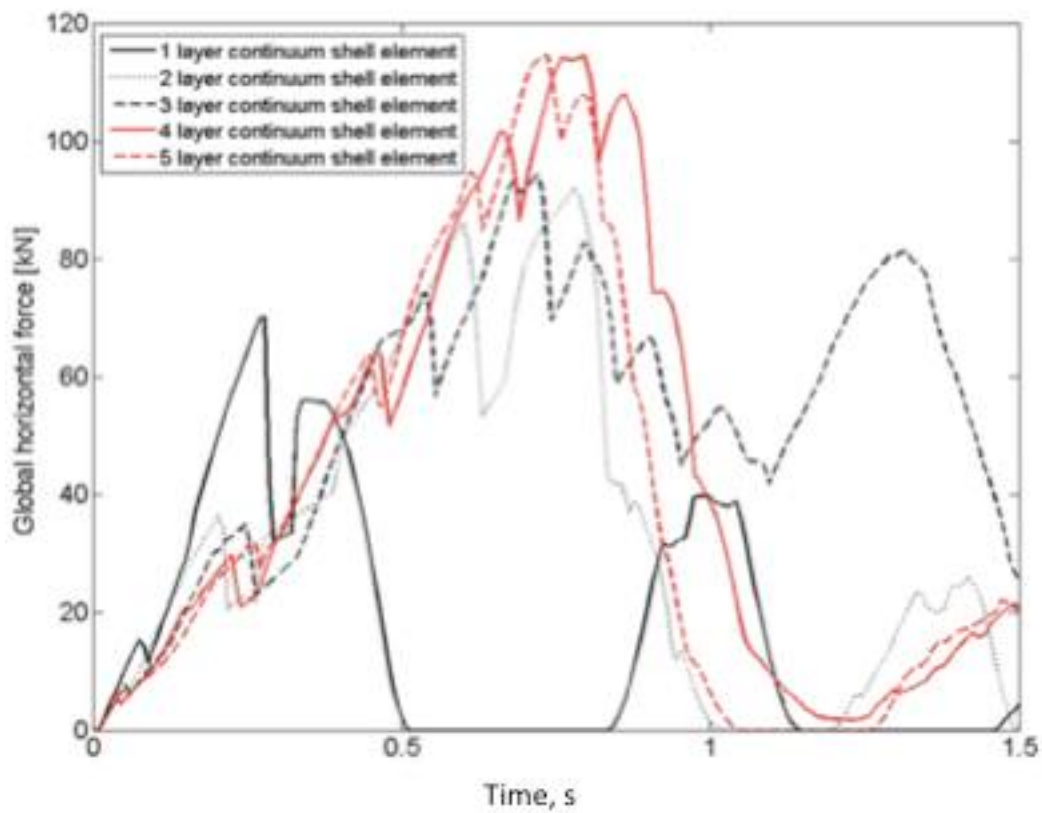


Figure 7.3: Bending failure tests with different layers of continuum element (Lu et al., 2012).

As described in Chapter 7.1 the CEM, the DEM and the conventional FEM with erosion control are heavily mesh dependent. Lu et al. (2012) carried out the mesh sensitivity analysis for the conventional FEM combined with the erosion control (fig.7.3). It was found that the loading history tended to converge when four layers of the continuum elements were applied. However, it might be not correct to directly apply this result obtained by Lu et al. (2012) for the problems discussed in this thesis because another type of the FEM software, the geometry of interacting bodies, the material models, etc. were used for the said simulations.

Additionally, the erosion technique is highly sensitive to the mesh size, which causes significant uncertainties related to the implementation of this result of the study done by Lu et al. (2012) to the model used in this thesis. Due to this, only three layers of the continuum elements have been used in this thesis in order to achieve acceptable simulation time (see fig.8.1, fig. 8.5).

7.2.5 Erosion

Note that the term “erosion” in this chapter does not refer to the physical mechanism of failure. It is a numerical mechanism providing automatic removal of elements from the model during simulations.

An element is damaged, when the failure initiation criterion is reached. After this, the failed element of the mesh is entirely removed from the model. Thereby, the erosion technique numerically provides the ‘creation’ of cracks in the material. In Ansys 15.0 Workbench, the erosion of an element might be initiated either by the geometric strain limit or by the material failure. In the first option, an element is removed when the material effective strain reaches the geometric strain limit. Typical values of the geometric strain limit vary from 0.5 to 2.0, but in the most cases the value of 1.5 might be used (ANSYS Inc., 2009b). On the other hand, an element erodes immediately when the damage initiation criteria reaches 1.0. However, the element will be assumed as eroded if any of these criteria are met.

Note that, along with removing failed elements from the simulation, their inertial components are removed as well. This can be avoided by application of a free mass point, which retains the inertia of the removed node so the corresponded momentum is transferred by this free node (see fig.7.5).

The erosion control technique introduced above has been implemented into the numerical model in order to attain more accurate results.

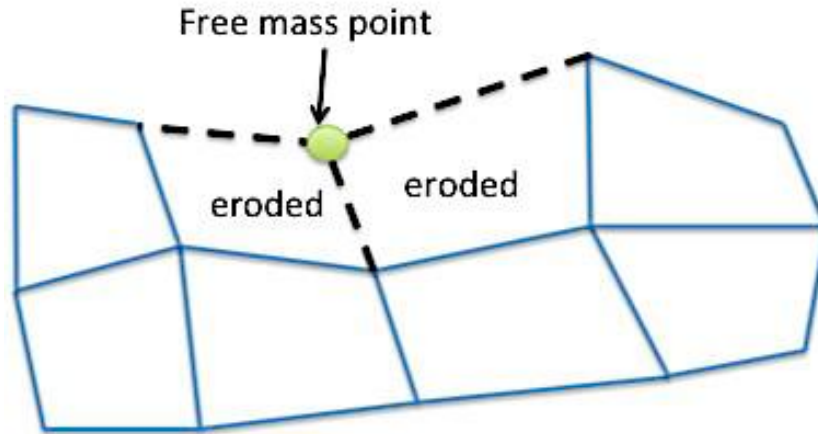


Figure 7.4: Representation of the erosion technique (based on ANSYS Inc., 2009b).

7.2.6 Boundary, initial and loading conditions

The proper design of boundary, initial and loading conditions is a vital step during finite element simulations. Moreover, the set up of these conditions is interfaced with the software graphics so that appropriate loads could be applied either on the geometry bodies or on the elements in the model. However, this should reflect to the design basis because the results of the solution depend on accuracy of the set-up of each of these conditions.

Another issue related to this step is the interaction between water and the ice sheet. The common way to get a correct model that considers the liquid behaviour is to apply specialized tools within the Ansys 15.0 Workbench environment. However, since the available version of the software doesn't include such systems, the water base has been assumed as an elastic foundation consisting of springs attached to the nodal points of the submerged part of the ice sheet. This approach has been implemented into the finite element model by using the elastic foundation with constant hydrostatic coefficients. It should be noted that Sand (2008) reports that such approach might be not fully correct and a sophisticated model consisting of nonlinear discrete springs should be applied. However, despite that this assumption satisfactory accounts buoyancy forces on the ice sheet. All of these conditions that have been realized in the finite element analysis are described in Chapter 8.

7.3 Summary

The chapter provides a brief and comprehensive description of the finite element method with erosion technique.

In general several numerical methods exist, but the FEM combined with erosion technique is one of the most effective from computational point of view. There are several steps that should be performed in order to obtain an adequate numerical model. The material constitutive model and the damage initiation criteria are crucial steps. The material model should reflect to the real model behaviour. Since the classical yield conditions do not comply the pressure dependency of ice, the hyperbolic Drucker-Prager plasticity model is selected for the material description. The main idea of this method is that when the yield criterion of the constitutive model is reached the material follows to a plastic behaviour until the damage initiation criterion is exceeded. After that a damaged element eroded, i.e. removed from the simulations. The erosion technique is modified in order to account masses of removed elements.

The selected numerical method is mesh dependent, so the number of meshing layers should be chosen so that the accuracy of the numerical solution will be not suffered. Because of this, three layers of the continuum elements are anticipated to implement into the numerical model.

Finally, the special approach is used to simulate the water base that will be replaced by an elastic foundation consisting of springs with constant hydrodynamic coefficients.

Chapter 8. The Finite Element Analysis of ice-structure interaction in shallow waters of the North Caspian Sea

The common practices for ice loads calculation discussed in Chapter 6 are based on empirical or semi-empirical approaches. Moreover, the magnitude of ice loads on the same structure might considerably vary depending on which code has been used for the calculations. As discussed, these methods might provide overestimated ice loads in shallow waters when grounded ice rubbles adjacent to the structure partially dissipate the ice loads into the seabed.

The application of the finite element analysis (FEA) may avoid the discussed shortcomings of the empirical practices if all steps established in Chapter 7.2 have been correctly done.

The present section is focused on non-linear finite element simulations of the ice-structure interaction in shallow waters of the Northern Caspian Sea. The finite element analysis is introduced in ANSYS 15.0 Workbench involving the simulations in accordance with the theoretical background presented in Chapter 7. The numerical set-up of the model as well as the parameters of each material model is described. The obtained results will be compared with the theoretical models described in Chapter 6.

8.1 Interaction scenarios realized in the finite element analysis

Even though the ice interaction with different structures has been intensively studied, there are still significant uncertainties related to the application of different empirical equations. Hence, it is of interest to compare the results obtained during the FEA with the empirical ones.

Initially, it was proposed to simulate the ice-structure interaction process, which involved three stages described in Chapter 6.4: (i) the initial interaction of the ice sheet with the structure, (ii) the rubble build up stage and (iii) the coming ice sheet fails against the grounded ice rubble adjacent to the structure.

Then it was realized that such approach demanded significant computational efforts. In order to optimize the numerical model, different numerical models have been realized for the analysis of vertical and sloping structures.

8.2 Finite element analysis of ice loads on vertical structures

The simulation accuracy is heavily affected by the shape/the size of the ice rubble model that has been implemented into the finite element model, not to mention the consolidation issue and the sliding resistance of the grounded ice rubble (see Chapter 6.3). Unfortunately, the author could not find any reliable observations of ice rubble in the vicinity of vertical structures (barges) in the North Caspian Sea, while ISO 19906 (2010) provides a limited guidance in this case. Due to this, only the first stage of the ice-structure interaction process, when the sliding resistance of ice rubble adjacent to the vertical structure is still not enough to reduce the ice load, is examined (see Chapter 6.4).

On basis of this assumption, the interaction of the 0.96-m ice sheet with the vertical structure (barge) has been simulated, since this value corresponds to the 100-year ice thickness (see table 3.2). Note that this provides simulation of the worst case, i.e. the maximal ice action will be due to the interaction of the 0.96-m ice sheet with the barge (see fig. 6.7,a) when there is no grounded ice rubble. Hence, the described model should predict conservative results.

8.3.1 Geometry

In order to achieve a compromise between calculation efficiency and the solution accuracy, the length, height and width of the barge are 30 m, 10 m and 15 m respectively, while the width and the length of the 0.96-m ice sheet are 50 m and 30 m respectively (see fig.8.1). The

soil base has not been involved into the simulation because its dimensions substantially increase the simulation time. Seawater was not implemented into the model because of complexity of the simulation of the liquid behaviour. Instead, the elastic foundation base with constant hydrodynamic coefficients has been applied as established in Chapter 7.2.6. The models of the vertical sloped barge and the ice sheet were created in the AutoCAD Inventor 14 software.

The barge fixed in place is considered being rigid. The velocity of the ice sheet has been set 0.5 m/s (see Chapter 3.8.2) and the water depth is assumed 4 m, which corresponds to the average water depth in the North Caspian Sea. All environmental loads (including wind, currents and ice action) are replaced with the velocity of the coming ice sheet constrained in horizontal direction. It worth mentioning that all models consisting of these bodies symmetrically interact with each other in order to avoid any additional forces and internal stresses caused by the asymmetric interaction.

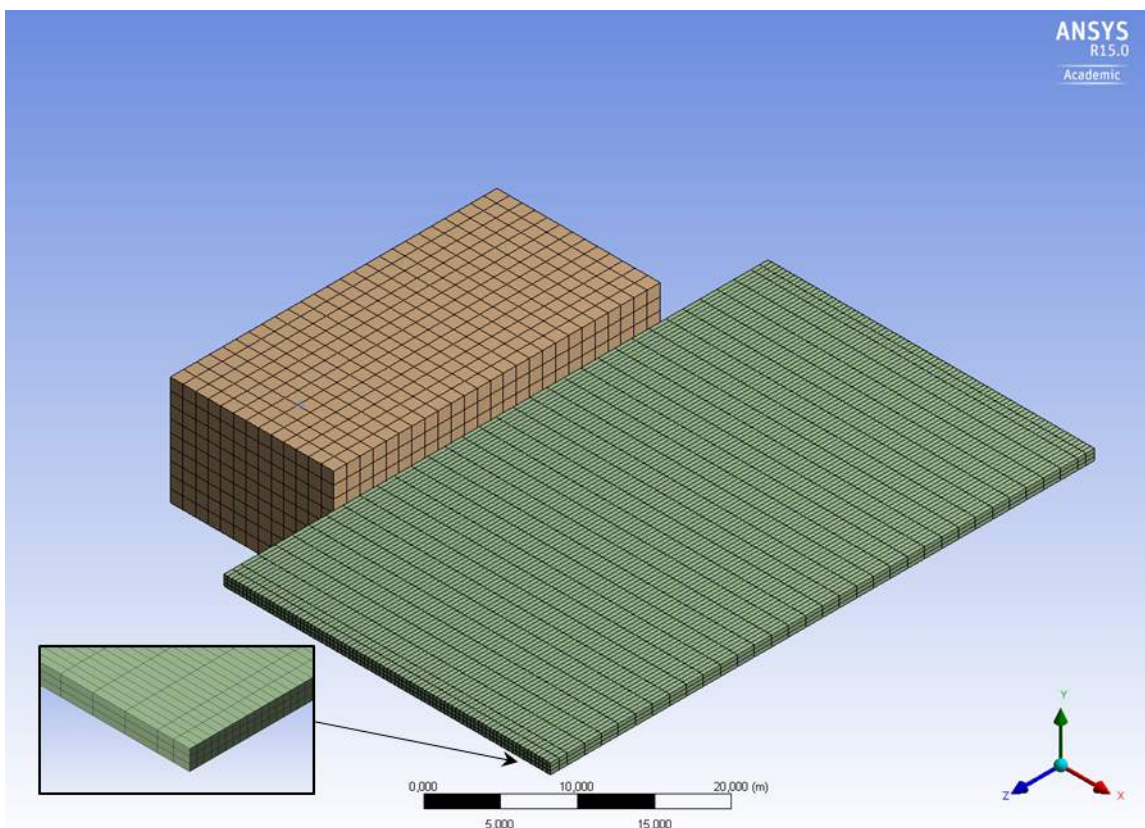


Figure 8.1: Mesh for the ice-structure simulation model.

Meshing was applied in accordance with recommendations discussed in Chapter 7.4, e.g. the minimal number of mesh layers applied for the ice sheet was chosen three. In order to

achieve high speed of the model realization, rough mesh has been constructed for the barge without trading of the accuracy of results

In addition to the geometric shape of the bodies, the parameters of the materials model will heavily affect the magnitude of the ice loads on the barge. Hence, all materials used in the model should reflect the design basis when they are defined in the finite element software. The model is described by the following set of materials: ice and concrete (see fig. 8.1), the properties of which have been defined in Chapters 2-3, 6-7. Drucker-Prager parameters implemented for the ice model are:

- The material friction angle $\beta = 50^\circ$ (Kajaste-Rudnitski and Kujala, 2014),
- The tension cut-off is 250 kPa (Lu et al. 2012),
- The cohesion is 580 kPa (Fish, 1991),
- The maximum tensile pressure is 517 kPa (Tippman, 2011).

All material properties of sea ice are summarized in Appendix A. It should be noted that the nonlinear material model of concrete applied for the barge has been taken from the ANSYS material library. In addition, the data accrued in Chapters 2-3 is used for input values of the models.

8.3.2 The simulation results

Ice drift onto the vertical barge has been simulated to investigate the ice interaction process and to calculate the maximal ice loads.

A typical force curve as a function of time shown in fig. 8.2 was obtained during the non-linear simulations for the first second of the interaction. The highest peak load was due to the dynamic interaction, which is out of interest of this thesis. The force fluctuates around a load of 74.29 MN.

Fig. 8.3 shows that the ice fails in crushing that is typically observed when the appearing ice interacts with a vertical structure as discussed in Chapter 6.4. So the characteristic fluctuating load is due to the crushing failure of the ice. Finally, fig. 8.3 reveals the erosion process when damaged elements are removed as introduced in Chapter 7.2.5.

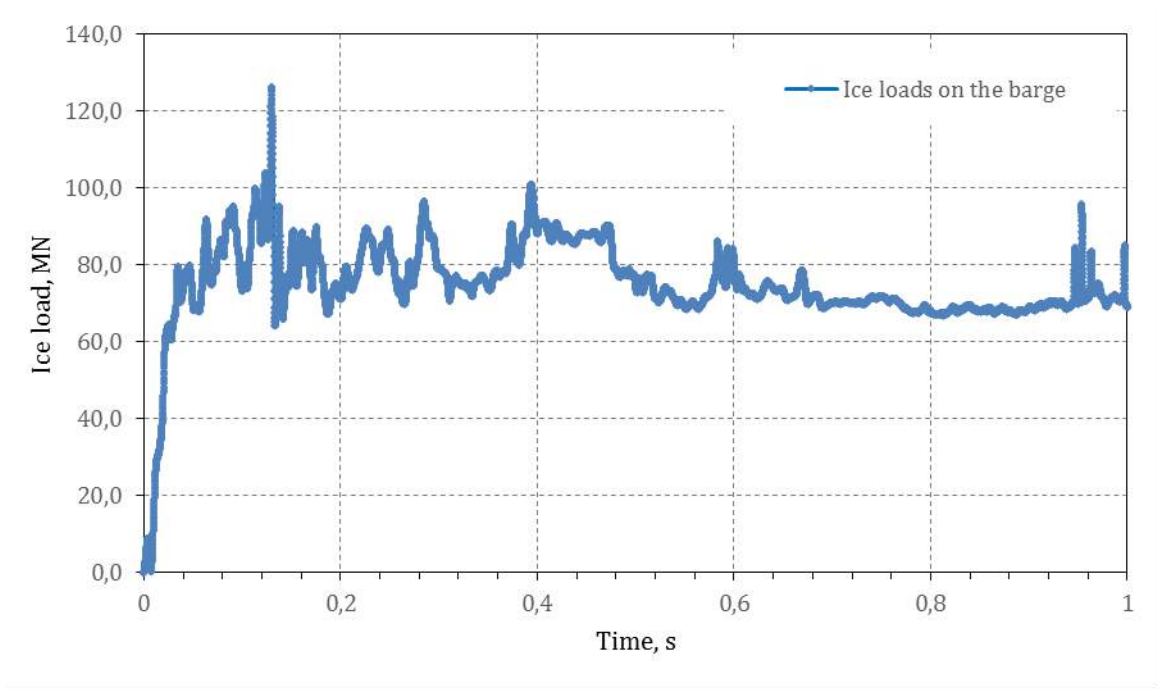


Figure 8.2: Simulated horizontal ice forces exerted onto the barge.

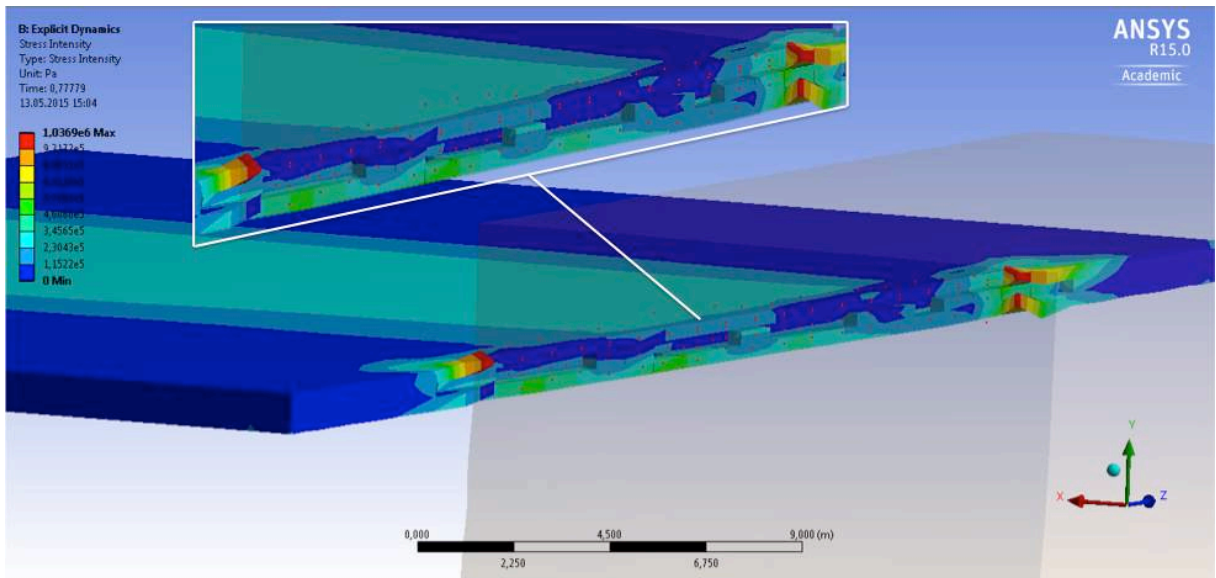


Figure 8.3: Interaction of the ice sheet with the barge. Note that the red dots correspond to the free mass points as established in Chapter 7.2.5.

8.3.3 Comparison of numerical results and analytical solution

Ice loads exerted onto the barge are also calculated by the semi empirical approach given by Eq. 6.2, Korshavin's formula (Eq.6.3) and Michel and Thussaint (Eq.6.4). As described in Chapter 6.4, these solutions treat the ice floe as an isotropic elastic material by assuming that

ice loads are assumed as distributed uniformly on the structure's face and the ice properties are homogenous. The geometry of the ice sheet and the barge used for the calculations is taken as in Chapter 8.3.1, i.e. the effective diameter is 30 m and the ice thickness is 0.96 m.

One can notice that the unconfined compressive strength σ'_c is a governing parameter used in these equations. Løset S. (2014c) reported that the unconfined compressive strength could be defined as $\sigma'_c = 0.3 \cdot \sigma_c$, where the compressive strength of ice σ_c is equal to 4.5 MPa (see Chapter 2.2.1). Assuming that the rate of indentation v is 0.5 m/s, the strain rate $\dot{\epsilon}$ is equal to $4.17 \cdot 10^{-3}$. The results of the calculations are summarized in fig.8.4.

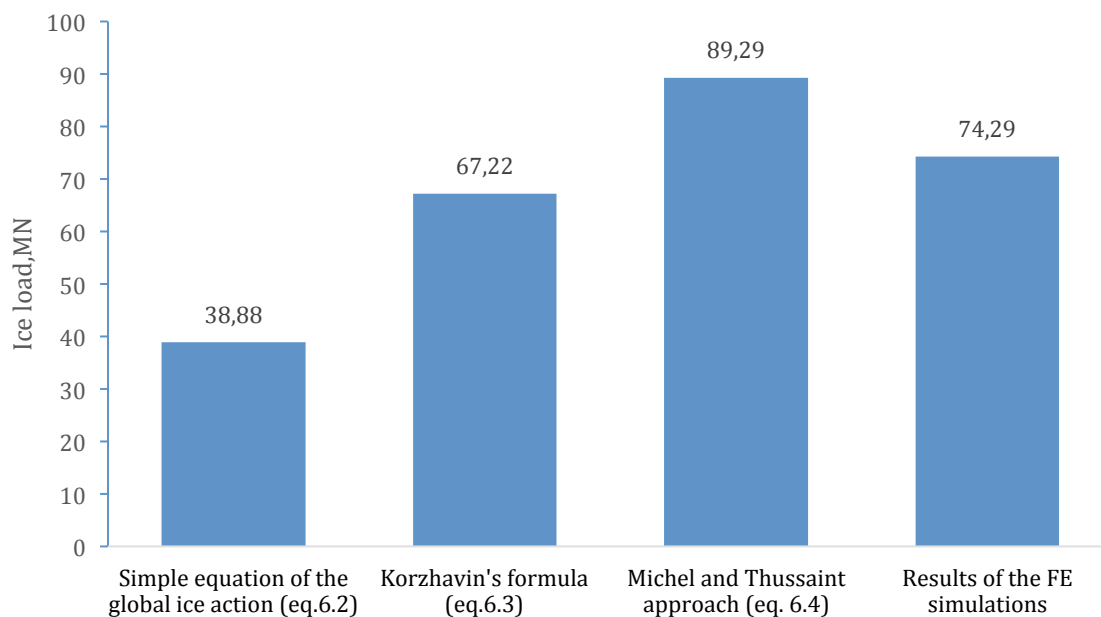


Figure 8.4: Comparison of the FEA and the semi empirical solutions described in section 6.4.

In general, Eq.6.2 predicts lower ice loads leading to underestimation of the ice action. Obviously, the approach given by Eq.6.2 could not be used for calculations of the design ice load due to the factors discussed in Chapter 6.4.1. It was anticipated that Korzhavin's equation would provide an overestimated result as reported by Løset et al. (1998). However, despite the drawbacks of this approach discussed in Chapter 6.4.2, its result is comparable with the outcome of the FEA, while Michel and Thussaint method predicts the ice forces that are higher than the numerical result.

The analysis of the results obtained by the finite element simulation and those obtained by the semi-empirical equations demonstrate that there is a gap between these methods. This is due to drawbacks of the semi-empirical methods, which do not consider the total stress and

the strain rate distribution around the barge due to the non-simultaneous ice failure (see Chapter 6.4).

8.4 Finite element analysis of ice loads on sloping structures

In case of a sloping structure only the first (the initial interaction) and the third (the interaction of an ice sheet with ice rubble) stages were taken into consideration. The rubble build-up (consolidation) process has not been implicitly involved into the simulations, since this substantially increases the simulation time.

It should be mentioned that the empirical approaches described in Chapter 6.5 could successfully predict ice loads during the first and the second stages, i.e. when the generated ice rubble is not grounded. Hence, it is of interest for to compare the accuracy of the FEA with the empirical methods described in Chapter 6.5 for different stages of the ice interaction process.

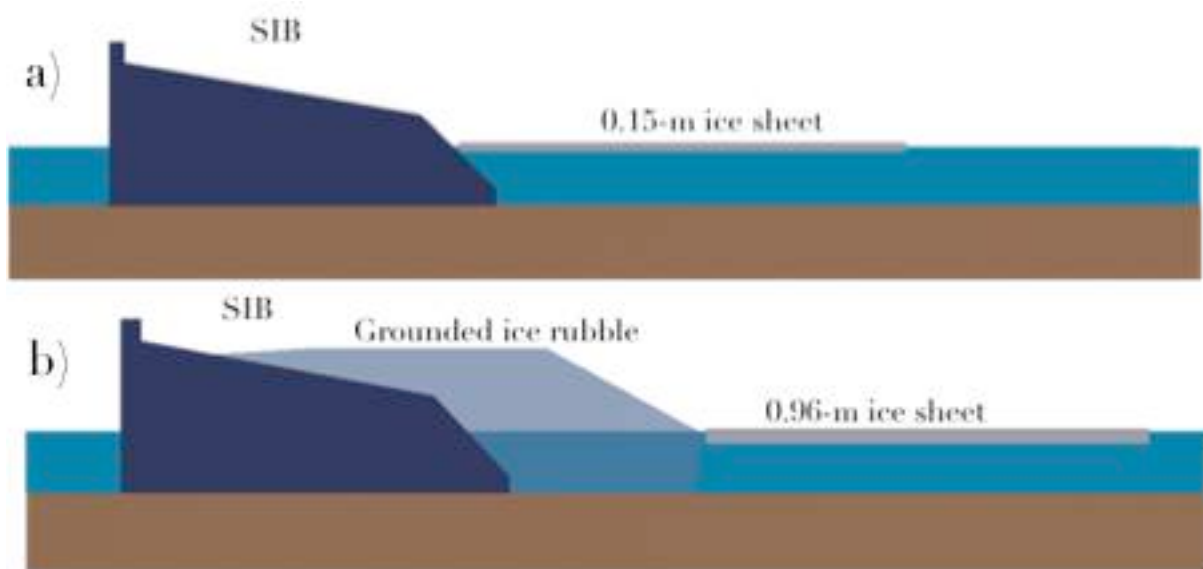


Figure 8.5: a) The initial stage of the interaction and b) the final stage when the ice rubble is grounded (not to scale).

The numerical model of the initial stage considers the interaction of the 0.15-m ice sheet with the first slope of a shoulder ice barrier (see fig. 8.5, a). Essentially, this can be assumed as interaction of the ice sheet with the 45-degree sloping face. The chosen ice thickness corresponds to the average predominant thickness, when ice freeze-up occurs.

For the final stage includes the 0.96-m ice sheet exerting onto the grounded ice rubble adjacent to the SIB. The soil base is used as a foundation for this arrangement (see fig. 8.5,b).

This ice thickness corresponds to the 100-year ice thickness in the Northern Caspian Sea (table 3.2).

It should be noted that the SIB model has been implemented into both simulations since the experimental observations shown in fig. 5.15, c) provide a reliable shape of the ice rubble in front of the structure. On the other hand, the SIB concept shown its high efficiency in shallow waters, so it is of interest to numerically simulate the interaction of ice with this type of ice barriers.

8.4.1 Geometry

Thus the width and the length of the 0.96-m/0.15-m ice sheets are 50 m and 30 m respectively. The length of the SIB is 30 m, while other dimensions are specified in Appendix C.

In the model of the initial interaction stage the soil base has not been involved into the simulation because its dimensions substantially increase the simulation time. For the model of the final stage of interaction the length, the width, the height of the soil base are 80 m, 40 m and 2 m respectively. The size and the shape of the ice rubble have been selected on basis of the tests carried out by Gürtner (2009) (see fig.5.15, c) and they are described in Appendix C. The numerical models consisting of these bodies were created in the AutoCAD Inventor 14 software.

The SIB fixed in place is considered being rigid. The soil foundation is fixed from all directions except the top (i.e. the seabed) in order to achieve some realness of the simulations. Seawater was not implemented into the model because of complexity of the simulation of the liquid behaviour. Instead, the elastic foundation base with constant hydrodynamic coefficients has been implemented as established in Chapter 7.2.6.

All environmental loads (including wind, currents and ice action) are replaced with the velocity of the coming ice sheet constrained in horizontal direction. The velocity of the ice sheet has been set 0.5 m/s (see Chapter 3.8.2) and the water depth is assumed 4 m, which corresponds to the average water depth in the North Caspian Sea. It worth mentioning that all models consisting of these bodies symmetrically interact with each other in order to avoid any additional forces and internal stresses caused by the asymmetric interaction.

Meshing was applied in accordance with recommendations discussed in Chapter 7.4, e.g. the minimal number of mesh layers applied for the ice sheet was chosen three (fig.8.6). In

order to achieve high speed of the model realization, rough mesh has been constructed for the soil foundation of the models without trading of the accuracy of results

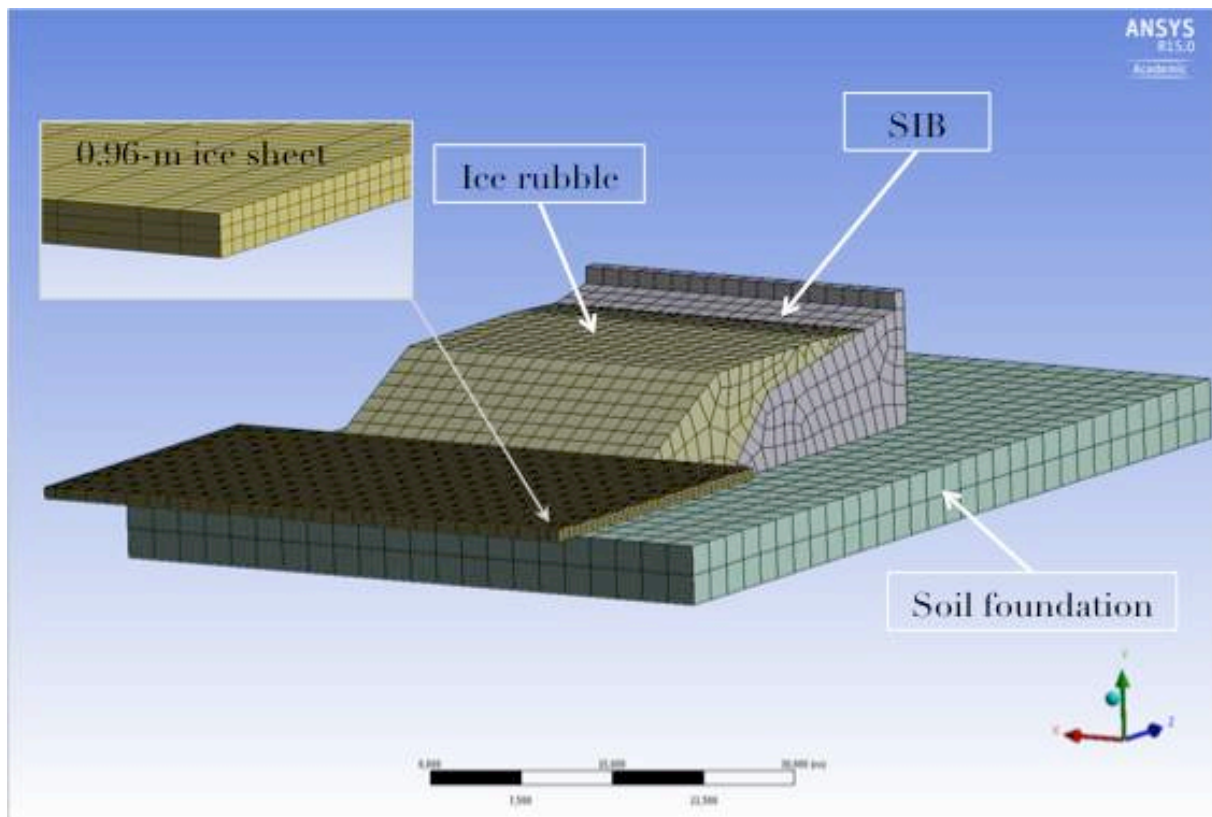


Figure 8.6: Mesh for the ice-structure simulation model when the ice rubble is grounded.

The model shown in fig.8.6 is described by the following set of the materials: ice, ice rubble, soil and concrete, which the properties have been defined in Chapters 2-3, 6-7. DP parameters for the actual ice model are taken as for the barge simulations (see section 8.3.1).

It should be noted that the soil conditions of the Caspian Sea are beyond of the scope of this thesis. Lengkeek et al. (2003) report the Caspian soil parameters of MC model described in Chapter 7.2.2 (see table A.3). Additionally, since there is no available data related to reported measurements of Young's module and Poisson's ratio in the Caspian Sea, their values have been suggested 140 MN and 0.33, respectively, according to Duplenskiy (2012). On basis of these data, the corresponding parameters of DP model have been implemented into the model. It should be noted that the nonlinear material model of concrete used for the barge has been taken from the ANSYS material library. All material properties of sea ice are summarized in Appendix A.

8.4.2 The simulation results

On basis of the numerical set-up described above, the finite element simulations have been realized. The typical force curves as a function of time obtained during the non-linear simulations are presented in Appendix C.

It should be noted that the peak loads observed during simulations were due to the dynamic interaction, which is beyond the scope of this thesis. For the model of the initial stage involving the 0.15-m ice sheet, the horizontal ice load is seen to fluctuate around a load of 558 kN. For the model of the final stage the same component of the ice load fluctuate around 3.91 MN, which is significantly lower than the horizontal force acting on the barge modelled in the previous section (74.29 MN). Ice loads vs. time graphs for each stage can be found in Appendix C.

On the other hand, the simulations have shown that the bending failure of the ice sheet is initiated at the bottom layer of meshing (see fig. 8.7), i.e. ice fails in bending rather in compression. Fig. 8.7 also demonstrates the erosion of failed elements as introduced in Chapter 7.2.5.

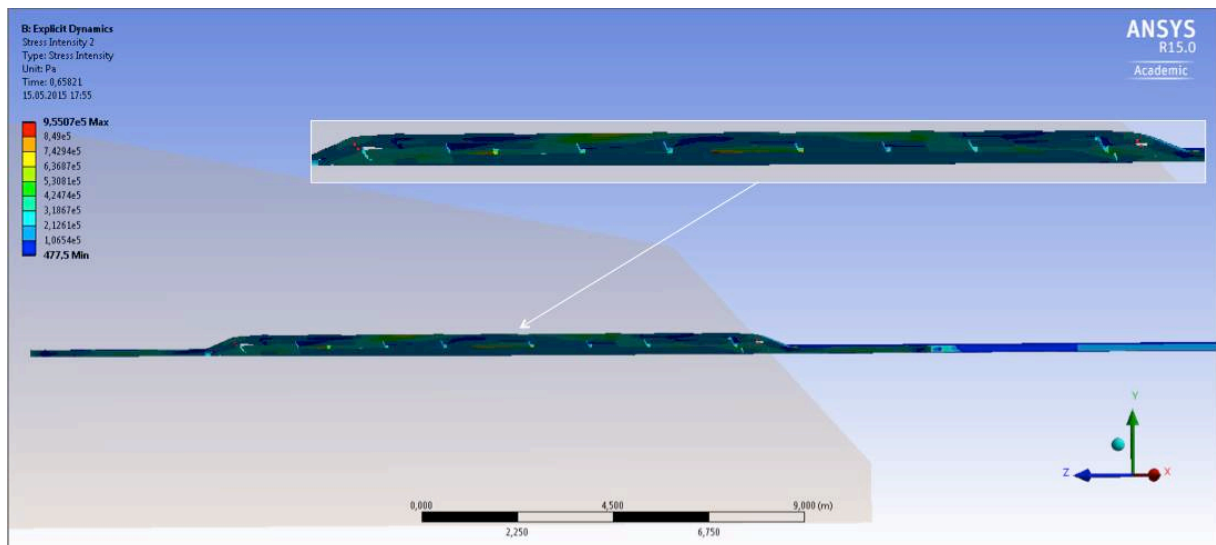


Figure 8.7: Interaction of the 0.15-m ice sheet with the sloping face of the SIB.

8.4.3 Comparison of numerical results and analytical solution

Ice loads on the sloping structure (SIB) are also calculated by Croasdale's analytical solution (Eq. 6.8) and by ISO approach (Eq.6.13).

One can notice that the ice flexural strength $\sigma_f = 0.78 \text{ MPa}$ (see Chapter 2.2.3) is a key factor governing the magnitude of the ice loads in this equations. The same parameters that

are the input values for the numerical simulations are used for these methods (see Appendix A). The geometry of the ice sheet, the SIB and the ice rubble is taken the same as in Chapter 8.4.1. Note that for calculations of the ice action when there is ice rubble adjacent to the SIB, the vertical distance z in Eq.6.8 is assumed 2.3 m, while the height of the ice rubble in ISO approach is taken 6.3 m (the same as for the finite element model).

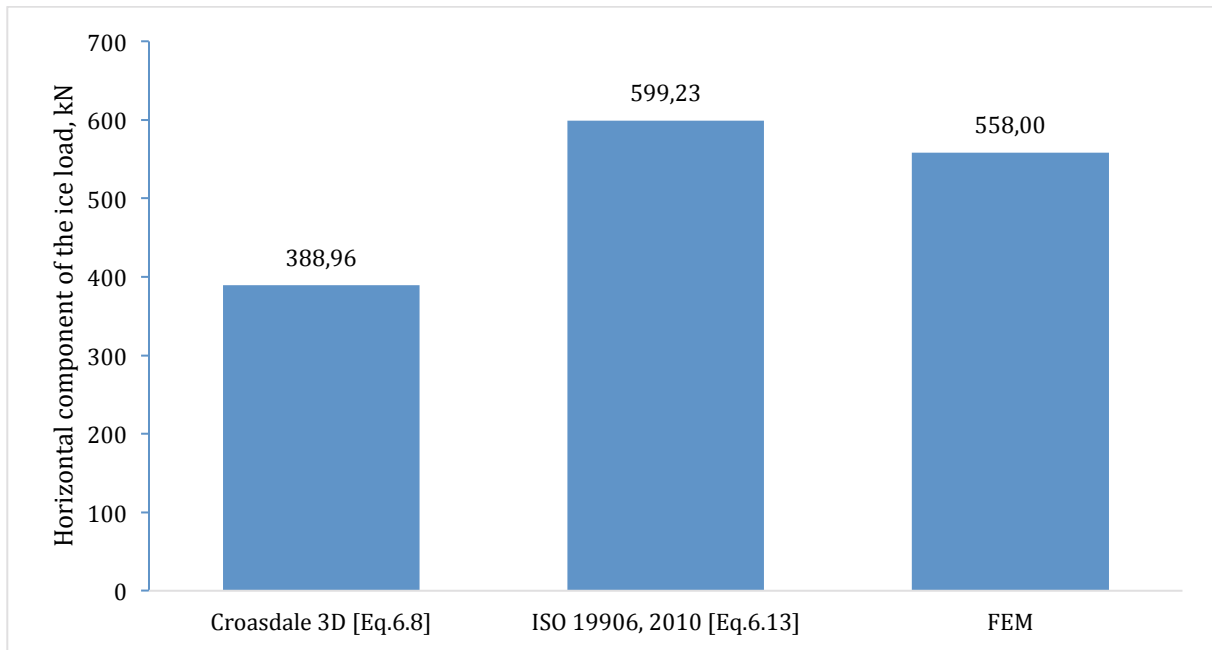


Figure 8.8: Comparison of ice loads on the SIB (the initial stage) obtained with the finite element simulations and the semi empirical solutions.

Fig.8.8 summarizes the results of the analytical solutions and the FEA for the initial stage. Primary, these methods provide satisfactory results when the 0.15-m ice sheet acts on the 45deg face and no rubble is involved into the model. Croasdale’s 3D solution predicts lower ice loads as compared with the finite element simulations and ISO 19906 (2010) method. The maximal deviation is about 30% (between the FEA and Croasdale’s 3D solution), while the results of ISO approach and the FEA are close. In general, the difference between the results might be assumed as acceptable.

However, comparison of loads obtained by the FEA and those obtained by the analytical approaches have shown a considerable discrepancy between these approaches when ice rubble is grounded. By comparing of the results of the calculations presented in fig. 8.9, it can be stated that both analytical approaches predict overestimated ice loads. The gap between Croasdale 3D and the FEA is 2.62 MN MN or 40% while the discrepancy between the results

of ISO approach and the FEA is 3.55 MN or 48%, respectively. This is mainly due to the effect of grounded ice rubble in shallow water discussed in Chapter 6.3.

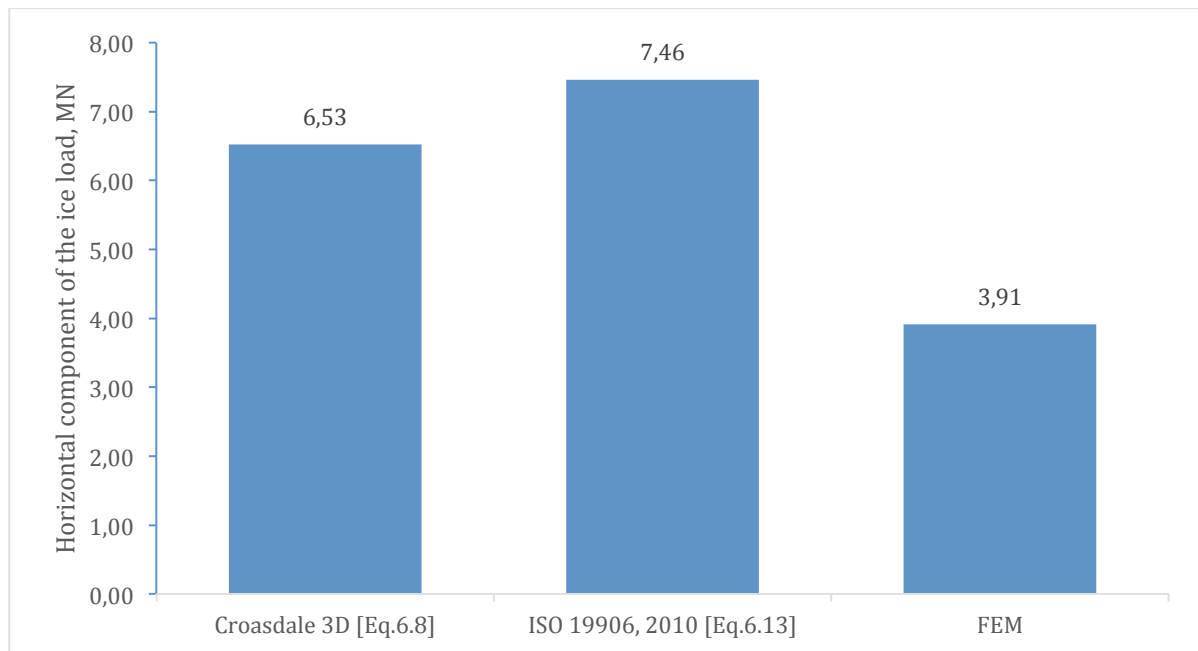


Figure 8.9: Comparison of ice loads on the SIB (when the ice rubble is grounded in front of the SIB) obtained with the finite element simulations and the semi empirical solutions.

8.5 Discussion of the results

The numerical models presented above focuses on the ice-structure interaction process in shallow water.

Primary, the constitutive model of ice provided the required level of realness, because crushing and bending failure modes were observed during the FEA for vertical and vertical structures. The force histograms have been obtained during the FEA. One can notice that the initial peak loads are observed during each simulation. The artificial shape of the ice sheet and the inertial force during the initial contact might cause this. Furthermore, it is possible that the assumption treating the barrier model (the barge or the SIB) as rigid might somewhat influence the interaction process due to the absence of the energy dissipation by structural deflections.

Furthermore, the results show a significant discrepancy between the FEA and the theoretical solutions. In addition to the causes described in the previous chapters, the finite element models in contrast to the semi-empirical equations consider the buoyancy forces acting on the submerged part of ice.

Finally, even though the FEA was performed for the vertical barge and the SIB, the findings obtained from the simulations can be applied for other aspects related to the ice action in shallow water.

8.6. Summary

The FEA of the ice-structure interaction in shallow water proved the main field observations, introduced in sections 5.3 and in chapter 6.

The results predictably show a discrepancy between the numerical results and those defined by the empirical formulas. In addition, the finite element simulations allow analysing the effect of ice rubble grounded in front of the structure as discussed in this thesis. It has been proved grounded ice rubble can significantly reduce the ice action.

Chapter 9. Conclusions and Suggestion for further work

9.1 Conclusions

Being a promising area for the for oil and gas growth, the Northern Caspian Sea imposes a unique combination of challenges. Hence, the further development of hydrocarbon fields in this region requires a proper selection of systems that can provide safe and effective production, transportation, processing and production drilling.

The present study discusses development concepts that are suitable for the Northern Caspian Sea. It addresses the findings to the next conclusions:

Production drilling. The most optimal options for production drilling include ice islands, drilling barges and conventional jack-ups protected by ice barriers. Primary, an ice island is recommended for temporary operations due to challenges related to the island operability time. Despite that a conventional jack-up with external ice protection is an attractive solution from economical point of view, its implementation heavily depends on the efficiency of an ice protection system. A drilling barge is only option currently used in the Northern Caspian Sea and some experience of their utilization has been gained. However, these structures still require additional ice protection. Finally, a conventional rig installed on a production structure can provide production drilling.

Production. Generally, Production structures for the Northern Caspian Sea can be fully ice resistant (“stand alone” platforms) or semi ice resistant with external ice protection.

A concept of a semi ice resistant platform presented by a sheet pile island protected by ice barriers is optimal for the development of fields located in extreme shallow water. In order to

attain high flexibility of this concept, two kinds of production islands can be constructed: (i) large hub islands for field processing and (ii) small islands tied back to the hub islands.

A stand-alone platform presented either by caisson retained islands or by gravity based structures can be, in turn, implemented for fields located in relatively deep locations within the Northern Caspian Sea (e.g. the Ural furrow) where the employment of semi-tolerant structures protected by ice barriers is challenging.

In addition wellheads platforms tied back to the main structures could be implemented to provide production from small/satellite fields and might be used to improve drainage strategy of extended reservoirs.

Processing and Transportation systems. There are several options depending on the type of the hydrocarbons producing from the reservoir. The pipeline transportation is only option for the field development in the Northern Caspian Sea. The main drivers (such as routing, flow assurance, H₂S corrosion protection) for the pipeline design as well as the seabed gauging issue are discussed. Pipelines should be buried below the seabed to the depth that is larger than the depth of the deepest scour.

Ice protection systems. The implementation of either non-ice tolerant structures (jack-ups) or semi ice tolerant platforms makes ice barriers a crucial component of these development concepts. They are designed to take the ice action so that the leeward lying structure can be normally operated even under extreme conditions. The reliability of the entire system is improved while the barriers take the potential threats.

The main factors governing the efficiency of a protection system are the geometry of barriers and spacing between the barriers and the leeward lying structure. The following ice barriers have been established as beneficial in this region: (i) breakwaters, (ii) ice protection piles, (iii) satellite barges, (iv) grounded ice and (v) ice rubble generators. Currently, breakwaters and ice protection piles are utilized in the Northern Caspian Sea, but the results of their application are not reported. The analysis of these structures shows advantages for the utilization of ice rubble generators, though there is no field experience of their employment.

The ice barrier arrangement depends on the ice tolerance of the leeward located structure. An ice protection alignment for sheet pile islands or jack-ups should be more intensive while an ice protection system for the Sunkar drilling barge could be simpler so that ice barriers should be deployed only in the main direction of ice drift.

The effect of ice rubble grounded in the vicinity of structures. Since the design of ice barriers and other structures is mainly governed by ice action, the ice-structure interaction process in shallow water has been examined. The study shows that ice rubble grounded adjacent to structures affect the interaction mechanism. It also has been proved that current semi-empirical approaches cannot provide correct ice loads due this phenomenon. Furthermore, depending on which approach has been used, the magnitude of ice loads on the same structure significantly vary. The finite element analysis has been carried out in ANSYS 15.0 Workbench in order to analyse the effect of ice rubble in front of the structure. The results establish some discrepancy between the numerical results and those defined by the empirical formulas. In addition, it has been demonstrated that grounded ice rubble decreases ice loads on a structure. Hence, it is beneficial to take advantage of the ice rubble in the vicinity of structures, while the shallowness of the sea favours to this process. Finally, the FEA proved the efficiency of the ice mitigation measures proposed in section 5.3.

9.2 Further work

Even though some aspects related to the development of hydrocarbon fields in the Northern Caspian Sea have been discussed, the process of ice-structure interaction in shallow water is not well understood due to the lack of knowledge and complicity of the problem. In this regard the following suggestions for further work (but not limited to):

- Improvement of the numerical simulations. It is recommended to make a sensitivity analysis of the simulations and to determine the optimal meshing approach. To compare results obtained from different numerical methods. The challenge here is a computational capacities available for the simulations, so cluster techniques should be applied.
- Scaled physical modelling of the discussed scenarios of ice-structure interaction. It is advised to improve the used FEM on basis of the results obtained from the physical modelling.
- A probabilistic approach for the calculation of ice loads in shallow water should be used on basis of long-term statistics acquired in this region.
- Physical testing of different barriers arrangement in order to achieve the optimal alignment. It is recommended to study the ice protection efficiency of different ice arrangement approaches.

References

ANSYS Inc. (2009a): Chapter 1. Introduction to Explicit Dynamics. Website: <http://wenku.baidu.com/view/005bf1ece009581b6bd9eb26.html?re=view> [Date accessed: 20/05/2015]

ANSYS Inc. (2009b): Chapter 8. Explicit Dynamics: Analysis Settings. Website: <http://wenku.baidu.com/view/893c4119227916888486d7e3> [Date accessed: 20/05/2015]

ANSYS Inc. (2009c): Chapter 9. Explicit Dynamics: Material Models. Website: <https://ru.scribd.com/doc/15222317/Explicit-Dynamics-Chapter-9-Material-Models> [Date accessed: 20/05/2015]

Atyrau-city.kz (2011): Great "powder keg" laying at the bottom of Caspian Sea. Website: atyrau-city.kz/img_ecology/Kashagan-D.jpg [Date accessed: 02/05/2015]

Bailey, A. (2009): Arctic Directory: Platforms for Arctic offshore? Published at the Journal Petroleum News, Vol. 14, No. 4, January, 2009.
Website: <http://www.petroleumnews.com/pntruncate/816813876.shtml> [Date accessed: 18/12/2014]

Barents-2020, Russian-Norwegian Cooperation Project (2011): Assessment of international standards for safe exploration, production and transportation of oil and gas in the Barents Sea. Harmonization of Health, Safety, and Environmental Protection Standards for The Barents Sea. Final Report Phase 4. p.159-170. Website: http://tksneftegaz.ru/fileadmin/f/activity/barents2020/Оценка_международных_стандартов_для_безопасной.pdf [Date accessed: 19/12/2014]

Barker, A., Croasdale, K. (2004): Numerical Modelling of ice interaction with Rubblr mound berms in the Caspian Sea. Proceedings of IAHR Symposium on Ice, IAHR'04, 2, pp.257-264, 2004-06-21

Barrette, P. (2011): Offshore pipeline protection against seabed gouging by ice: An overview. Published in the Cold Regions Science and Technology journal, 69 (2011).
Website: http://ac.els-cdn.com/S0165232X11001091/1-s2.0-S0165232X11001091-main.pdf?_tid=c0248136-7efe-11e4-b075-00000aacb360&acdnt=1418059513_82af574c26d459e6d9c982e63e3d500a [Date accessed: 8/12/2014]

Bastian, J., Strandberg, A.G., Graham, W.P. and Mayne, D. (2004): Caspian Sea Sprayed Ice Protection Structures. International Association of Hydraulic Engineering and Research. 17th International Symposium on Ice. Saint Petersburg, Russia, Vol. 2 pp. 58-67.

Been, K., Croasdale, K., Jordaan, I., Verlaan, P. (2013): Practice for Pipeline Design in Ice Scoured Environments: Application to the Kashagan Project. Proceedings of the 22nd International Conference on Port and Ocean Engineering under Arctic Conditions June 9-13, 2013, Espoo, Finland.

Brinker, T. (1980): Construction of grounded ice island for drilling in Beaufort Sea, Alaska. Presented at the 50th Annual California Regional Meeting of the Society of Petroleum Engineers of AIME, Los Angeles, California, April 9-11, 1980, SPE-8915

Britner-Shen Consulting Engineers Inc.: Caissons. Website: <http://www.bittner-shen.com/caissons.html> [Date accessed: 02/05/2015]

Bruun, P.K., Gudmestad, O.T., Gürtner, A., Zheng, P. (2006): Issues for Development of Shallow Water Offshore Hydrocarbon Fields in Moderate Ice Conditions. Proceedings of The Seventh (2006) ISOPE Pacific/Asia Offshore Mechanics Symposium, Dalian, China, September 17-21, 2006, ISBN 1-880653-67-2

CDE (2015): Sur les îles artificielles du gisement géant de Kashagan. Website: <http://www.connaissancedesenergies.org/sur-les-iles-artificielles-du-gisement-geant-de-kashagan> [Date accessed: 06/05/2015]

Comyn, M. (1984): Beaufort Sea Caisson retained Islands. Published in the Journal of Canadian Petroleum Technology, July-August, 1984, PETSOC-84-04-01. Website: <https://www.onepetro.org/journal-paper/PETSOC-84-04-01> [Date accessed: 1/11/2014]

Croasdale, K.R. (2001): Final report Ice research & Field Measurements Programme North Caspian Sea, Confidential Report, prepared for Offshore Kazakhstan Operating Company (now Agip KCO), Calgary, Canada

Croasdale, K.R. (1988): Ice Forces: Current Practices. Esso Resources Canada Limited. Calgary, Alberta, Canada, 1988 (not publicly available)

Croasdale, K., Jordaan, I., Verlaan, P. (2011): Offshore platforms and deterministic ice actions. Kashagan phase 2 Development: North Caspian Sea. Proceedings of the 21st International Conference on Port and Ocean Engineering under Arctic Conditions, July 10-14, 2011, Montréal, Canada, POAC11-117

Devon Canada Corporation: Comprehensive Study Report; Devon Beaufort Sea Exploration Program. Submitted to National Energy Board Canada August 2004. Website:

http://www.devonenergy.com/operations/canada_pages/Beaufort_Sea_CSR_August_2004.pdf [Date accessed: 15/10/2014]

Dobrovolskiy, A.D., Zaloghin, B.S. (1982): The USSR's oceans. Moscow, Publishing House of Moscow University, 1982, 192 p.

Duplenskiy, S.V. (2012): Protection of Subsea Pipelines against Ice Ridge Gouging in Conditions of Substantial Surface Ice. Master's Thesis, University of Stavanger

Eldesov, D. (2013): The collapse of the Caspian myth: there is no oil! Website: http://www.galiya.kz/index.php?option=com_content&view=article&id=70%3A2013-03-28-20-31-35&catid=3%3A2011-02-12-11-11-41&Itemid=4&lang=ru [Date accessed: 19/12/2014] Russian: Ельдесов Д. (2013): Крушение каспийского мифа: нефти нет!

Espergen, R.A. (2006): Development of oil and gas production in the Kazakh sector of the Caspian Sea. Vestnik OGU, №8, August, 2006. Website: <http://cyberleninka.ru/article/n/razvitie-neftedobychi-v-kazahstanskom-sektore-kaspiyskogo-morya> [Date accessed: 1/10/2014] Russian: Есперген Р.А. (1982): Развитие нефтедобычи в Казахстанском секторе Каспийского моря.

European Environment Agency (2005): Caspian Sea physiography (depth distribution and main currents). Website: <http://www.eea.europa.eu/data-and-maps/figures/caspian-sea-physiography-depth-distribution-and-main-currents> [Date accessed: 12/10/2014]

Fish, A.M. (1991): Creep and Yield Model of ice under Combined Stress. U.S. Army Corps of Engineers. Cold, Regions Research & Engineering Laboratory. Special Report 91-31

Fitzpatrick, J.P., and Stenning, D.G. (1983): "Design and Construction of Tarsiut Island in the Canadian Beaufort Sea", Proceedings of 15th Annual OTC in Houston, Texas, May 2-5, 1983, OTC 4517

Frederking, R., Barker, A., (2002): Friction of sea ice on various construction materials. Proceedings of the 16th IAHR International Symposium on Ice, Dunedin, New Zealand, vol. 1, pp. 442–449.

Frederking, R.M.W., Timco, G.W., (1986): Field measurements of the shear strength of columnar-grained sea ice. Proceedings 8th International Association for Hydraulic Research Symposium on Ice, vol. I, pp. 279–292. Iowa City, U.S.A.

Ghoneim, G. A. (2011): Arctic Standards – A Comparison and Gap Study. Proceedings of the Arctic Technology Conference, 7–9 February 2011, Houston, Texas, USA, OTC 22039

Gorelits, O.V. (1995): the Caspian Sea level fluctuations. Review of the papers of S.N.Rodionov and R.E.Nikonov, Moscow (not published).

Granneman, C., Goris, A. (2001): Kazakhstan, Offshore Exploration in the Caspian Sea. Website: <https://www.iadc-dredging.com/ul/cms/terraetaqua/document/1/0/3/103/103/1/terra-et-aqua-nr82-03.pdf> [Date accessed: 15/10/2014]

Gudmestad, O.T. (2014): Marine Technology and Operations. Theory and practice. University of Stavanger. Norway, pp. 40-45

Gudmestad, O.T., Zolotukhin, A.B., Jarlsby, E.T. (2010): Petroleum Resources with Emphasis on Offshore Fields. WIT Press, Southampton, May 2010, pp. 73-77, 159-170

Gürtner, A. (2005): Design options of offshore facilities for the Northern Caspian Sea. Confidential report submitted to Statoil July 25th, 2006

Gürtner, A. (2009): Experimental and Numerical Investigations of Ice-Structure Interaction. Doctoral theses at NTNU, Trondheim, January 2009

Gürtner, A., Gudmestad, O.T., Tørum, A. and Løset, S. (2006): Innovative Ice Protection for Shallow Water Drilling - Part I: Presentation of the Concept. Proceedings of the 25th International Conference on Offshore Mechanics and Arctic Engineering, Hamburg, Germany. OMAE2006-92181

Helman, C. (2014): Troubled Kazakhstan Project Shows The Value Of U.S. Shale Oil. Website: <http://www.forbes.com/sites/christopherhelman/2014/04/01/troubled-kazakhstan-project-shows-the-value-of-u-s-shale-oil/> [Date accessed: 18/12/2014]

Henni, A. (2014): The Mystery of the Kashagan. Website: <http://www.spe.org/news/article/the-mystery-of-the-kashagan> [Date accessed: 12/11/2014]

Hewitt, K. (2007): Offshore Arctic Exploration & Development Challenges based on 25 years of experience. Proceedings of the TEKNA Conference, Oslo, January, 2007

Hewitt, K. (2014): Arctic Offshore Islands – Lessons Learned. Proceedings of the Arctic Technology Conference, Houston, Texas, USA, 10-12 February 2014, OTC 24559

Imani, M., You, R-J., Kuo, C-Y. (2014): Forecasting Caspian Sea level changes using satellite altimetry data (June 1992–December 2013) based on evolutionary support vector regression algorithms and gene expression programming. Website: <http://www.sciencedirect.com/science/article/pii/S0921818114001210> [Date accessed: 20/09/2014]

IMPac Offshore Engineering Gmbl (2011): Kashagan Field Development – Kazakhstan. Website: <http://www.impac.de/index.php?id=kashaganfielddevelopment> [Date accessed: 19/12/2015]

International Standards Office, 2010. ISO/FDIS 19906:2010(E) Petroleum and natural gas industries — Arctic offshore structures, Geneva: ISO

Iskaziev, K.O. (2013): Development of the Caspian shelf. Official report of KazMunayGas, Atyrau, 2013. Website:

http://www.kursiv.kz/upload/post/iskaziev_k_exploration_prospect_s_work.pdf

[Date accessed: 20/09/2014] Russian: Исказиев К.О. (2013): Доклад «Развитие Каспийского шельфа», Казмунайгаз.

Jochman, P., Evers, K-U., Kuehiein, W. (2003): Model testing of ice barriers used for reduction of ice design loads. Proceedings of 22th International Conference on Offshore Mechanics and Arctic Engineering, Cancun, Mexico, June 8-13, 2003

Juurmaa, K., Wilkman, G. (2002): Supply Operations in Ice Conditions. Website: <http://offshore-industry.net/info/SupplyOperationsInIce.pdf> [Date accessed: 1/09/2014]

Kaltayev, A., Sokolsky, A. (2007): The Northeast Caspian Sea: Oil Developments in a Sensitive Environment. Proceedings of the SPE Asia Pacific Health, Safety, Security and Environment Conference and Exhibition held in Bangkok, Thailand, 10–12 September 2007, SPE 108913

Karluk Spray Ice Island. Website: <http://www.ausenco.com/case-studies/karluk-spray-ice-island> [Date accessed: 20/10/2014]

Karulin, E.B., Karulina, M.M., Blagovidov, L.B. (2007): Ice Model Tests of a Caisson Platform in Shallow Water. Proceedings of the 17th International Offshore and Polar Engineering Conference (ISOPE), July 1-6, 2007, Lisbon, Canada, ISOPE-I-07-301

Karunakaran, D. (2014): Pipeline design. Lecture 2, the course "Pipeline and risers", University of Stavanger

Kajaste-Rudnitski, J. and Kujala, P. (2014): Ship propagation through ice field. Rakenteiden Mekaniikka (Journal of Structural Mechanics) Vol. 47, No 2, 2014, pp. 34-49

Kouraev, A.V., Papa, F., Mognard, N.M., Biharizin, P.I., Cazenave, A., Cretaux, J., Dozortseva, J. and Remy, F. (2004), Sea ice cover in the Caspian and Aral Seas from historical and satellite data, Journal of Marine Systems, Vol. 47, pp. 89-100

Kry, P.R. (1977): Ice rubble fields in the vicinity of artificial islands. Proceedings of the first International Conference on Port and Ocean Engineering under Arctic Conditions, St. John's, Canada

Kuehnlein, W.L. (2002): The North Caspian Project. Proceedings of the Twelfth (2002) International Offshore and Polar Engineering Conference Kitakyushu, Japan, May 26–31, 2002. I-02-003 ISOPE

Kuehnlein, W.L., Evers, K-U., Jochmann, P. (2003): Model testing of ice barriers used for reduction of design ice loads. Proceedings of the 22nd International Conference on Offshore Mechanics and Arctic Engineering Cancun, Mexico, June 8-13, 2003, OMAE-2003-37385

Lebedev, S.A. (2014): Satellite altimetry of the Caspian Sea. PhD Thesis at the Federal State Institution of Science "Geophysical Center of the Russian Federation", 2014, pp. 59-65

Lebedev, S.A., Kostianoy, A.G. (2006): The Caspian Sea Level, Dynamics, Wind, Waves and Uplift of the Earth's Crust Derived from Satellite Altimetry. Proceedings of the Pan Ocean Remote Sensing Conference, November 2-4, 2006, Busan, South Korea. Website: http://www.alticore.eu/Publications/Presentation_lebedev_et_al_PORSEC_Busan_Korea_2006.pdf [Date accessed: 12/10/2014]

Lengkeek, H.J., Croasdale, K.R., and Metge, M. (2003): Design of Ice Protection Barrier in the Caspian Sea. Proceedings of OMAE03: 22ND International Conference on Offshore Mechanics and Arctic Engineering June 8-13, 2003, Cancun, Mexico, OMAE2003-37411

Lengkeek, H.J., Croasdale, K.R., Metge, M.: Design of ice protection barrier in Caspian Sea. Proceedings of OMAE03: 22ND International Conference on Offshore Mechanics and Arctic Engineering June 8-13, 2003, Cancun, Mexico, OMAE2003-37411

Li, Z., Kong, X., Zhang, L., Li, G., Lu, P.: A New Concept of Attached Ice-breaking Structure in Shallow Water Area. Proceedings of The Seventh (2006) ISOPE Pacific/Asia Offshore Mechanics Symposium, China, September 17-21, 2006, ISBN 1-880653-67-2

Lu, W., Raed Lubbad, R., Sveinung Løset, S. and Høyland, K (2012): Cohesive Zone Method Based Simulations of Ice Wedge Bending: a Comparative Study of Element Erosion, CEM, DEM and XFEM. 21st IAHR International Symposium on Ice "Ice Research for a Sustainable Environment", Dalian University of Technology Press, Dalian, ISBN 978-7-89437-020-4

Løset, S. (2014a): Arctic Offshore Structures/Fields. Lecture 1, the course AT-327 "Arctic offshore engineering", UNIS, 2014

Løset, S. (2014b): Ice Physic. Structure and Formation of Ice Part I. Lecture 3, the course AT-327 "Arctic offshore engineering", UNIS, 2014

Løset, S. (2014c): Global and Local Ice Loads. Lecture 7, the course AT-327 "Arctic offshore engineering", UNIS, 2014

Løset, S., Shkhinek, K. and Høyland. K.V. (1998): Ice physics and mechanics. Trondheim, NTNU, pp. 73-87

Løset, S., Shkhinek, K.N., Gudmestad, O.T. and Høyland. K.V. (2006): Action from Ice on Arctic Offshore and Coastal Structures. Student's Book for Institutes of Higher Education. St.-Petersburg: Publisher "Lan", p.9

Matskevitch, D.G. (2007): Technologies for Arctic Offshore Exploration and Development. Presented at the SPE Russian Oil and Gas Technical Conference and Exhibition, 3–6 October, Moscow, SPE-102441

McKenna, R. (2012): Safety and Ice Design Criteria in the ISO 19906 Standard for Arctic Offshore Structures. OGP Structural Reliability Seminar 4-6 December 2012. Website: <https://www.yumpu.com/en/document/view/24598301/safety-and-ice-design-criteria-in-the-iso-19906-standard-for-arctic-> [Date accessed 14/05/2015]

McKenna, R., McGonigal D., Stuckey, P., Crocker, C. and Marcellus, B. (2011): Modelling of Ice Rubble Accumulations in the North Caspian Sea. Proceedings of the 21st International Conference on Port and Ocean Engineering under Arctic Conditions July 10-14, 2011 Montréal, Canada. POAC11-003

Michel, B. and Toussaint, N.: Mechanisms and theory of indentation of plates, Journal of Glaciology, Vol. 19, No.81, pp.285-301, 1977

Mirzoev, D.A. (2009): Basics of offshore oil and gas engineering. Vol.1. Construction and exploitation offshore oil and gas fields. "Serebro", Moscow, p.51. Мирзоев Д.А. Основы морского нефтегазового дела. Том 1 - Обустройство и эксплуатация морских нефтегазовых месторождений

MODIS (2013): Ice in the Northern Caspian Sea. Satellite image. Website: http://modis.gsfc.nasa.gov/gallery/individual.php?db_date=2013-03-07 [Date accessed 15/05/2015]

NCOC (2011): North Caspian Sea Project: from Vision to Reality. Brochure, website: http://www.google.no/url?sa=t&rct=j&q=&esrc=s&source=web&cd=1&cad=rja&uact=8&ved=0CB4QFjAA&url=http%3A%2F%2Fwww.ncoc.kz%2Fpdf%2Fpublications%2Fncoc_brochure_2011_en.pdf&ei=uRKSVLPUlsnfywOb4IG4BQ&usg=AFQjCNF24ViG4bfqDTcWbnHZy8jVmQbRVw&sig2=_SBf6zMDaw_ViWXZQsyHYA&bvm=bv.82001339,d.bGQ [Date accessed: 01/10/2014]

NCOC (2013): The project of the Kalamkas-offshore field development. Aqtau. Website: <http://www.doc4net.ru/doc/3139097588808/> [Date accessed:17/12/2014]

Nilsen, R., Verlaan, P. (2011): The North Caspian Sea Ice Conditions and how Key Ice Data is Gathered. Proceedings of the 21st International Conference on Port and Ocean Engineering under Arctic Conditions July 10-14, 2011 Montréal, Canada. POAC11-112

Nisja, H.A. (2014): Numerical Modelling of Brittle Failure in Ice Structures. Master's thesis NTNU, Trondheim

Noyonews.net (2013): Prirazlomnaya. Website: <http://noyonews.net/wp-content/uploads/2013/09/> [Date accessed: 10/06/2015]

Nymo (2010): Kashagan D Island - Design of piping systems. Website: <http://www.nymo.no/Default.aspx?ID=110> [Date accessed: 06/05/2015]

Palmer, A. and K. Croasdale (2012). Arctic offshore engineering. Singapore, World Scientific Publishing Co. p. 129-136

Petrovich, J. (2003): Mechanical properties of ice and snow. Material Science and Technology Division, Los Alamos National Laboratory

Planeta (2015): Caspian Sea. Ice cover chart-maps. Website: http://planet.iitp.ru/english/products/p_6_5_eng.htm [Date accessed: 20/05/2015]

Polonskii, V.F., Ostroumova, L.P. (2007): Long-term and Intraannual Changes in Run-off and Water Levels in the Volga River Delta. Published in Meteorologiya i Gidrologiya, 2010, №2, pp. 63–72. Website: <http://link.springer.com/article/10.3103/S1068373910020068> [Date accessed: 20/09/2014]

Ramseur, J. L. (April 17, 2015). Deepwater Horizon Oil Spill: Recent Activities and Ongoing Developments (PDF) (Report). CRS Report for Congress. Congressional Research Service. R42942. Retrieved 01 May 2015. Website: <http://www.fas.org/sgp/crs/misc/R42942.pdf> [Date accessed: 04/03/2014]

Remontowa Shipbuilding S.A. (2006): Ice Breaking Emergency Evacuation Vessel. Website: http://pdf.nauticexpo.com/pdf/remontowa/ibeev/31521-45365-_2.html [Date accessed: 08/11/2014]

Repetto-Llamazares, A.H.V., Gürtner, A., Gudmestad, O.T., Høyland, K.V. (2013): Qualitative Description of A shoulder Ice Barrier–Ice Interaction During Model Tests. Journal of Offshore Mechanics and Arctic Engineering-Transactions of The Asme. vol.135 (3).

Rigzone (2015): Rig Data: SDC. Website: http://www.rigzone.com/data/offshore_drilling_rigs/984/Drill_Barge/SDC_Drilling_Inc/SDC [Date accessed: 1/10/2015]

Sand, B. (2008): Nonlinear finite element simulations of ice forces on offshore structures. Doctoral Thesis at Luleå university of technology, Luleå, Sweden, June 2008

Sarybekova, L. (2004): North Caspian Project – Challenges and Successes. Presented at the 7th SPE International Conference on Health, Safety, and the Environment in Oil and Gas Exploration and Production held in Calgary, Alberta, Canada, March 29-31, 2004, SPE 86685

Shahnazaryan, A. (2012): Kashagan suffers a natural disaster? Website: <http://www.respublika-kz.info/news/business/27587/> [Date accessed: 8/12/2014]. Russian: Кашаган терпит природное бедствие? Публикация от 19.12.2012. Газета Республика –kz

Shlyamin, B.A. Caspian Sea. Website: <http://stepnoy-sledopyt.narod.ru/geologia/kmore/priroda2.htm> [Date accessed: 8/12/2014]

Sodhi, D.S., Borland, S.L., and Stanly, J.M. (1996): Ice action on riprap. Small scale tests. US Army Corps of Engineers, Cold regions Research and Engineering Laboratory, CRREL Report 96-12. Website: <http://www.dtic.mil/docs/citations/ADA318069> [Date accessed: 5/05/2015]

SpatialEnergy.com (2010): Caspian Sea. World View. Website: <http://www.spatialenergy.com/documents/caspian-sea-no-ice-low.pdf> [Date accessed: 14/09/2014]

Sultanov, E. (2010): Follow the law, investors! Foreign mining companies ignore the Kazakh goods and services. Kazakstan Today magazine. Aqtau. Website: <http://82.200.130.64/print/1274394760> [Date accessed: 05/05/2015] Russian: СУЛТАНОВ Е. (2010): Соблюдайте закон, господа инвесторы! Иностранные недропользователи игнорируют казахстанские товары и услуг. Актау, газета Kazakstan Today

Terziev, F.C., Kosarev, A.N., Kerimov, A.A. (1992): Hydrometeorology and hydrochemistry of the seas. Vol. 4. The Caspian Sea. St.-Peterburg, Gydrometoeizdat, 1992

Timco, G.W. and Weeks, W.F. (2010): A review of the engineering properties of sea ice. Cold Regions Science and Technology 60 (2010) p.107–129

Timco, G.W., Croasdale, K., Wright, B. (2000): An overview of first-year sea ice ridges. Technical report HYD-TR-047. Perd/CHC Report 5-112.

Tippmann, J.D. (2011): Development of a strain rate sensitive ice material model for hail ice impact simulation. Master's Thesis, University of California, San Diego

Topaz Energy and Marine (2015): An offshore drilling structure on D Island in Kazakhstan. Website: <http://www.topazworld.com/en/press-room/image-library/an-offshore-drilling-structure>, [Date accessed: 3/05/2015]

Unified state system of the World Ocean (ЕСИМО) (2005): The Caspian Sea. Website: http://esimo.oceanography.ru/esp2/index/index/esp_id/2/section_id/2/menu_id/779 [Date accessed: 20/10/2014]

Verlaan,P., Croasdale, K. (2011): Ice Issues Relating to the Kashagan Phase II Development, North Caspian Sea. Proceedings of the 21st International Conference on Port and Ocean Engineering under Arctic Conditions July 10-14, 2011 Montréal, Canada, POAC11-171

Volga Ltd. Report (1992): The fundamental points of the technical-economic report. Protection of the National economic objects and populated areas of the Caspian Sea coastal zone within Russian Federation. Moscow. pp.7-20

Weeks, W. F. and Gow, A. J. (1980): Crystal Alignments in the Fast Ice of Arctic Alaska. J. Geophysical Research. Vol. 85, pp. 1137–1146.

Weihrauch, A., Berger, J., Bartels, M. (2005): Ice Loading of Jack-Up Platforms. Proceedings of the 24th International Conference on Offshore Mechanics and Arctic Engineering, June 12-17, 2005, Halkidiki, Greece, OMAE 2005-67285

Wikipedia (2011): Map of the Kazakh oil and gas fields
Website:http://commons.wikimedia.org/wiki/File:Карта_нефтегазовых_месторождений_Казахстана.jpg [Date accessed: 25/05/2015]

Weiss, R.T., Prodonovic, A. and Wood, K.N. (1981): Determination of ice rubble shear properties. Symposium on Ice, Quebec City, pp. 861-872.

WMO (1989): Sea Ice Nomenclature. World Meteorological Organization. Website: http://www.aari.nw.ru/gdsidb/docs/wmo/nomenclature/WMO_Nomenclature_draft_version1-0.pdf [Date accessed: 31/03/2015]

Wong, T. T., Gale, A. D., Sego, D. C., Morgenstern, N. R. (1988): Shear Box Tests on Broken Ice. Proceedings of the ninth International Conference on Port and Ocean Engineering under Arctic Conditions, St. John's, Canada.

Zolotukhin, A.B. (2014a): Development of Russian shelves. Lecture 4, the course “Technical and economic analysis. Development of offshore oil and gas fields”, Gubkin Russian State University of oil and gas

Zolotukhin, A.B. (2014b): Basics of Offshore field development. Lecture 5, the course “Technical and economic analysis. Development of offshore oil and gas fields”, Gubkin Russian State University of oil and gas

Appendix A. Summary of the materials properties

Table A.1. Summary of ice properties used for the FEA.

Parameter	Unit	Value	Comments
Density	kg/m ³	920	Used for the FE model, Chapter 2.1.1
Compressive strength	MPa	4.5	Chapter 2.2.1
Tensile strength	MPa	0.13-0.67	Chapter 2.2.2
Flexural strength	MPa	0.78	Chapter 2.2.3
Shear strength	kPa	550-900	Chapter 2.2.4
Young's modulus	GPa	3.5	Chapter 2.2.5
Poisson ratio		0.33	Chapter 2.2.5
The maximum tensile pressure	kPa	517	Chapter 8.3.1, Chapter 7.2.3
Cohesion, <i>d</i>	kPa	580	Chapter 8.3.1, Chapter 7.2.2
The angle of internal friction, β	Deg	50	Chapter 8.3.1, Chapter 7.2.2
Tension cut-off	kPa	250	Chapter 8.3.1, Chapter 7.2.2
The static friction of sea ice on rough concrete (the relative velocity is 30cm/s)		0.13	Chapter 2.2.6
The kinetic friction of sea ice on rough concrete (the relative velocity is 30cm/s)		0.05	Chapter 2.2.6
The friction coefficient for the ice-ice interaction		0.09	Chapter 2.2.6
The ice-sand/gravel friction coefficient		0.4	Used for the FE model, Chapter 2.2.6

Table A.2. Summary of ice rubble properties (Duplenskiy, 2012)

Parameter	Unit	Value	Source
Density	kg/m ³	920	Chapter 2.1.1
Young's modulus	GPa	8	Chapter 2.2.5
Poisson ratio		0.33	Chapter 2.2.5
Cohesion, d	kPa	15	Chapter 6.3
The angle of internal friction, β	Deg	20	Chapter 6.3

Table A.3. Soil properties implemented into the model (Sediments layer of silty sand and soft clay).

Parameter	Unit	Value	Source
Density	kg/m ³	1750	Lengkeek et al.,2003
Young's modulus	MPa	140	Duplenskiy, 2012
Poisson ratio		0.33	Duplenskiy, 2012
Cohesion, d	kPa	1	Lengkeek et al.,2003
The angle of internal friction, β	Deg	25	Lengkeek et al.,2003

**Appendix B. A concrete armor block with improved
interlocking ability**



A CONCRETE ARMOR BLOCK WITH IMPROVED INTERLOCKING ABILITY

Arkhat Sultabayev
Ove Tobias Gudmestad

ABSTRACT

A concrete interlocking armor block with improved interlocking ability is suggested to be used with other similar blocks in construction of marine structures, such as breakwaters, seawalls, groins for protecting reservoir banks and other coastal structures from hydrodynamic forces of waves and currents. The blocks are arranged at random or so that they create an integrated assembly, in which said blocks are interlocked to provide residual stability of the assembly.

Each block is constructed with two hook-shaped outer members integrally joined by a central cylinder. The outer members are arranged such that when one of them is in the upstanding position the other one is in the horizontal position.

10 Claims, 7 Figures

DESCRIPTION

Background of the invention.

The presented invention relates to a concrete interlocking armor block for protecting shorelines and reservoir banks. These concrete multiple legged structures provide improved interlocking characteristics and a set of these modules form a stable interlocked assembly, which resists the waves and currents action. The assembly of the adjacent blocks is arranged on a layer of stones or gravel and the gravity force coupled with the interlocking force provided by the hook-shaped outer members of each block fixes the assembly in situ.

Brief description of the prior art.

The utilization of riprap and/or rectangular blocks as coastal protection structures has some challenges leading to washing away and losing of these blocks during storms due to the absence of or minimal interlocking ability of the blocks which results in problems related to the breakwater assembly maintenance.

Interlocking concrete armor or erosion prevention modules of various shapes (such as Kolos, Dolos, tetrapods, etc.) are well known. One of the primary drawbacks of such modules is that these individual modules might not be interlocked in situ due to low interlocking forces produced by their appendages such that the stability of the assembly of these modules basically relies on a gravity force of an individual module.

The present invention was developed in order to avoid these drawbacks of the prior modules by utilization of concrete interlocking armor blocks of an improved shape that provides a high interlocking capability in situ.

Summary of the invention.

According to the invention the concrete interlocking armor block comprises two hook-shaped outer members integrally joined by a central cylinder.

The outer members joined to the central member (cylinder) on opposite sides thereof at their central portions are constructed so that when one of them is in the vertical position the other one is in the horizontal position.

FREMLAGT SOM ORIGINAL
PRESENTED AS ORIGINAL
STAVANGER TINGRETT

13/04-15

Keth Husvold
NOTARIUS PUBLICUS



KETH HUSVOLD
1.konsulent

1
Alyo

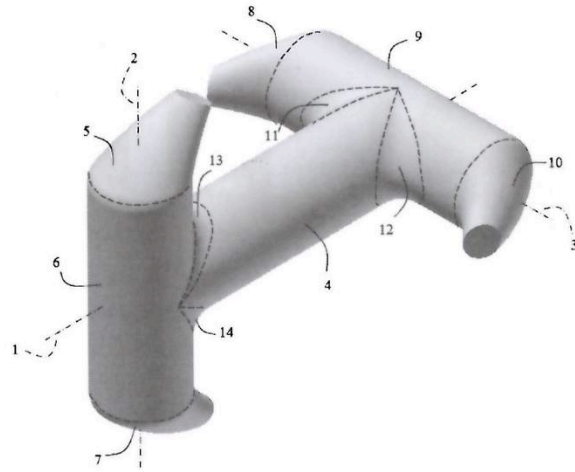


FIG.1

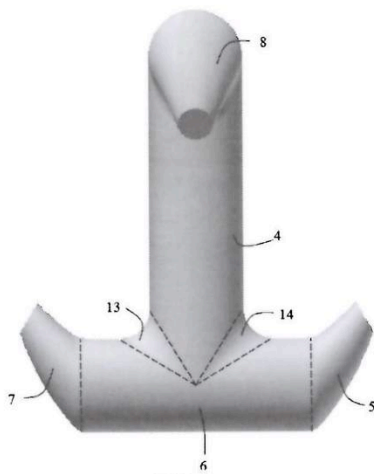


FIG.2

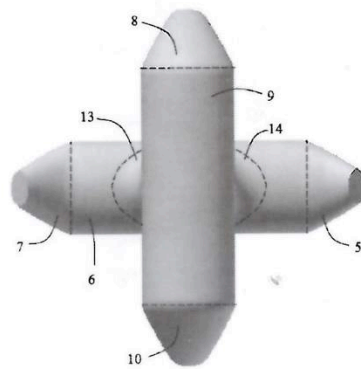


FIG.3

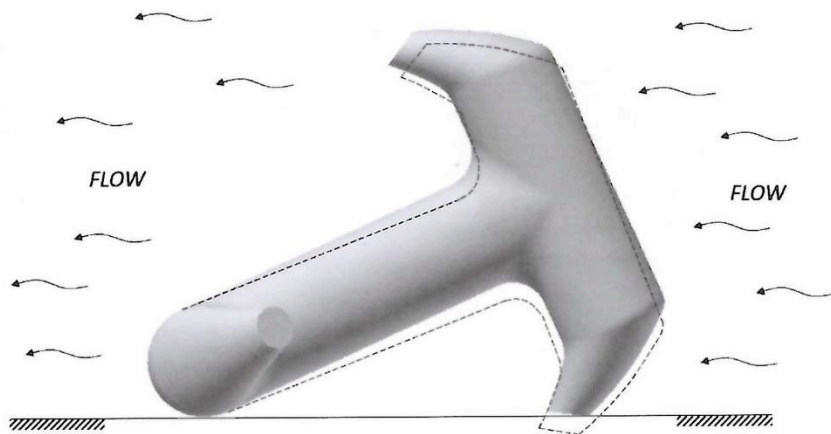


FIG.4

FREMLAGT SOM ORIGINAL/
PRESENTED AS ORIGINAL
STAVANGER TINGRETT

a)

NOTARIUS PUBLICUS



KETH HUSVÆG
1.konsulent

2

Handwritten signature

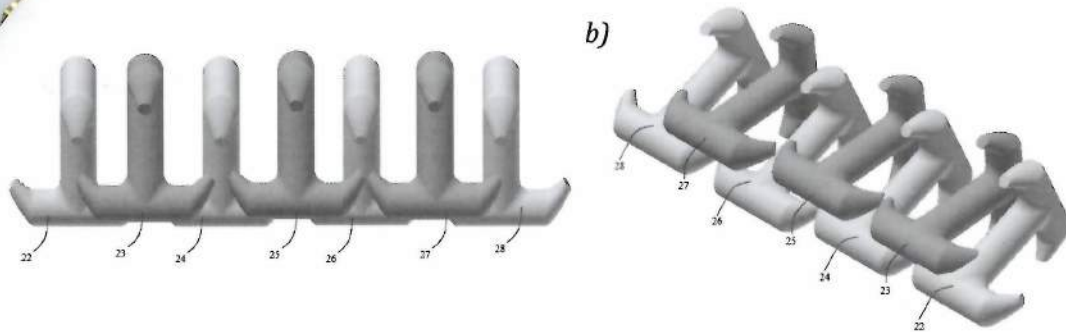


FIG. 5

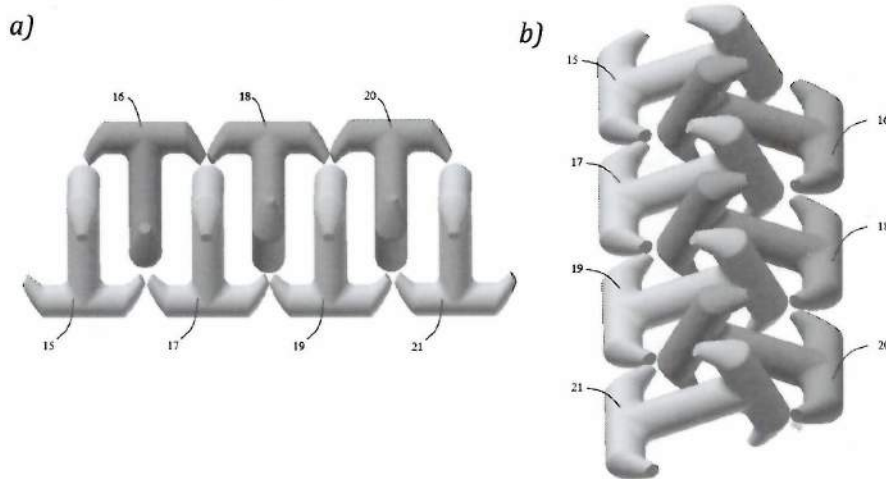


FIG. 6

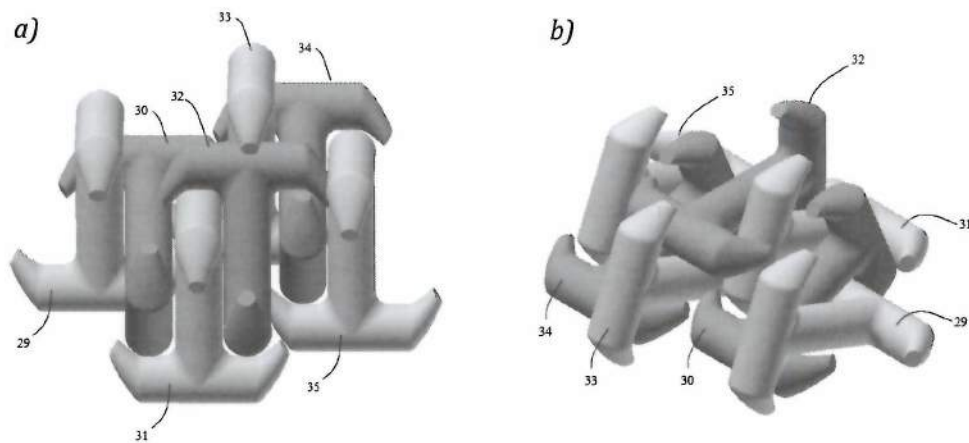


FIG. 7

FREMLAGT SOM ORIGINAL/
PRESENTED AS ORIGINAL
STAVANGER TINGRETT

Keth Husvæg

NOTARIUS PUBLICUS

KETH HUSVÆG
1.konsulent



3

Algeir

Each of the outer members is arranged as a cylinder, which has two arcuate, inward-curved, hook-shaped end segments joined to the cylinder's bases. The end segments are configured such that their cross-sectional areas decrease from the bases connected to the outer member's cylinder toward their opposite ends.

According to the further object of the invention, the outer members include chamfered surfaces at the connections to the central cylinder.

Brief description of the figures.

Other features and advantages of the invention will be better understood from the following specification and drawings in which:

Fig.1, is a perspective view of one embodiment of a concrete interlocking armor block according to the invention;

FIG.2, is a front plan view of the concrete interlocking armor block of fig.1;

FIG.3, is top plan view of the concrete interlocking armor block of fig.1;

FIG.4, is a side elevation view of the concrete interlocking armor block of fig.1;

FIG.5, is a plan (a) and perspective elevation (b) view of an erosion prevention structure assembled from concrete interlocking armor blocks according to the invention;

FIG.6, is a plan (a) and perspective elevation (b) view of a marine arrangement or a barrier constructed with said blocks for shore protecting and erosion control;

FIG.7, is a plan (a) and perspective elevation (b) view of a marine assembly of concrete interlocking armor blocks according to the invention.

Detailed description.

Referring to FIGs1-3, the interlocking block of the present invention comprises a central cylinder 4 having a longitudinal axis 1 and two hook-shaped outer members having longitudinal axes 2 and 3 respectively.

The first outer member is arranged as a cylinder 9 with arcuate, inward-curved, end segments 8 and 10, respectively, connected at two opposite bases of the cylinder. The cylinder 9 has the same diameter and shape of the cross-section as the central cylinder 4. The end segments 8 and 10 are configured such that their cross-sectional areas decrease from the bases connected to the cylinder 9 toward their opposite ends. The dimension of these shaped segments 8 and 10 is less than the diameter of the central cylinder 4. The other outer member is identical in shape and dimensions to the first outer member.

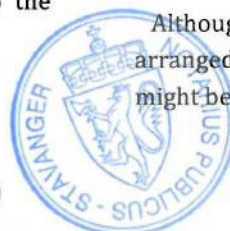
The outer members are connected to the central cylinder 4 on opposite sides thereof at their central portions such that the longitudinal axes 3 and 2 of the members are at 90° to each other. The connections between the central cylinder 4 and the outer members comprise chamfered surfaces 11, 12, 13 and 14 in order to improve the integrity of the block by reducing stresses at the area of possible concentration.

The breakwater block illustrated in FIGs1-3 is demonstrated in FIG.4 in position in use. In this instance one of the outer members is disposed in the horizontal position while the other one is in the upstanding position toward the flow. The seaway flowing straight ahead the concrete interlocking armor block according to the innovation as illustrated in FIG.4 provides the block embed itself as demonstrated by broken lines.

Although breakwater blocks can be arranged as shown in FIGs 5-7, said blocks might be arranged at random as well.

FREMLAGT SOM ORIGINAL/
PRESENTED AS ORIGINAL
STAVANGER TINGRETT

Keth Husveg
NOTARIUS PUBLICUS



KETH HUSVÆG
1.konsulent

4

Agw

The blocks according to the innovation can be formed of concrete or of any appropriate materials.

Although the preferred forms and embodiments have been described in this report, the various modifications may be done with observance of the idea of the invention.

Claims.

The invention claimed is:

1) A concrete interlocking armor block usable in construction of marine structures for protecting shorelines, reservoir banks and other coastal structures from the hydrodynamic forces of waves and currents, comprising

(a) a central cylinder having a longitudinal axis and two outer members, each outer member comprising a cylinder with two arcuate, inward-curved, hook-shaped end segments that are integrally joined to the bases of the outer member's cylinder;

(b) the outer members disposed with their longitudinal axes at 90° to each other are integrally joined to the central member (cylinder) on opposite sides thereof at their central portions.

2) An interlocking block according to claim 1 a), wherein the cross-sectional area of each end segment decreases from the opposite bases of the outer member's cylinder to their opposite ends.

3) An interlocking block according to claim 1 b), wherein the regions of the central cylinder connection to the outer members are chamfered.

4) An interlocking block according to claim 1, wherein each the outer members are identical in length and in shape.

5) An interlocking block according to claim 1, wherein the central cylinder and two outer members have an internal reinforcement made of metal rods and are formed of concrete.

6) An interlocking block according to claim 1 that can be used with similar blocks whereby, when a set of similar interlocking blocks is arranged so that it creates an integrated assembly, said breakwater blocks interlock in situ and provide residual stability of the assembly.

7) A marine erosion prevention structure comprising a set of interlocking blocks, each interlocking block comprising a central rigid cylinder and two outer members integrally connected to the central cylinder in the fixed relative position such that their longitudinal axes are at 90° to each other, each outer member comprising a cylinder with two rigid, inward-curved, arcuate, hook-shaped end segments that are integrally joined to the bases of the outer member's cylinder.

8) A marine structure according to claim 5, wherein each said block is alike in configuration.

9) Any marine structure comprising at least one layer of said blocks.

10) A marine structure according to claim 5, wherein said interlocking blocks are arranged at random.

Arkhat Sultabayev

Notarius Publicus i Stavanger bekrefter at
The Notary Public of Stavanger certifies that

ARKHAT SULTABAYEV

har undertegnet dette dokument
has/have signed this document
Stavanger tingrett og Notarius Publicus
Stavanger District Court and Notary Public

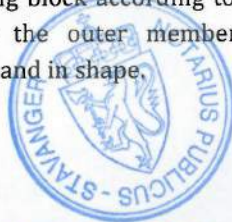


Keth Husveg
KETH HUSVÆG
1.konsulent

13/04-15
5

[Handwritten signature]

FREMLAGT SOM ORIGINAL/
PRESENTED AS ORIGINAL
STAVANGER TINGRETT



Keth Husveg
NOTARIUS PUBLICUS

KETH HUSVÆG
1.konsulent

Appendix C. Simulation results

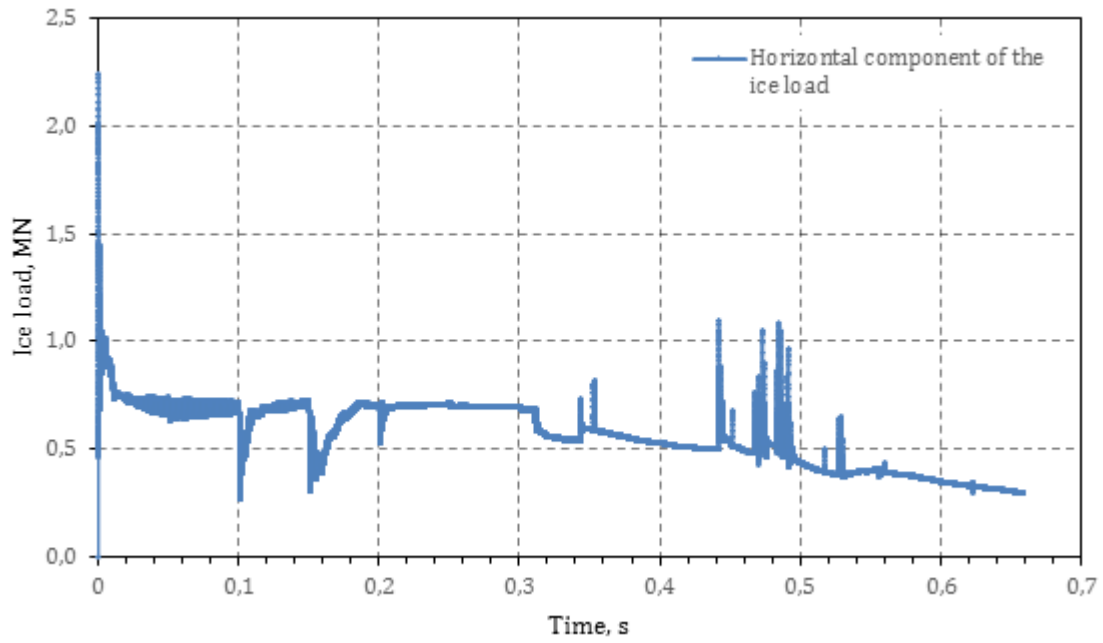


Figure C.1: Simulated horizontal component of ice forces exerted onto the SIB (the 0.15-m ice sheet acting on the 45-degree slope).

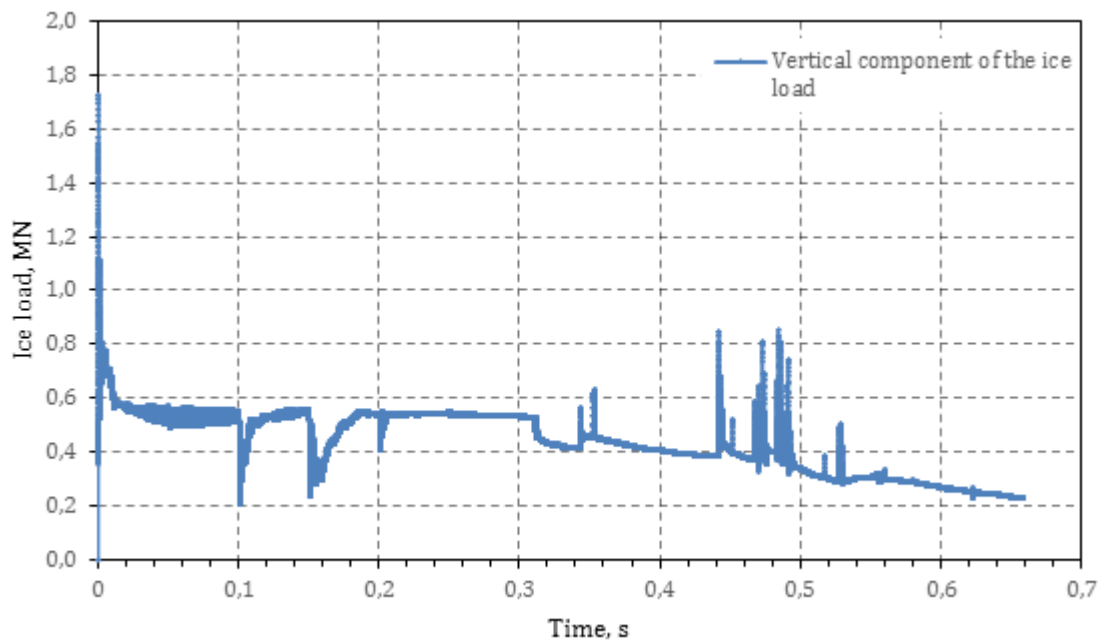


Figure C.2: Simulated vertical component of ice forces exerted onto the SIB (the 0.15-m ice sheet acting on the 45-degree slope).

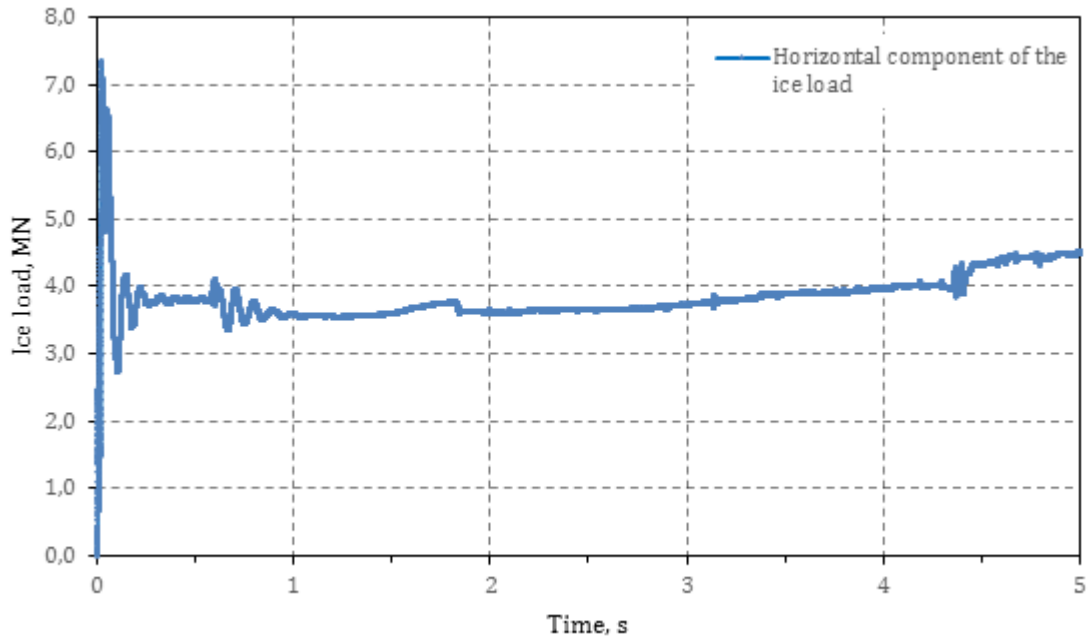


Figure C.3: Simulated horizontal component of ice forces exerted onto the SIB (the 0.96-m ice sheet acting on the grounded ice rubble in front of the SIB).

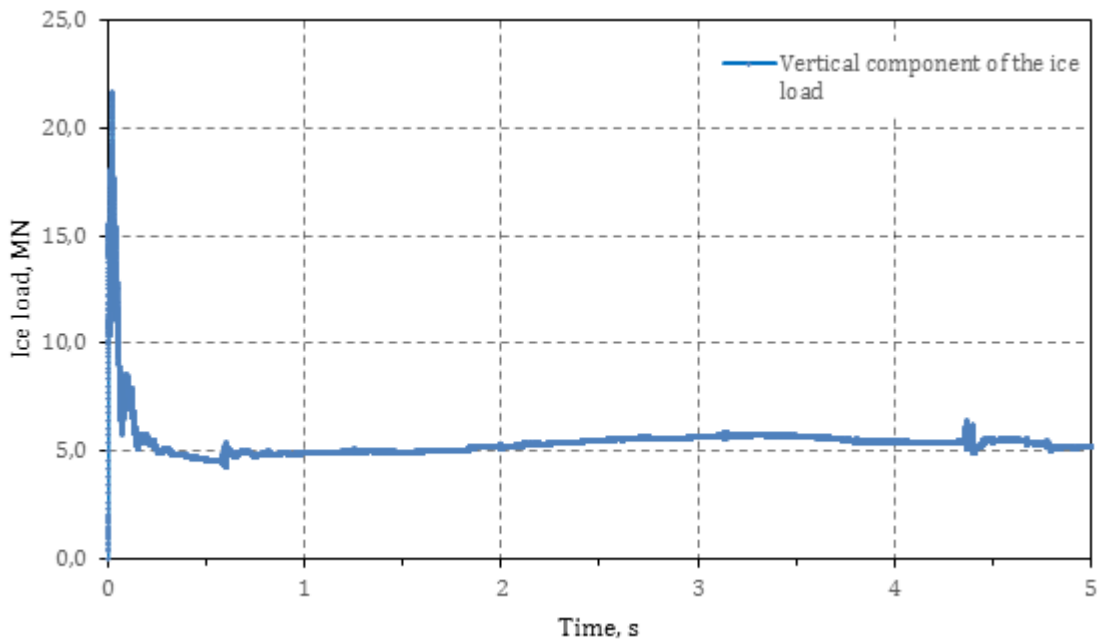


Figure C.4: Simulated vertical component of ice forces exerted onto the SIB (the 0.96-m ice sheet acting on the grounded ice rubble in front of the SIB).

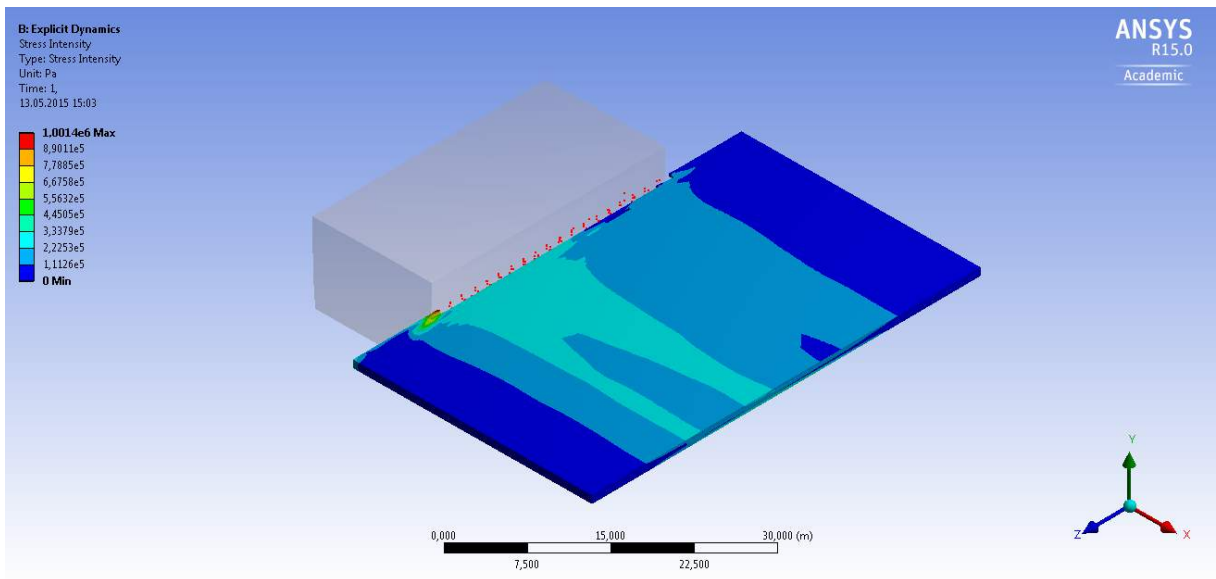


Figure C.5: Snapshot of ice interaction on the barge revealing the ice failing in crushing. Note that red dots are free mass points (see Chapter 7.2.5)

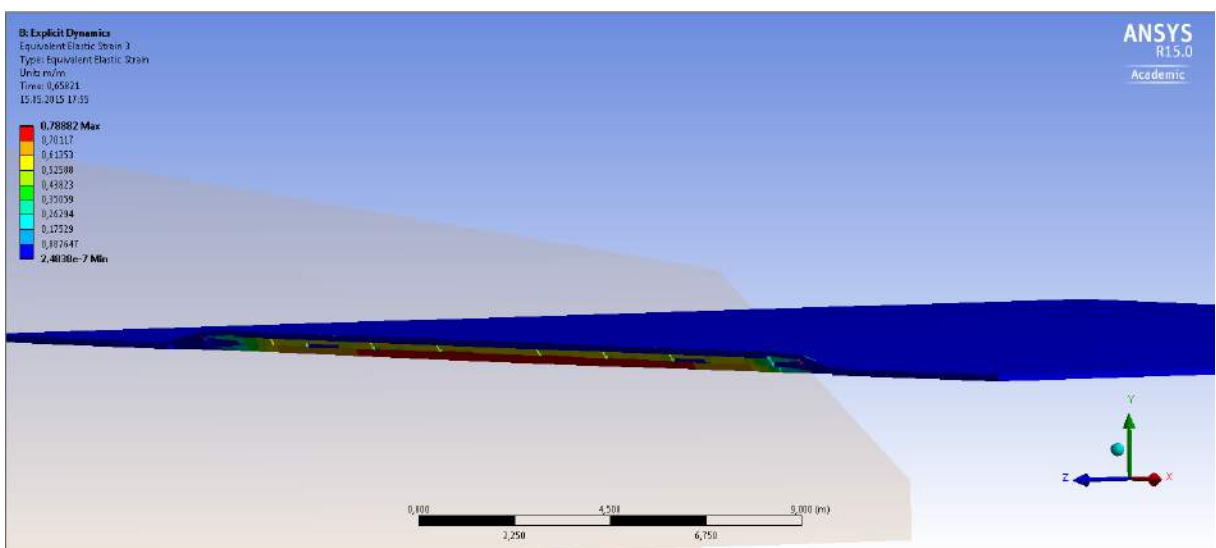


Figure C.6: Snapshot of the 0.15-m ice sheet acting on the SIB revealing the ice plasticity before the ice failing in bending and before initiation of circumferential cracks.

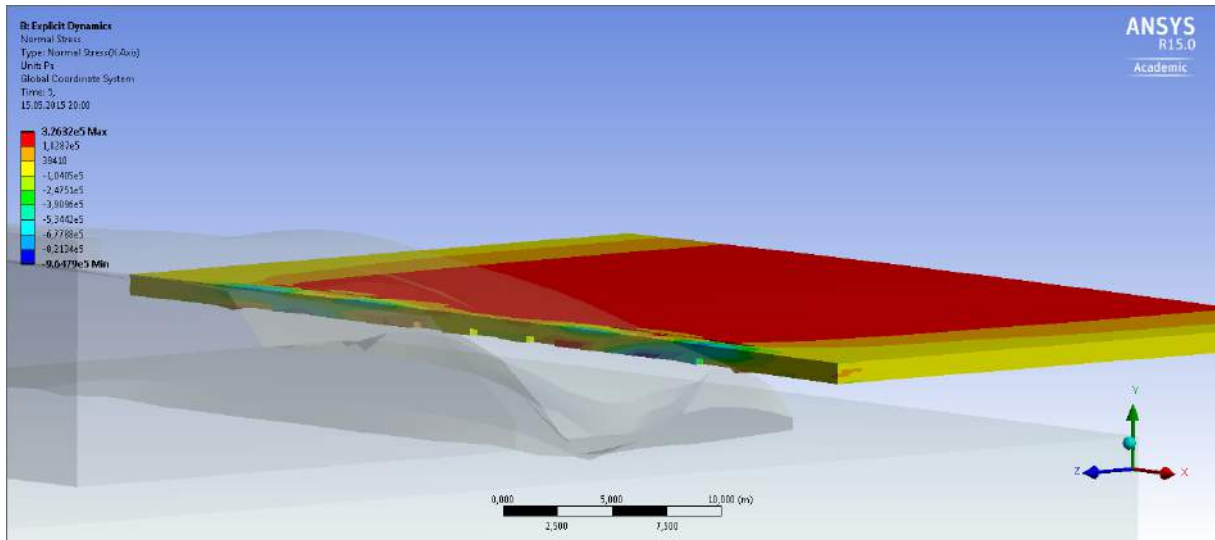


Figure C.7: Snapshot of the 0.96-m ice sheet acting on the grounded ice rubble in front of the SIB revealing the ice failing in rubbling.

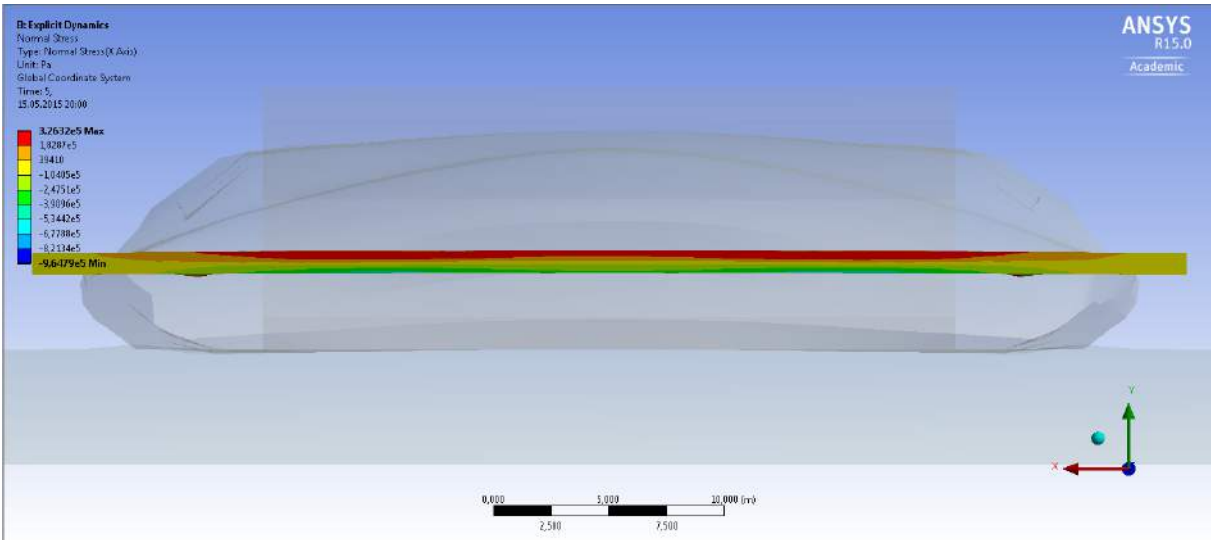


Figure C.8: Snapshot of the 0.96-m ice sheet acting on the grounded ice rubble in front of the SIB revealing the ice failing in rubbling.(back view).

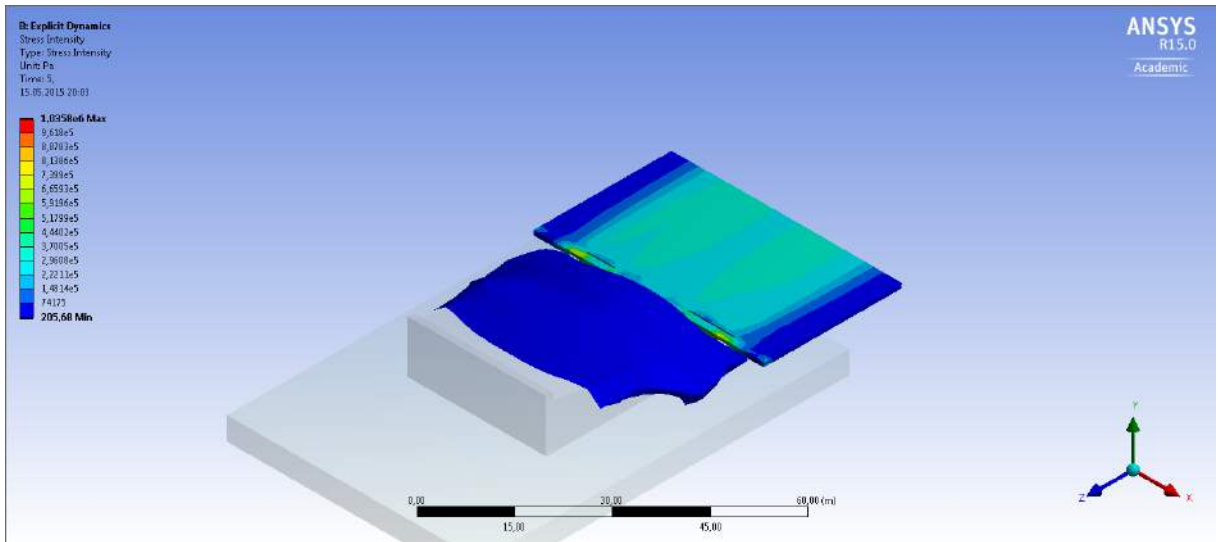


Figure C.9: Snapshot of the 0.96-m ice sheet acting on the grounded ice rubble in front of the SIB revealing the ice failing in rubbling (general view).

Appendix D. Dimensions of the SIB and ice rubble

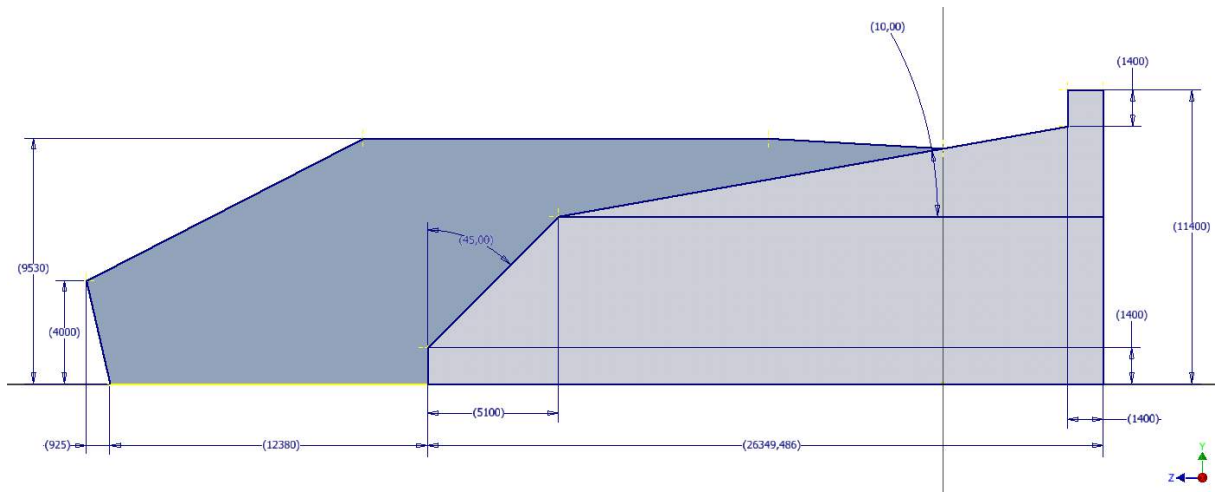


Figure D.1: The dimensions of the SIB and grounded ice rubble implemented into the simulations. Note that all dimensions are in mm and in degrees.